UCGE Reports
Number 20188

Department of Geomatics Engineering

Hydrological Modelling Using MODIS Data for Snow Covered Area in the Northern Boreal Forest of Manitoba

(URL: http://www.geomatics.ucalgary.ca/links/GradTheses.html)

by

Samantha K.M. Poon

January 2004

UNIVERSITY OF CALGARY

Hydrological Modelling Using MODIS Data for Snow Covered Area in the Northern Boreal Forest of Manitoba

by

Samantha Ka Man Poon

A THESIS
SUBMITTED TO THE FACULTY OF GRADUATE STUDIES
IN PARTIAL FULFILMENT OF THE REQUIREMENTS FOR THE
DEGREE OF MASTERS OF SCIENCE

DEPARTMENT OF GEOMATICS ENGINEERING

CALGARY, ALBERTA
January, 2004

Abstract

Satellite derived snow cover area (SCA) is a critical parameter in snowmelt modelling, and is used in numerous hydrological and climatological studies. A major limitation of current SCA modelling when using optical satellite sensors is mapping snow in forested areas. The most ideal case for mapping snow in dense forested areas is to have landcover data indicating the location of forested regions and then use separate classification criteria for forested and non-forested areas. This study investigates the MODIS (Moderate Resolution Imaging Spectroradiometer) snow-mapping algorithm "*Snowmap"* and its ability to map snow in the Northern Boreal Forest of Manitoba. Landcover data enhanced snow-mapping algorithms were developed and compared with MODIS snow products during the snowmelt period of 2001 and 2002. The use of Normalized Difference Snow Index (NDSI) and Normalized Difference Vegetation Index (NDVI) values in the MODIS Snowmap algorithm to detect snow in forested areas was proven successful in this study. Landcover based algorithms and the MODIS algorithm both mapped similar amounts of SCA during the melt period in each study year. The algorithm-derived SCA data for both years showed an exponential correlation with accumulated degree-days. In addition, because the variation in SCA provides an indication of the amount and rate of runoff produced by snowmelt in a watershed, snowmelt runoff computations using the derived SCA data at a daily time step were conducted in two watersheds located in the study area. A quick verification with streamflow data indicated the inclusion of SCA data in runoff computation could yield better runoff estimates than the exclusion of SCA data. Snow depletion behavior at different elevation ranges in the study area was also investigated. Results show that snow located at higher elevation ranges melt faster compared to snow located at lower elevation ranges. This study also provides a relationship between SCA and accumulated degree-days at different elevation ranges.

Acknowledgements

I would like to thank Dr. Caterina Valeo for giving me research and teaching opportunities in my studies. She had also given me exposure to many different aspects of engineering. It was a great honour for me to be one of her graduate students. I am really grateful for all the mentoring and encouragement she has given me.

I would also like to thank the University of Calgary and the Engineering for the Environment Program for research funding.

My gratitude goes out to Mr. Marc St. Laurent for providing landcover and DEM data, the Water Survey of Canada for the streamflow data, Environment Canada for meteorological data, and NASA Distributed Active Archive Centers for all the MODIS data. My research would not have been possible without any of these data sets.

I sincerely thank Dr. Dorothy Hall from the National Snow and Ice Data Center for answering all my questions; Dr. Isabelle Couloigner and Dr. Mryka Hall-Beyer for helpful comments and suggestions to improve my thesis.

Last but not least, I would like to thank my family and friends for all the unconditional love and support they had given me at all times. My family is the main source of my success in everyway. I have met a lot of great people during the course of my undergraduate and graduate study in this department. I will always value the friendships I have built throughout this journey. Special thank to Mr. Suen Lee for all the great editing he has done on this thesis. I also like to thank Mr. Damien Tsang for helping me on making the notation page.

Table of Contents

List of Figures

List of Tables

Notation

Abbreviations

ADC	Areal Distribution Curve
ADD	Accumulated Degree-days
AVHRR	Advanced Very High Resolution Radiometer
BOC	Basis of Comparison
CMG	Climate Modelling Grid
CSA	Canadian Space Agency
DAACs	Distributed Active Archive Centers
DEM	Digital Elevation Model
ECS	EOSDIS Core System
EDG	EOS Data Gateway
EOS	Earth Observing System
EOSDIS	Earth Observation System Data and Information System
ERS	European Remote Sensing
ESA	European Space Agency
FTP	File Transfer Protocol client
GAC	Global Area Coverage
GES DAAC	Goddard Earth Sciences DAAC
GF	Gap Fraction
HDF	Hierarchical Data Format
HDF-EOS	Hierarchical Data Format - Earth Observing System
HISDUMP	Image Histogram Export
ImageWorks	ImageWorks Data Browser or PCI Image Handler
IR	Infrared
ISIN	Integerized Sinusoidal

Abbreviations

L2	Level 2
L2G	Level 2G
L3	Level 3
L4	Level 4
LAC	Local Area Coverage
LBSM	Land-Based Snow-Mapping Algorithm
LP DAAC	Land Processes DAAC
LWIR	Longwave-IR
MODIS	Moderate Resolution Imaging Spectroradiometer
NDSI	Normalized Difference Snow Index
NDVI	Normalized Difference Vegetation Index
NIR	Near-Infrared
NOAA	National Oceanic and Atmospheric Administration
NOHRSC	National Operational Hydrologic Remote Sensing Center
NSIDC DAAC	National Snow and Ice Data Center DAAC
QA	Quality Assessment
RS	Remote Sensing
RSI	RADARSAT International
SCA	Snow Cover Area
SAR	Synthetic Aperture Radar
SDC	Snow Depletion Curve
SIN	Sinusoidal
SNR	Signal-to-Noise Requirements
SWE	Snow Water Equivalent
SWIR	Shortwave-IR
TM	Thematic Mapper
TOA	Top of the Atmosphere

Abbreviations

UTM	Universal Transverse Mercator
V001	Version 1
V002	Version 2
V003	Version 3
V004	Version 4
WSC	Water Survey of Canada

Symbols

α	significant
A	watershed area
a	exponential coefficient
a_1	coefficient
a_2	coefficient
b	exponential coefficient
C_1	albedos of channel 1
C_2	albedos of channel 2
Fr	fraction of SCA in the watershed
G_1	ground threshold for channel 1
G_2	ground threshold for channel 2
Im	snow cover percent in each pixel
K	proportional constant
M	amount of melt
Q	amount of runoff
Q_{sw}	shortwave (solar) energy flux
Q_{lw}	longwave (terrestrial) energy flux

Symbols

Q_{le}	latent heat flux
Q_h	sensible heat flux
R	rainfall intensity
S_1	snow threshold for channel 1
S_2	snow threshold for channel 2
Sn	amount of snow
T	daily mean temperature

Chapter 1
Introduction

1.1 Background

In the province of Manitoba, electricity generated by water resources accounts for over 90% of the total electricity produced, with runoff from spring snowmelt being the largest single source of this power. As reservoir operations are critical to hydropower generation, stream flow forecasts are used in planning electricity production and reservoir operation. Hence, there is a need to accurately model snow hydrology in northern Manitoba. Accurate monitoring of snow-covered areas (SCA) will yield better estimates of the stream flow levels that are produced by melting snow. Typically, snow accumulation and melt are usually modelled using meteorological observations. But with only a sparse meteorological network in many parts of Manitoba, there is great interest in using remotely sensed data to increase the accuracy of the information on snow cover (Johansson *et al,* 2001).

According to Donald *et al.* (1995), SCA and other snow cover attributes such as average snow depth are important factors for modelling snowmelt runoff. Uniform snow cover of constant depth and complete areal coverage is the simplest representation of snow cover and is often assumed in snow modelling. They also stated that vegetation roughness tends to dominate the snow cover distribution in lowland regions. This indicated that the surface cover type, which caused the response of snow cover distribution, could be summarized into three general vegetation classes: little to low vegetation, low vegetation and high vegetation. Ploughed fields or pasture grassland are considered little to low vegetation. Corn stubble and marsh grasses are classified as low vegetation. Finally, forests are classified as high vegetation. The vegetation in northern Manitoba can

generally be classified into seven specific types: coniferous forest, deciduous forest, mixed forest, muskeg, treed rock/impervious, lakes/rivers, and marsh/beaver flood. The study area contains a large amount of black spruce treed muskeg amounting to 22% of the total coverage. The boreal forest of northern Manitoba has a sub-arctic climate, and the terrain is relatively flat.

Traditional methods of measuring SCA involve manually measuring precipitated snow fall or snow depth at a number of locations within a basin. With these measurements, an overall estimate of the amount of snow cover can be produced. The equivalent amount of water runoff that will be produced during snowmelt can be determined if the snow water equivalent is known or assumed. However, due to the limited number of measurements, these methods may produce erroneous results. In order to create a more reliable and efficient hydrological model, and improved runoff predictions, a more accurate and less user-intensive method is needed to predict the SCA. Some researchers have indicated that remotely sensed data can provide better estimates of SCA in a basin than traditional surveying methods. Remote sensing (RS) algorithms can help to increase point measurements in larger spatial scale models (Metcalfe and Buttle, 1998). It is still undetermined however, if using remote sensing algorithms can improve the hydrological modelling process significantly. A major limitation of current SCA modelling using RS is snow-mapping in forested areas. Snow reaches the ground after filtering through the forest canopy and the dense forest can obscure the underlying snow. A basin may contain less dense types of deciduous forest or denser types of coniferous forest. Under these conditions, a reliable interpretation is required to identify snow under forest cover (Singh and Singh, 2001).

While there are several existing satellite sensors in orbit already that provide data for snow cover, they all have certain flaws, such as low spatial and temporal resolution that limit their usefulness. The MODIS (Moderate Resolution Imaging Spectroradiometer) instrument launched aboard Terra EOS AM-1 in late 1999 is designed to observe and

monitor Earth changes. MODIS has a wide range of spectral bands in the visible and near-infrared (IR) regions, high spatial resolution and near daily global coverage. It is a new tool that improves on the deficiencies of current sensors and can help to improve the representation of SCA.

1.2 General Thesis Objectives

The primary objectives of this thesis are:

1) To determine the effectiveness of daily MODIS data for determining SCA and areal snow depletion in the northern Boreal Forest.
2) To use the MODIS data in a conventional model of snowmelt to see if snowmelt modelling improves.

1.3 Thesis Layout

Chapter Two will describe general snow cover distribution and snowmelt properties. Methods for carrying out snow cover analysis will also be covered. Also, important characteristic of snow for remote sensing and four remote sensing sensors currently used for snow-mapping will be reviewed. Detail description of the MODIS snow-mapping algorithm, "*Snowmap*", will be addressed along with its gaps and limitations. The detailed thesis objectives are also given in this chapter.

Chapter Three will describe the thesis study area, the methodology, database construction and data pre-processing of acquired spatial and temporal data. Three test snow-mapping algorithms, "*LBSM*", "*LandSnow" and "Simulated Snowmap"*, are developed and described in this chapter.

Different case studies that help to illuminate the results and differences between the three test algorithms and the MODIS daily snow product will be addressed in Chapter 4. These case studies compare the percentage of daily SCA and other coverage features mapped by the algorithms. Besides a comparison of the differences in percent coverage, the spatial agreement will also be covered. SCA correlation to degree-days and elevation range between different algorithms will also be covered. This is detailed in Chapter 5. Chapter 6 describes the study conclusions.

Chapter 2
Literature Review

2.1 Introduction

Snow cover is the focus of this chapter. Important factors that affect snow cover distributions and methods of snow cover analysis will be discussed. Finally, remote sensing for snow cover will be examined, including a closer look at four remote sensing sensors that are currently in use. A detail description of the MODIS snow-mapping algorithm, "*Snowmap*" will be given, along with its limitations.

2.2 Snow Cover Distribution

Snow cover is heavily impacted by the environment. Weather, terrain and landcover all cause different accumulation and melt patterns and are important factors in creating an accurate SCA model.

2.2.1 Meteorological Conditions

Meteorological factors, such as temperature, precipitation, atmospheric circulation patterns, frontal activity, lapse rate, stability of the air mass (American Society of Civil Engineers, 1996) and wind, have a great effect on the distribution and characteristics of snow in a basin. The amount of snowfall can vary significantly across a large area. Similarly, the temperature over the area will not be homogenous, affecting the amount of snow accumulated and the melting rate. However, the single most important meteorological factor is wind. It can cause snow to vary throughout the basin, creating different depths and making it more difficult to model SCA. The wind affects seasonal

snow cover significantly by reducing snow deposition and increasing sensible heat flux during periods of low solar flux. Even calm winds in the best of conditions are capable of hindering the occurrence of sublimation from, or condensation to the snow cover (Marks *et al.,* 2001). This leads to differences in the energy balance of the snow cover, especially during melt periods, between windy and calm areas since thinner snow cover distributed by the wind does not persist into late spring (Marks *et al*, 2001). Consequently the snow will not melt simultaneously across the basin. The unequal distribution of snow complicates the snowmelt modelling process.

2.2.2 Terrain Conditions

Parameters such as slope, aspect, elevation, vegetation cover, exposure (American Society of Civil Engineers, 1996) and land use (Burkard *et al.,* 1991) are factors in the spatial variation of snow accumulation and ablation. Snowmelt rate is a function of these same terrain factors. Normally it is important to incorporate an accurate model for the elevation and topography when modelling SCA, but it is unlikely to be a factor in northern Manitoba as the terrain is relatively flat. With low relief, as in this study's area, the boreal forest and its vegetation properties becomes the primary control for the snow accumulation and energy exchanges during snowmelt (Metcalfe and Buttle, 1998).

2.2.3 Landcover

Differences in landcover types significantly impact snow accumulation and melt. The amount or depth of snow that can accumulate in the winter and its melting rate during the spring differs depending on the vegetation cover. Burkard *et al.* (1991) determined that at least three cover types need to be used in any model of snow cover distribution to be accurate. These cover types differed by vegetation height, ranging from ploughed fields which have low vegetation heights, grass fields for medium heights and forests for high heights. The roughness of the vegetation cover also dictated the range of snow depths.

Rougher cover, such as forests resulted in a larger range of measured snow depths as compared to more uniform cover types.

Ward and Elliot (1995) had noted that most research in snowmelt focused on forests because they often determine the timing and extent of snowmelt. A forest canopy opening and an open wetland might have the same gap fraction (GF). However, these sites would represent two different extremes of snow water equivalent values (Metcalfe and Buttle, 1998). Forest shade, which is dependent on the type and density of trees and their heights, greatly impacts solar radiation in the daytime. The shade ultimately reduces the amount of shortwave radiation that reaches the snowpack.

Canopy density in a forest, can be represented as a gap fraction (Metcalfe and Buttle, 1998), and controls the amount of shortwave radiation that reaches the snowpack surface. It can also affect the wind speed over the snow surface, which controls the sensible and latent heat fluxes. The reductions in incoming shortwave radiation, along with changes in sensible and latent heat fluxes were the dominant impact of the canopy.

Snow accumulation is affected by airflow perturbations created from canopy openings. For example, parts of a snowfall received in a wind-swept wetland would be redistributed to the wetland fringes (Metcalfe and Buttle, 1998). The tree height and the size of the canopy opening also affected the magnitude of snow redistribution by wind in a forest opening. The forest reduced wind speed and turbulence which resulted in less air movement, especially moist air over the snow, which leads to a lower snowmelt rate.

In the study of Klein *et al.* (1997), forests were a major stumbling block for the global mapping of snow cover as a forest canopy could obscure and add shadow to the snow underneath it. This resulted in the reflectance of snow cover beneath a forest being significantly different from pure snow. It depended on reflectance, transmittance, geometry and areal extent of the canopy, the surface cover and the conditions that

determined the proportion of shadowed and lighted areas. Colombo *et al.* (1999) had also noted that while snow and forest had different behaviors, a pixel with a mixture of snow and forest could be easily confused with cloud.

There is also a tendency for the snowpack to follow consistent patterns from year to year (Donald *et al.,* 1995). Burkard *et al.* (1991) indicated the snow cover distribution on the same landcover type from site to site in southern Ontario did not appear to have significant differences. This means that only a few detailed snow measurements within a common area or region are necessary as inputs for models that use areal depletion curves (ADCs).

2.3 Snowmelt Processes

The snowmelt process is the final physical process of snow. The snow particles undergo melting and refreezing throughout the snow-covered months. Once, the temperature of the snowpack rises above 0ºC, the snowpack will reach its liquid water holding capacity and any additional energy absorbed will cause the snowpack to melt. It may take several weeks to several months for the complete snowmelt to occur.

In Singh (1992), the snowmelt process has been described as thermodynamic with various factors that affect the transmission of heat to the snowpack. These factors, ranked in order of their importance, are (1) sensible heat conducted from moist air, (2) latent heat of condensation, (3) solar radiation, (4) heat transmitted by rain fall, and (5) heat conducted from the ground. The first two factors are formed by warm moist air turbulent diffusion. One further factor not mentioned in this literature is the snowpack condition. New-snow melts faster than old-snow that has been transformed into ice.

Murray and Buttle (2003), also looked at whether other factors could impact snowmelt rates. They found that clear-cutting did cause a small increase in melt rate compared to nearby forested areas, but the impact of the aspect was greater.

The snowmelt rates in the boreal forest vary spatially. This can be explained by the differences in canopy density (Metcalfe and Buttle, 1998). Under different canopy densities, the melt rate did not change proportionally according to the amounts in the total energy available for melting. As available energy increases with decreasing canopy density, the snowmelt rate increases. However, this relationship can vary depending on climatic conditions.

An energy balance considers the fluxes of all of the above mentioned forms of energy to find the net energy flux, shown in Figure 2.1. In this figure, Q_{sw} is the shortwave (solar) energy flux, Q_{lw} is the longwave (terrestrial) energy flux, Q_{le} is the latent heat flux, Q_h is the sensible heat flux. All flux units are usually presented as energy per unit time, e.g. watts. When trying to calculate snowmelt, it is easiest to consider the primary surface at the top of the snowpack and the bottom surface of the soil. As stated in the American Society of Civil Engineers (1996), each heat transfer process is dependent on atmospheric, environmental, and geographic conditions for a particular location and a particular time or season.

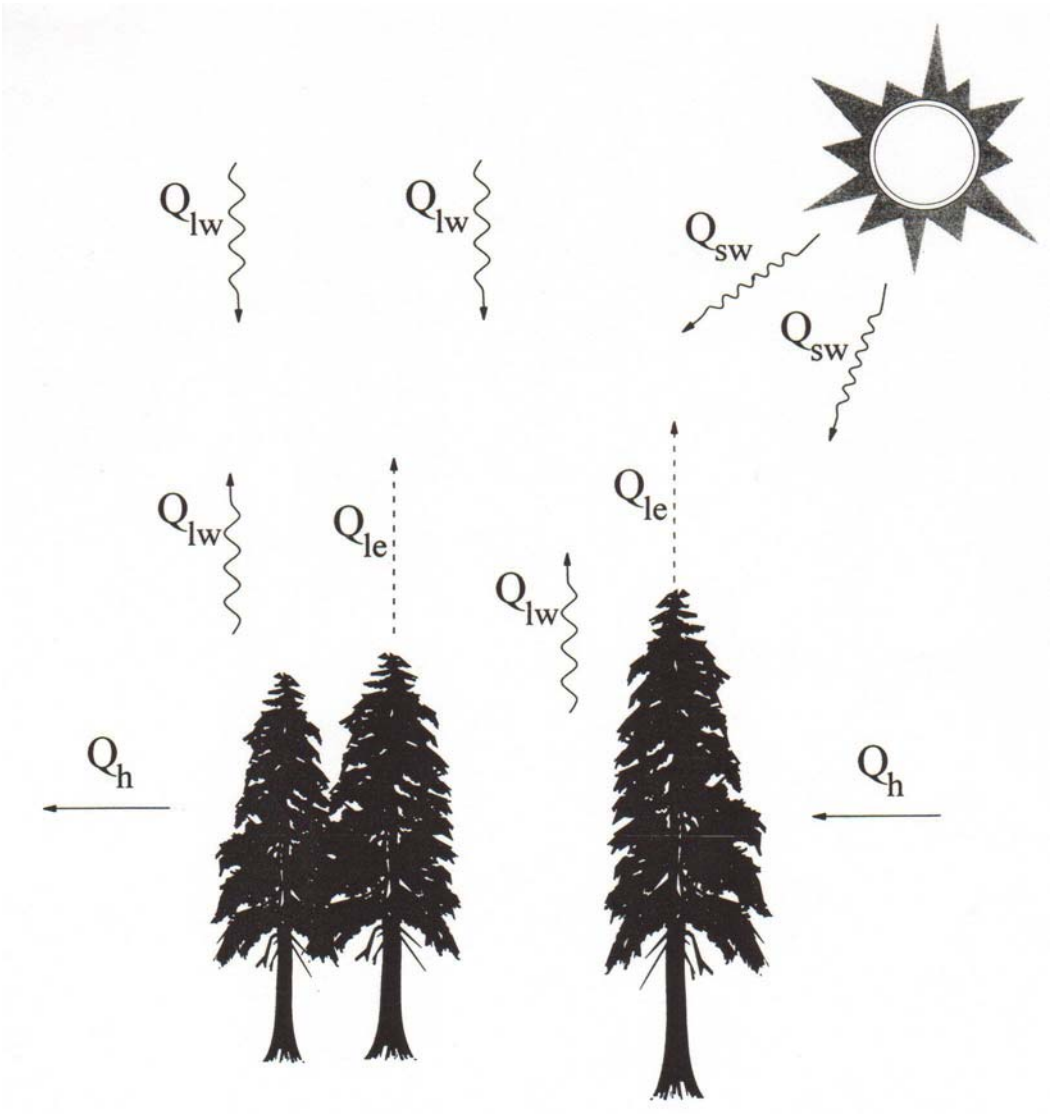

Figure 2.1 Energy Balance in a Forest (Ward and Elliot, 1995)

Singh (2003) has found that the depletion of SCA and cumulated mean temperature are exponentially correlated. As temperature is a critical determiner for snowmelt runoff (McCuen, 1998), the Temperature Index method is a simple and commonly used method for determining snowmelt. This method is highly popular because in most cases, temperature is the only reliable and consistently available weather variable measured at weather stations (Ward and Elliot, 1995). The Temperature Index method used in this

study employs the daily mean temperature as the fundamental prediction element for snowmelt. No matter if the method employs hourly or daily time steps, the amount of heat represented in the Temperature Index method has been proven to be useful in determining point-snowmelt and runoff from snowmelt (Viessman *et al.,* 1977). The Temperature Index method is a purely linear relationship that takes a general form as follows:

$$M = \begin{cases} K(T-32) & T \geq 32^{\circ}F \\ 0 & T < 32^{\circ}F \end{cases} \qquad [2.1]$$

where M is the daily snowmelt (inches/day), K is a proportional constant, and T is the daily mean temperature (ºF). When T the daily mean temperature in degree Celsius, then (T - 0ºC) is the number of degree-days for a given day. The value K in this equation represents a number of factors like the time of year, watershed orientation, the percent of forest cover, the slope and the depth of snow present at the watershed (McCuen, 1998). It reflects the potential of a watershed to produce daily melt. By multiplying M by the drainage area or the snow covered area (A), the amount of runoff (Q) can be computed.

$$Q = MA = K(T-32)A \qquad [2.2]$$

When calculating snowmelt runoff, the snow water equivalent (SWE) is usually used as an indicator of the quantity of snowmelt runoff that can be expected. SWE is the amount of water obtained by melting the snow cover, usually expressed in units of water depth per unit of snow depth. In most studies the assumption of 1mm of rainfall is equivalent to 10mm of snowfall (Environment Canada, 2004). The SWE measurement at the beginning of snowmelt period provides information on the amount of snow storage in a basin. Stated in the American Society of Civil Engineers (1996), snow density is generally expressed as the ratio of the weight of a unit snow volume to the weight of a unit volume of liquid water. Snow density is usually computed using SWE divided by the snow depth.

2.4 Snow Cover Analysis

In Donald *et al.* (1995), a study that examined areal distribution of snow cover for dominant landcover units, it was stated that the simplest representation of snow cover was one which was uniform with constant depth and complete areal coverage. As mentioned previously, to define the state of a snow cover at a given time, an ADC can be used. ADC summarizes the areal distribution of snow cover within a landcover type. An observed ADC is a point on the snow depletion curve (SDC) since an SDC is a summary plot of observed ADCs. The average snow cover depth or water equivalent in the ADCs, including bare area, is plotted against the percentage of SCA in an SDC plot (Donald *et al.,* 1995).

Average snowpack densities can be assigned with a reasonable degree of confidence, since the variability of snowpack density is considerably less than snow depth variability (Donald *et al.,* 1995). The impact of the SDC on a snow cover estimate varies greatly depending on the variability of the snow depth. With a highly variable snow cover, the SDC will have a higher importance for the snow cover estimate.

The landcover based SDCs in Donald *et al.* (1995) provided a snow cover conceptualization that better approximated the melt of the snow in a watershed than the watershed-wide SDC approach. The snow cover parameters developed for landcover based SDCs are expected to be more stable than those based on watershed-wide SDCs. During periods of partial cover within any of the specified landcover units, the benefits of using landcover based SDCs should be most apparent.

2.5 Application of Remote Sensing for Snow Cover Modelling

Remote Sensing techniques used in snow cover mapping have included surveys by both airborne and spaceborne devices. However, the reduced costs and large coverage areas

make spaceborne remote sensing a more popular choice. Numerous sensors have been used to map snow cover and new models are developed as additional sensors are launched into space. Popular sensors have included the Advanced Very High Resolution Radiometer (AVHRR) sensors that have been used in a large number of National Oceanic and Atmospheric Administration (NOAA) satellites, Synthetic Aperture Radar (SAR) sensors used on the European Remote Sensing (ERS) satellites, and higher resolution sensors offered by modern Landsat satellites.

Snow cover area is the most reliable snowpack parameter that can be obtained from satellite data (Singh and Singh, 2001). Certain properties of snow have been found to be especially useful in identifying and discriminating snow from other surfaces. These properties form the basis for the remote sensing of snow. Snow's importance is well-recognized in remote sensing, with numerous orbiting sensors used to monitor snow cover. Four of the most important sensors are Landsat 5 Thematic Mapper (TM), NOAA-AVHRR, SAR and MODIS. However, models based on different types of sensors can produce estimates that vary greatly from one another. For the purposes of validating or updating modelled SCA, users cannot treat the SCA estimates from different sensors to be equivalent (Caves *et al.,* 1999).

2.5.1 The Properties of Snow Important to Remote Sensing

To properly use remote sensing images in modelling snow, the physical properties of snow and snowmelt must be well understood. In the visible and near-infrared (NIR) regions, freshly fallen snow has a much higher reflectance than other Earth surface materials, such as water, vegetation and soil. This characteristic of fresh snow makes it easy to distinguish from clouds, and can be seen in Figure 2.2. However, snow has a lower reflectance than other materials in the middle IR region. Masters (1997) stated that albedo is the fraction of total incoming radiation that is reflected. The reflectance of snow is dependent on the following factors: size and shape of the snow grains, wavelength,

temperature, depth of snow cover, liquid content of the snow, surface roughness, refreezing, impurity content of the snow, solar elevation, drift effects, and angle of reflectance.

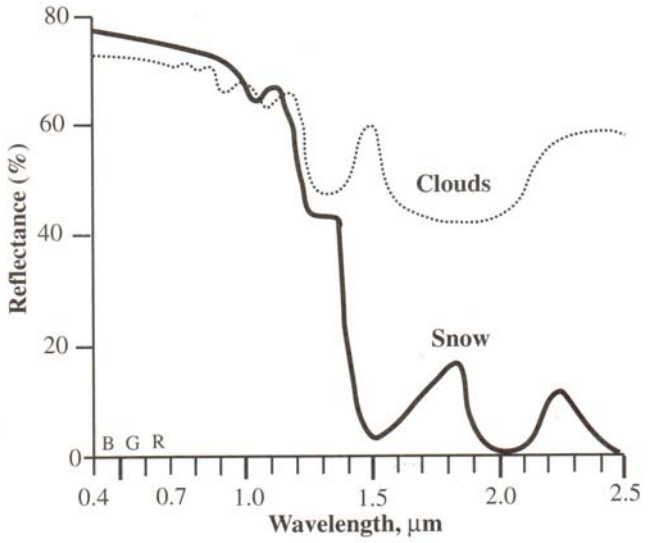

Figure 2.2 Reflectance of Clouds and Snow in the Wavelength Interval 0.4 to 2.5μm from (Jensen, 2000)

Many of these factors are time dependent and will cause the snow reflectance to change as the snow ages. For example, as snowmelts and refreezes the radius of the snow particles will increase and lead to a decrease of the snow reflectance in the NIR band. Also, as the snow remains on the ground for a long period of time, the impurities present in the snow will increase due to accumulation of particles in the atmosphere, such as carbon and dust. This leads aged snow to have a lower reflectance value in the visible region.

The size of a basin being modelled and the temporal resolution required are generally the factors that govern the choice of a sensor (Singh and Singh, 2001). Another factor that affects the choice of a sensor is the spectral bands available from each sensor. Polar

orbiting and geostationary meteorological satellites are found more appropriate for large scale snow-mapping.

2.5.2 Landsat 5 TM

The first Landsat satellite was launched in July 1972. Landsat 5 was launched on July 16th 1982 as a back up for Landsat 4 (personally communication with Dr. Mryka Hall-Beyer, University of Calgary), with the Thematic Mapper (TM) sensor onboard. The TM sensor monitored seven spectral bands in the visible, near, and thermal infrared regions of the electromagnetic spectrum. It has a swath width of 185km, 30m resolution and a repeat coverage interval of 16 days, or every 233 orbits.

Caves *et al.* (1999) stated that Landsat TM with its high resolution is considered to be the best source of Earth observation data for use with snow cover mapping. Automated snow-mapping techniques exist that use the high resolution Landsat TM data to produce snow maps that are comparable in accuracy to maps created using airborne methods, but at lower cost, using less time and covering much larger areas (Rosenthal *et al.,* 1996). It was also found that these techniques are insensitive to factors like snow grain size, level of particulate illumination and variable lighting conditions (Rosenthal *et al.,* 1996). Often, when no ground data exists, TM maps are held to be the closest estimate of the true snow cover area. The major drawback to TM is its long repeat time (Winther *et al.,* 1999).

In a study by Schaper *et al.* (2001), Landsat data was able to improve the runoff modelling accuracy in a high alpine basin by enabling separate evaluation of the snow cover over glaciers and over glacier-free areas for each elevation zone. Specific melt factors of ice and the actual elevation of glaciers within the respective elevation zones were taken into account in this approach. The test selected in the case study was the River Rhône above Sion in the Swiss Alps, with a study area of 3371km^2 and elevation ranging

from 488m to 4634m above sea level. The total area of the glaciers amounts to 580km^2 or 17%. The basin was divided into seven elevation zones to model the runoff. The runoff in high mountain basins was determined by using changing areas of the seasonal snow cover and of the exposed glacier ice throughout the snowmelt season. It was possible to distinguish between snow and ice in Schaper *et al.* (2001), using advanced satellite data processing methods and high spatial resolutions from Landsat. They were also able to periodically determine snow and ice respective areas in each elevation zone. The scenes were classified with multivariate statistics into snow, ice, and snow and glacier-free classes. In order to complement the images in areas obscured by clouds, a GIS analysis of the snow cover units was generated.

2.5.3 NOAA-AVHRR

The United States operates the National Oceanic and Atmospheric Administration (NOAA) satellites, which were first launched in 1979. Each satellite carries the Advanced Very High Resolution Radiometer (AVHRR) sensors. The AVHRR sensor is a four or five channel scanner, depending on the model. It senses in the visible, near-infrared, and thermal infrared portions of the electromagnetic spectrum. It has a swath width of 2399km and orbits 14 times each day around the Earth from a mean altitude of 833km. The repeat coverage interval for this satellite is 12 hours. AVHRR data are available in two formats: Local Area Coverage (LAC) and Global Area Coverage (GAC). LAC data have a spatial resolution of 1.1 km at nadir, while GAC data spatial resolution varies from 1.1km to 4km. These sensors collect daily global data for different land, ocean and atmospheric applications. Specific applications include: vegetation analysis, forest fire detection, weather forecasting and analysis, ocean dynamics research and search and rescue, global sea surface temperature measurements, water resource management, flood defense and SCA determination (Archer *et al.,* 1992).

While the AVHRR sensor provides relatively low resolution data, in Caves *et al.* (1999), Landsat TM data was used to determine that AVHRR actually gave better estimates of SCA than using SAR and could provide for real-time forecasts because of its short repeat time.

Engeset, *et al.* (2003) used AVHRR and SAR derived snow covered area to assess whether operational runoff simulations could be improved. The authors noted that AVHRR data provided better estimates of SCA than SAR data. The HBV model was used to simulate snow reservoirs and snowmelt. Satellite derived SCA was not found to appreciably improve modelling results when used as an independently observed variable but was useful in detecting errors in the model's simulation of the snow reservoirs.

Two different methods with AVHRR data were tested in Johansson *et al.* (2001): (1) a station data with subjective weighting, and (2) an optimal interpolation with an automatic weighting. On average with in the calibration period, the two model set-ups performed equally well with respect to runoff. However, they differed for the melt season for 1999. With no correction of the remote sensing input snowpack value, model (1) estimated the total runoff volume well, while model (2) underestimated the total spring flood runoff volume considerably.

The effect of the remote sensing input was marginal for model (1). There was an improvement for model (2). Two conclusions where made in the study from Johansson *et al*. (2001): (a) when the snowpack is well estimated by the model, remote sensing input has no impact on the forecast runoff. However, remote sensing input can be used as a confirmation of the model estimate. And (b) when the model underestimates the snowpack, remote sensing input could improve snowmelt forecasts, although the original error in the model simulation cannot be completely corrected.

As new satellite data have been available, NOAA snow cover maps have been continually improved. Despite such improvements, these snow cover maps are not available globally and analysts fine-tuning are required. Analysts fine-tuning makes these snow cover maps subjective, and not appropriate for long-term climate studies (Hall *et al.,* 2002). Clouds are also a great hindrance in the usefulness of AVHRR data for SCA analysis (Archer *et al.,* 1992). Significant efforts have been and are still being expended to improve the cloud-discrimination capabilities of AVHRR (Simpson *et al.,* 1997).

2.5.4 SAR

The Synthetic Aperture Radar (SAR) sensor is an active microwave sensor. This instrument is classified as an "active" sensor, because it emits microwave energy to image the Earth's surface. On the other hand, "passive" or "optical" sensors rely on the Sun's reflected energy to image the Earth. Regardless of cloud, haze or smoke over an area, this sensor is capable of imaging the Earth any time of the day. Early airborne SAR and simulated SAR results had suggested that SAR could provide 80% or better classifying results for mapping wet snow in open fields. However, SAR offered much poorer results at the edges of SCA, in heavily forested areas and for dry snow (Donald *et al.,* 1993).

SAR sensors exist onboard several satellites. Two well known ones are on the European Remote Sensing (ERS) satellites and the Canadian RADARSAT satellite. ERS satellites are operated by the European Space Agency (ESA). The first ERS satellite ERS-1 was launched on July 17th 1991, and the second one ERS-2 followed on April 20th 1995. The ERS satellites carries a C-band SAR sensor that has five different modes of operation. The SAR incidence angle is 23º with a swath width of 100km and a spatial resolution of 30m. The satellite's repeat coverage interval ranges from 16 to 35 days. The RADARSAT satellite was launched on November 4th 1995. This sensor can operate in a variety of imaging modes to suit different applications. The RADARSAT satellite is

managed by the Canadian Space Agency (CSA), with RADARSAT International (RSI) of Canada performing data processing and distribution. The SAR sensor has the unique capability to acquire data in any one of the 25 imaging modes. RADARSAT carries a configurable C-band SAR. With respect to swath width, resolution, incidence angle and number of looks, they vary between each mode. The swath width is adjustable from 45 to 500km, with spatial resolutions from 8 to100m, and incidence angle ranging from 20 to 58°. The satellite repeat coverage interval ranges from 4 to 6 days.

From Caves *et al.* (1999), Landsat TM detected much finer spatial detail in comparison with SAR, even though the resolutions of these two sensors are comparable. The SAR method for determining dry snow overestimated quantities at higher elevations but underestimated at lower elevations. Problematic features included high steep ridges, which TM found to be snow free, and shallow or patchy snow-covered areas at lower elevations. These problems resulted in difficulties when comparing snow cover estimates made by SAR-based models to snow-mapping models based on TM data. It is not yet clear how to deal with the differences in SCA derived by TM and ERS SAR. These differences are caused partially by the method used to infer dry snow cover and vary with elevation and time.

2.5.5 MODIS

The Moderate Resolution Imaging Spectroradiometer (MODIS) instrument, launched on December 18th 1999 onboard Terra EOS (Earth Observing System) AM-1, is designed to observe and monitor Earth changes. MODIS has a wide range of spectral bands in the visible and infrared (IR) regions, spatial resolution ranges from 250m to 1000m, and near daily global coverage, making MODIS especially well suited for monitoring global changes. It is the primary tool on the EOS satellites for this purpose. The MODIS instrument is a scanning imaging radiometer with a viewing swath width of 2330km (±55º) by 2030km along track (Hall *et al.*, 2002). Due to the fact that MODIS is a

relatively new sensor, most of its details are not mentioned in literature reviews. Please note that some of the following MODIS information is found on NASA related websites. Most of these resourceful websites are listed in the references and Table 2.1.

Table 2.1 NASA Related Websites Used in Research

Website Title	URL Link	Last Visited
MODIS Home Page	http://modis.gsfc.nasa.gov/	December 15, 2003
National Snow and Ice Data Center	http://nsidc.org/	December 15, 2003
MODIS Land Quality Assessment (QA) Home Page	http://landdb1.nascom.nasa.gov/QA_WWW/newPage.cgi	December 15, 2003
The MODIS Snow/Ice Global Mapping Project	http://modis-snow-ice.gsfc.nasa.gov/intro.html	December 15, 2003
EOS Data Gateway	http://redhook.gsfc.nasa.gov/~imswww/pub/imswelcome/	December 15, 2003

MODIS is a space instrument designed to use the near-infrared (NIR) and IR bands. MODIS has 36 channels: 11 channels in the visible range, 9 in the near-IR range, 6 in the thermal range, 4 in the shortwave-IR (SWIR) range and 6 in the longwave-IR range (LWIR). Channels 1-2's primary use is for Land/Cloud Boundaries while channels 3-7's primary use is for Land/Cloud properties. Spectral properties of the MODIS channels are given in Table 2.2.

MODIS has two channels with 250m spatial resolution, five with 500m resolution and 29 channels with 1000m resolution. The 1000m channels have 10 detectors each; the 500m have 20 detectors; and the 250m channels have 40 detectors. Channels 13 and 14 have

high signal-to-noise (SNR) requirements; hence dual 10-element arrays are used for each. In total, MODIS has 490 detectors.

The MODIS sensor has 36 spectral bands and spatial resolution varies by band from 250m to 1000m. Shown on Table 2.3, the SAR sensor has the finest spatial resolution but is only equipped with one spectral band since it is a microwave sensor. It is not considered reasonable to compare the SAR sensors with the other optical sensors; though, in SCA modelling applications, SAR sensors are also applied. Landsat TM, as mentioned before, gives the most promising results. However, it also has the worst revisit time. The most commonly used sensor for snow-mapping is AVHRR and by contrast it has the fastest revisit time but only offers spatial resolutions of 1.1km or 4km. Comparing to these sensors, MODIS offers both good spatial resolution and fast revisit times. With the large variety of specified spectral bands, MODIS should be a more suitable sensor for mapping daily SCA.

Table 2.2 MODIS Spectral Characteristics (Conboy, 2003)

Channel	Wavelength (µm)	Spectrum	Spectral Radiance (W/m^2 -µm-sr)	Ground Resolution (km)	Primary Use
1	0.620-0.670	visible	21.8	0.25	Land/ Cloud/ Aerosols Boundaries
2	0.841-0.876	near IR	24.7	0.25	
3	0.459-0.479	visible	35.3	0.5	Land/ Cloud/ Aerosols Properties
4	0.545-0.565	visible	29.0	0.5	
5	1.230-1.250	near IR	5.4	0.5	
6	1.628-1.652	near IR	7.3	0.5	
7	2.105-2.155	near IR	1.0	0.5	
8	0.405-0.420	visible	44.9	1	Ocean Color/ Phytoplankon/ Biogeochemistry
9	0.438-0.448	visible	41.9	1	
10	0.483-0.493	visible	32.1	1	
11	0.526-0.536	visible	27.9	1	
12	0.546-0.556	visible	21.0	1	
13	0.662-0.672	visible	9.5	1	
14	0.673-0.683	visible	8.7	1	
15	0.743-0.753	visible	10.2	1	
16	0.862-0.877	near IR	6.2	1	
17	0.890-0.920	near IR	10.0	1	Atmospheric Water Vapour
18	0.931-0.941	near IR	3.6	1	
19	0.915-0.965	near IR	15.0	1	
20	3.660-3.840	thermal IR	0.45(300K)	1	Surface/ Cloud Temperature
21	3.929-3.989	thermal IR	2.38(335K)	1	
22	3.929-3.989	thermal IR	0.67(300K)	1	
23	4.020-4.080	thermal IR	0.79(300K)	1	
24	4.433-4.498	thermal IR	0.17(250K)	1	Atmospheric Temperature
25	4.482-4.549	thermal IR	0.59(275K)	1	
26	1.360-1.390	near IR	6.00	1	Cirrus Clouds Water Vapour
27	6.535-6.895	SWIR	1.16(240K)	1	
28	7.175-7.475	SWIR	2.18(250K)	1	
29	8.400-8.700	SWIR	9.58(300K)	1	Cloud Properties
30	9.580-9.880	SWIR	3.69(250K)	1	Ozone
31	10.780-11.280	LWIR	9.55(300K)	1	Surface/ Cloud Temperature
32	11.770-12.270	LWIR	8.94(300K)	1	
33	13.185-13.485	LWIR	4.52(260K)	1	Cloud Top Altitude
34	13.485-13.785	LWIR	3.76(250K)	1	
35	13.785-14.085	LWIR	3.11(240K)	1	
36	14.085-14.385	LWIR	2.08(220K)	1	

Table 2.3: Specifications of Different Satellite Sensors

Sensor	Number of Spectral Bands	Resolution Range	Repeat Time
TM	7	30m – 120m	16 days
AVHRR	5	1100m – 4000m	12 hours
SAR	1	8m – 100m	4 – 35 days
MODIS	36	250m – 1000m	1.5 days

Relative to the hemispheric-scale snow maps that are available nowadays, the MODIS snow cover maps represent a potential improvement due to its frequent global coverage, moderate spatial resolution and its snow/cloud discrimination capabilities. However, snow cover map accuracy has not yet been established; nor has the existing operational map accuracy (Hall *et al*., 2002). Due to the fact that different sensors use different techniques to map snow cover, and hence, create different products, it is not known which map can be considered the "truth", and thus, the accuracy of these maps is hard to establish.

A brief description of the MODIS snow products is given here to provide a view of the snow product creation process. The first product, MOD10_L2, is a snow cover map at 500m spatial resolution. It is created directly from the results of the algorithm identifying snow and other features in the scene. Geolocation data (latitude and longitude) at 5km resolution is also included in the product. The second product, MOD10L2G, is a multidimensional data set. That means that, pixels are mapped to their geographical data, and can be stacked up as there are data from different dates. MOD10A1, the third product, is a tile of daily snow cover at a 500m spatial resolution. It uses the MOD10L2G product as its basis, selecting the best data based on a scoring algorithm to produce the tile.

The fourth product, MOD10C1, is a geographic map projected daily global snow cover map. It is created by binning the 500m cell observations to the Climate Modelling Grid

(CMG) 0.05° spatial resolution cells and assembling MOD10A1 daily tiles. MOD10A2, the fifth product, is an eight-day snow cover composite, created by compositing anywhere from two to eight days worth of the MOD10A1 product. The sixth and final product, MOD10C2, is an eight day composite of the MOD10A2 product. General summaries of these MODIS snow cover products are presented in Table 2.4.

Table 2.4 Summary of the MODIS Snow Data Products (Riggs *et al.*, 2003)

Earth Science Data Type (ESDT)	Product Level	Nominal Data Array Dimensions	Spatial Resolution	Temporal Resolution	Map Projection
MOD10_L2	L2	1354 km by 2000 km	500m	swath (scene)	None. (lat,lon referenced)
MOD10L2G	L2G	1200km by 1200km	500m	day of multiple coincident swaths	Sinusoidal
MOD10A1	L3	1200km by 1200km	500m	day	Sinusoidal
MOD10A2	L3	1200km by 1200km	500m	eight days	Sinusoidal
MOD10C1	L3	360° by 180° (global)	0.05° by 0.05°	day	Geographic
MOD10C2	L3	360° by 180° (global)	0.05° by 0.05°	eight days	Geographic

The daily Level 3 snow product is constructed by selecting an observation from multiple observations and mapped to cells of the grid by the L2G algorithm (Riggs *et al.,* 2003). Areas at the Equator may be imaged by the sensor every other day, while areas at high latitudes may be imaged multiple times in a single day (Klein et al., 1998c). Hence, the number of observations for a particular cell will vary. A scoring algorithm is set up to

select the observation nearest to nadir with a greatest coverage at the highest solar elevation angle to represent a particular grid cell for the day (Riggs *et al.,* 2003).

This algorithm is based on the solar elevation and location of a pixel. Observations are selected based on the scores they obtain, the observation distance from nadir, area of coverage in a grid cell and the solar elevation. The scoring algorithm is listed in equation [2.3] (Riggs *et al.,* 2003).

$$score = 0.5(\text{solar elevation}) + 0.3(\text{distance from nadir}) + 0.2(\text{observation coverage}) \quad [2.3]$$

The MODIS land products are generated through hierarchy processing levels. Level 2 (L2) products are geophysical parameters retrieved at the same location as the MODIS instrument data. Level 2G (L2G) and Level 3 (L3) are Earth-gridded geophysical parameters, while Level 4 (L4) is Earth-gridded model outputs. The smallest unit of MODIS land data processed is defined as a granule at Level 2, and as a tile at Levels 2G, 3 and 4.

The MODIS land products have undergone processing several times. The best available calibration and geolocation information with the latest available version of the algorithm are applied to the MODIS instrument data. To differentiate between different reprocessing runs, a collection numbering scheme is used. Collection 1 product uses MODIS data sensed from 2000 to early 2001, approximately the first year after Terra was launched. Collection 3 represents reprocessed Collection 1 products and products using MODIS data from November 2000 to December 2002. Collection 4 represents reprocessed collection 1 and 3 products and data sensed from 2000 to present.

There are three levels of product quality for MODIS land products. These are the Beta, Provisional and Validated levels. Beta products are initial release products, and have not been checked thoroughly and may still contain large errors. These products should not be used for any serious conclusions or publications. The Provisional level feature products have undergone checking but may still not be optimal and improvements are still occurring. The Validated level products are well-checked with product uncertainties well-defined over a range of representative conditions. While improvements may still be possible, the data quality is adequate for scientific publications.

There are also three validation stages. Stage 1 products have accuracies estimated with only a small number of independent measurements. Stage 2 validation products have been assessed with numerous independent measurements made over a well-distributed set of locations and time periods. Finally Stage 3 products have had their accuracy assessed via a comprehensive and systematic validation effort that is both statistically robust and representative of global conditions.

2.5.6 MODIS Snowmap Algorithm

The MODIS snow-mapping algorithm "Snowmap" is an efficient and automated algorithm that produces daily global snow maps at 500m resolution using data from MODIS. Being automated, it avoids any subjective influence by human operators. It is important to have a data set that is developed using an objective technique for long-term climate studies (Hall *et al.,* 2002).

In the study of Klein *et al.* (1997), MODIS's cloud screening ability, unique spectral bands and 500m resolutions, offered significant improvement over older satellite sensors. Snowmap uses at-satellite reflectances in the 0.4 to 2.5μm region. The ratio techniques that the MODIS Snowmap algorithm is based on were proven to be successful for both local and regional scales (Hall *et al.,* 2001b).

2.5.6.1 Landsat Derived

Klein *et al,*'s (1998a) work, which was published when the MODIS sensor had not yet been launched, stated that the MODIS snow-mapping algorithm was developed using Landsat TM data. MODIS bands selected for the Snowmap algorithm were largely determined by research with the most comparable TM sensor wavelength data (Hall *et al.,* 1995). This, along with MODIS being able to scan ±55º off-nadir compared to the nadir-viewing Landsat, will lead to inaccuracies as Landsat TM cannot perfectly approximate MODIS (Klein *et al.,* 1998a).

The first proposed MODIS snow-mapping algorithm had two classification criteria (Klein *et al.,* 1998b). The first criterion is that the Normalized Difference Snow Index (NDSI), shown in equation [2.4], has values greater than or equal to 0.40. Compared to most other terrestrial surface features, snow has high reflectance in the visible wavelength and strong absorption in the infrared spectral regions (Figure 2.3). These characteristics make reflectance ratios the key in detecting snow (Riggs and Hall, 2002). NDSI also serves as a snow/cloud discriminator since clouds tend to have high reflectance in both visible and mid-infrared wavelengths (Figure 2.2). The second criterion constrains pixels with a reflectance at 0.9µm (MODIS band 2) so that pixels whose value are greater than 11% are considered as snow. This is used to separate snow against liquid water since water may yield high NDSI values.

$$NDSI = \frac{TM2(0.56\mu m) - TM5(1.65\mu m)}{TM2 + TM5} \qquad [2.4]$$

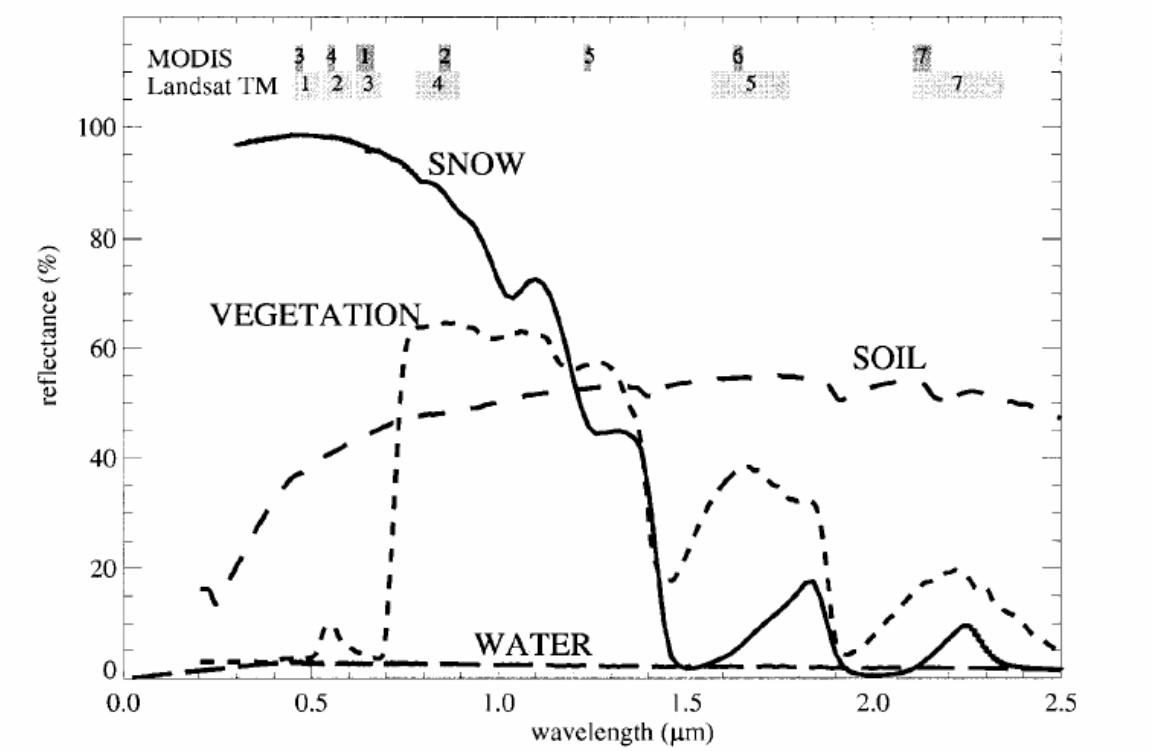

Figure 2.3: General Reflectance Curves for Snow, Soil, Vegetation and Water (Klein *et al.,* 1998b)

2.5.6.2 Snowfield Criteria for Snowmap

As previously mentioned, there are significant differences in the reflectance behavior between snow underneath forest and uncovered snow. To distinguish snow-covered from snow-free conditions underneath a forest stand, the significant changes in the spectral reflectance produced under a forest canopy can be used (Klein *et al.,* 1997). An increase in visible reflectance with respect to the near-infrared reflectance is the most obvious reflectance change (Hall *et al*., 2002). The shortwave infrared (1.6μm) reflectance in some tree species may also decrease. From these changes, a snow-covered forest will have a higher NDSI value than a snow-free forest, but lower than pure snow cover. This small increase may also be too low for Snowmap to classify data as snow.

The studies of Klein *et al.* (1997) and Klein *et al.* (1998b), also stated the Normalized Difference Vegetation Index (NDVI) for a snow-covered forest is lower than that of a snow-free forest. When snow is present, the red reflectance of forest will be closer to its near-infrared reflectance, and tends to lower the NDVI (Hall *et al*., 2002). Klein *et al*. (1998a) has stated the most ideal case for mapping snow in dense forested areas is to have landcover data indicating the location of forested regions and then use separate classification criteria for forested and non-forested areas. However, the ideal approach was not feasible due to the fact that a continuous high resolution global landcover data did not exist at the time of the study.

From pre-launch validation work, the study of Hall *et al.* (2001a) indicated that snow-mapping algorithms work best under conditions of continuous snow cover in short or sparse vegetation areas such as grass and agricultural fields and tundra. It can also map snow cover in dense forests but accuracy suffers. For areas with vegetation density greater than 50%, the algorithm mapped only 71% of snow-covered forested data properly as snow (Klein *et al,* 1998b).

The snow-free and snow-covered NDSI and NDVI values converge as the forest canopy cover increases (Klein *et al.,* 1998b). The proposed snow-mapping algorithm does not account for the seasonal changes that occur in forests. In Klein *et al.* (1997), two additions to the Snowmap algorithm have been proposed. The first addition is an NDSI-NDVI field that can identify snow-covered and snow-free forests better than the proposed algorithm. This field will be used to minimize inclusion of non-forested pixels while capturing as much of the variation in observed NDSI-NDVI values in the snow-covered forests as possible.

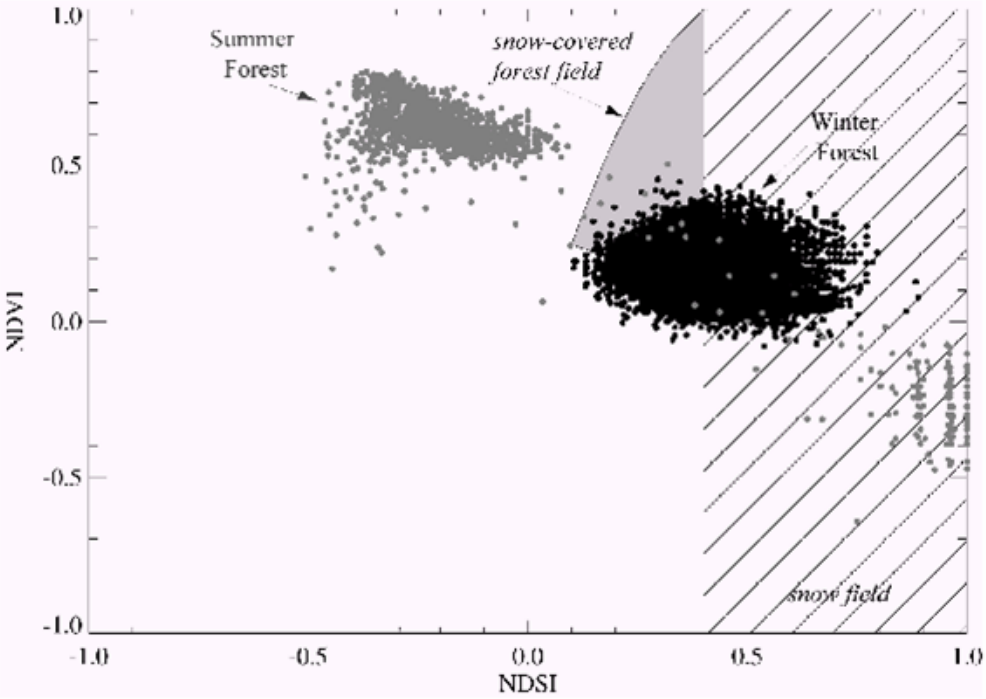

Figure 2.4 NDSI versus NDVI Plot (Klein *et al.*, 1998b)

Figure 2.4 is plotted for coniferous and deciduous forest stands in central Saskatchewan. Gray points are from an August 6th 1990 TM scene and black points are from a February 1994 TM scene. The hatched area contains NDSI values considered to be snow in the original algorithm, while the gray-shaded region represents the new field for capturing snow-covered forests in the enhanced MODIS snow-mapping algorithm (Klein *et al.,* 1998b).

The second possible improvement is to use MODIS band 7 instead of band 6 (Klein *et al.*, 1997). MODIS band 6 was originally selected because of its past use for cloud detection. The NDSI component of the MODIS snow-mapping algorithm filters out most of the clouds effectively except for high clouds (Hall *et al.,* 2002). These clouds contain ice that are often misclassified as snow. In the study of Tait *et al.* (2001), the reflectivity of snow is near zero in the AVHRR channel 3, a (1.58-1.64μm) spectral region. This

band is the key to the MODIS snow-mapping algorithm, and is thus referred to as a cloud/snow discriminator.

However, the study of Klein *et al.* (1997) stated that forest stands have lower NDSI values in MODIS band 6 since the reflectance is much higher for some forest species, especially deciduous species, than snow. There are two drawbacks in using band 7 for NDSI calculations, hence, the MODIS band 7 cannot replace band 6. First, using band 7 data for snow-covered coniferous forests, the modelled NDSI values are much closer to snow-free conditions than using band 6. Second, the original NDSI threshold would require recalculation if band 7 is used.

2.5.6.3 Dark Targets

Another criterion proposed by Klein *et al.* (1997) was a 10% reflectance in the green spectrum (MODIS band 4) being used as a lower limit to prevent forest stands with very low visible reflectances from being classified as snow. For a pixel to be classified as snow, a reflectance in MODIS band 4 greater than or equal to 10% is required. Despite high NDSI values, this prevents dark targets from being classified as snow (Klein *et al.,* 1998b). There is one potential drawback to this kind of visible threshold; snow-covered forests will have a visible reflectance under 10% if they happen to be on a slope facing away from the Sun or shadowed by the surrounding topography. Through personal communication with Dorothy K. Hall, dark targets that were detected in the MODIS snow-mapping algorithm are classified as land.

2.5.6.4 Land/Water Mask

The snow-mapping algorithm is implemented for inland water bodies only; it is not run on ocean waters. The MODIS 1km resolution land/water mask in the MODIS geolocation

product is used to mask large bodies of inland water. In the snow-mapping algorithm, the 1km mask is applied to four corresponding 500m resolution pixels (Hall *et al.*, 2002).

2.5.6.5 Liberal and Conservative Cloud Masks

The discrimination of snow from cloud is a challenging problem in snow-mapping (Riggs and Hall, 2002). There are three reasons why it is necessary to identify cloud. First, cloud obstructs information on what is underneath. Second, cloud usually creates shadow in a basin (Singh and Singh, 2001). Third, in order to improve the accuracy of snow-mapping; cloud has to be identified to avoid misclassification of clouds as snow (Riggs and Hall, 2002). Clouds and snow usually have similar spectral reflectance features and temperatures making discrimination difficult. Thermal wavelengths cannot be used to discriminate clouds from snow, since clouds maybe colder or warmer than the snow surface (Singh and Singh, 2001).

In the first proposed MODIS snow-mapping algorithm, there is only one solution to determine if clouds are present to obscure a pixel. This standard cloud mask uses the "unobstructed field-of-view" flag in the MODIS Cloud Mask product (MOD35_L2) as the cloud criteria to determine if a pixel is cloud-free. Based upon the amount of obstruction of the surface due to clouds and aerosols, the MODIS cloud mask product's main purpose is to identify scenes where land, ocean, and atmosphere products should be retrieved (Strabala, 2003). Following processing paths based on different surface types, geographic location and ancillary data input, the MODIS cloud mask algorithm uses fourteen of the 36 MODIS channels in 18 cloud spectral tests (Riggs and Hall, 2002). The cloud product includes a cloud mask summary flag as well as all the cloud spectral tests applied in the MODIS cloud mask algorithm.

Cloud is set in the snow-mapping algorithm if the summary flag is set to 'certain cloud' (Hall *et al.,* 2002). From observations, the cloud mask algorithm often misclassified snow

pixels as cloud (Riggs *et al.,* 2003). Later a more liberal criterion was proposed. Three tests in the cloud algorithm were available to be used in the snow algorithm to mask clouds where clouds obscured the surface completely and to minimize cloud obscuration over snow (Riggs and Hall, 2002). This liberal criterion has the advantage of still being able to analyze pixels that are obscured by very thin or transparent clouds. Besides the three criteria tests, an additional criterion was also included. A pixel is mapped as cloud if any of the following four liberal cloud-mask criteria is met:

- High cloud test [CO_2 cloud test] (bit 14) is set to cloud;
- Thermal difference test [cloud brightness temperature difference test] (bit 19) is set to cloud;
- Visible reflectance test (bit 20) is set to cloud and band 6 reflectance > 0.20 and that the confidence in the bit 20 test was high;
- NDSI >=0.4 and band 6 reflectance > 0.20.

However, this liberal cloud mask tends to misclassify ice clouds as snow (Riggs *et al*, 2003). Hence, to take advantage of both algorithms, generally the liberal cloud mask is used in winter time and other periods where snow is expected. The standard cloud mask is generally used when snow is not expected such as in the summer.

The standard cloud mask is still the most used cloud mask to create MODIS snow cover products. All Version 3 and earlier versions used this mask to create snow cover data. Only Level 2 data in Version 4 use both standard and liberal cloud masks to create snow cover. The higher level products also continue to use the standard cloud mask.

Another use of the cloud mask is to determine if the area of interest is dark or not. When the area of interest is dark, the snow-mapping algorithm will not be applied. The area of

interest is defined as dark when the solar zenith angle recorded in the cloud mask product is greater than 85°.

2.5.6.6 Thermal Mask

As stated in the study of Hall *et al.* (2002), the introduction of a thermal mask on October 3rd 2001 eliminated most of the spuriously detected snow cover found in earlier MODIS snow maps. Possible causes of these spurious snow cover stated in this study were confusion with cloud cover, aerosol effects and snow-sand on coastlines. A threshold temperature is set to exclude pixels with high ground temperature being classified as snow. This is especially useful in non-snowing areas. In MODIS Version 3, a threshold of 277K was used, while the threshold has changed to 283K in Version 4. MODIS IR bands 31 and 32 were used with a split-window technique to estimate ground temperature (Hall *et al*., 2002). Any pixel having a temperature greater than the threshold will not be classified as snow.

2.5.6.7 Snowmap Versions and Process Periods

A collection of MODIS land data with processing refinements made for algorithm, instrument, and calibration stabilization, is represented by a version number. In this version number, the data will have consistent quality in a continuous time frame. The older versions will still be available to users when a new version becomes available but only for a limited time period until the data are reprocessed.

The Version 1 (V001) snow cover products applied the original, at launch version, algorithms for only a five and a half month period. This period started from mid September to early March of 2001. The Version 2 (V002) products were never produced. The Version 3 (V003) products from 31 October 2000 to 31 December 2002 contain refinements accommodating algorithm, instrument and calibration stabilization.

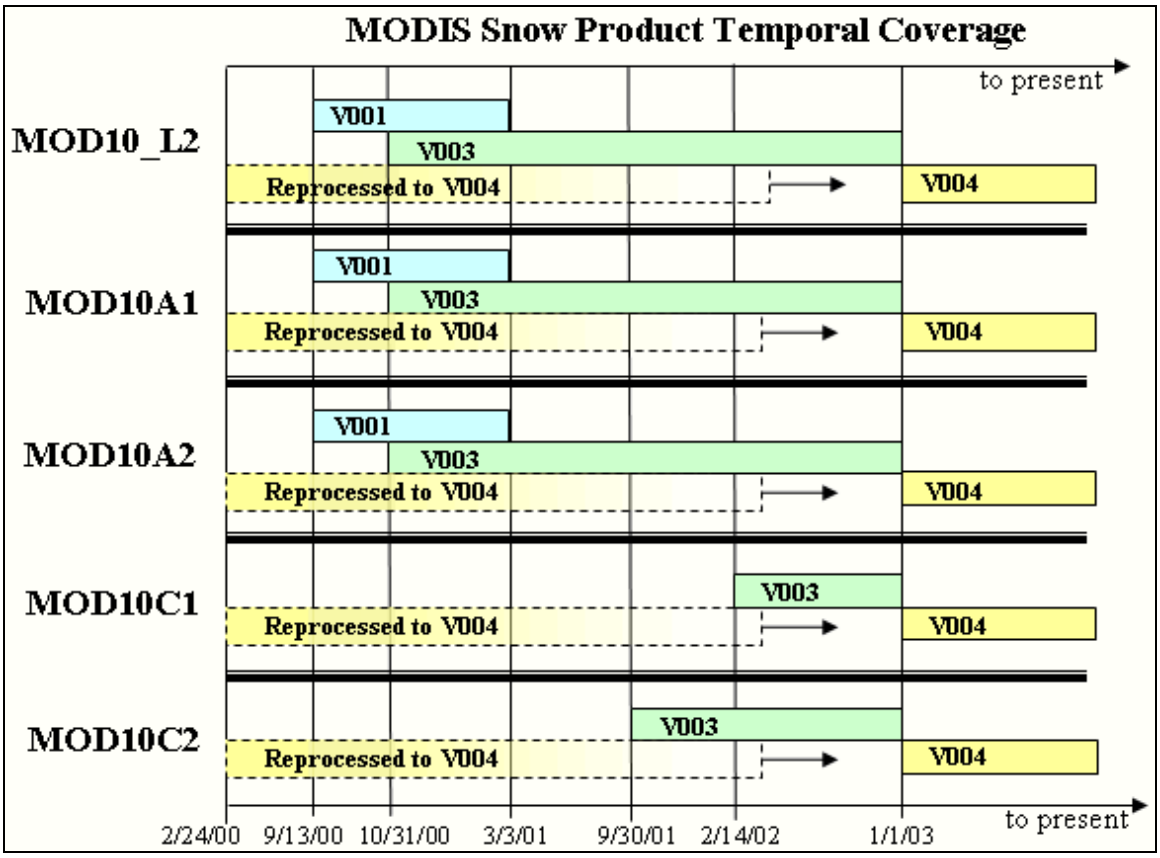

Figure 2.5 MODIS Snow Product Temporal Coverage (Masuoka, 2003)

MODIS Version 4 (V004) products from March of 2000 to present contain major refinements to the algorithms. In this version, the MOD10A1 and MOD10A2 products use a sinusoidal (SIN) grid projection to replace the original Integerized Sinusoidal (ISIN) grid projection. The ISIN is analogous to the Sinusoidal projection except that the ISIN projection is centered about 0° longitude and special coefficients are used to flatten the ellipsoid. Two separate snow cover data generated using two different cloud masks are offered in the MOD10_L2 product. The thermal mask threshold in the snow-mapping algorithm has changed from 277K to 283K. The process periods for different products are presented in Figure 2.5.

The change of projection grid in Version 4 products has two main advantages. First, the sinusoidal grid has less distortion at a pixel level, there are no brick-like shifts between rows, and it has better vendor support. It also resolves nesting problems between different resolution products. However, after testing, it has been found that at finer resolutions such as 250m the mapped coordinate differences between the different grid projections can differ by 75% of a pixel. The differences in 500m resolution range will be 37.5% of a pixel. The shift in 1km resolution is relatively small at 18.7% of a pixel, and can be ignored.

2.5.6.8 Snowmap Version 4 Algorithm

Some important details regarding the Snowmap algorithm used in MODIS snow product processing should be noted. Pixels must satisfy the following criteria:

1) Pixels have nominal Level 1B radiance data;
2) Pixels are on land or inland water;
3) Pixels are in daylight;
4) Pixels are unobstructed by clouds;
5) Pixels have an estimated surface temperature less than 283K.

These criteria are applied in the order listed and will result in only pixels that have daylight clear sky view of land surface being analyzed for snow (Riggs *et al.,* 2003). The automated MODIS snow-mapping algorithm uses at-satellite reflectances in MODIS bands 4 and 6 to calculate the NDSI values (Hall *et al.,* 1995), shown in equation [2.5]. The algorithm also uses MODIS bands 1 and 2 to calculate the NDVI values, shown in equation [2.6], to use with the NDSI values to map snow in dense forests (Klein *et al.,* 1998a).

$$NDSI = \frac{MODIS4(0.545 - 0.565\mu m) - MODIS6(1.628 - 1.652\mu m)}{MODIS4 + MODIS6} \qquad [2.5]$$

$$NDVI = \frac{MODIS2(0.841 - 0.867\mu m) - MODIS1(0.620 - 0.671\mu m)}{MODIS2 + MODIS1} \qquad [2.6]$$

Two groups of tests are performed to detect snow. The first case is to detect snow in many varied conditions. A pixel will be mapped as snow:

1) if NDSI ≥ 0.4;
2) and MODIS band 2 > 11%;
3) and MODIS band 4 ≥ 10%.

The second case will be applied in dense forested areas only. A pixel in dense forested regions will be mapped as snow:

1) if fit in NDSI-NDVI field (Figure 2.6);
2) and MODIS band 2 > 11%;
3) and MODIS band 4 ≥ 10%.

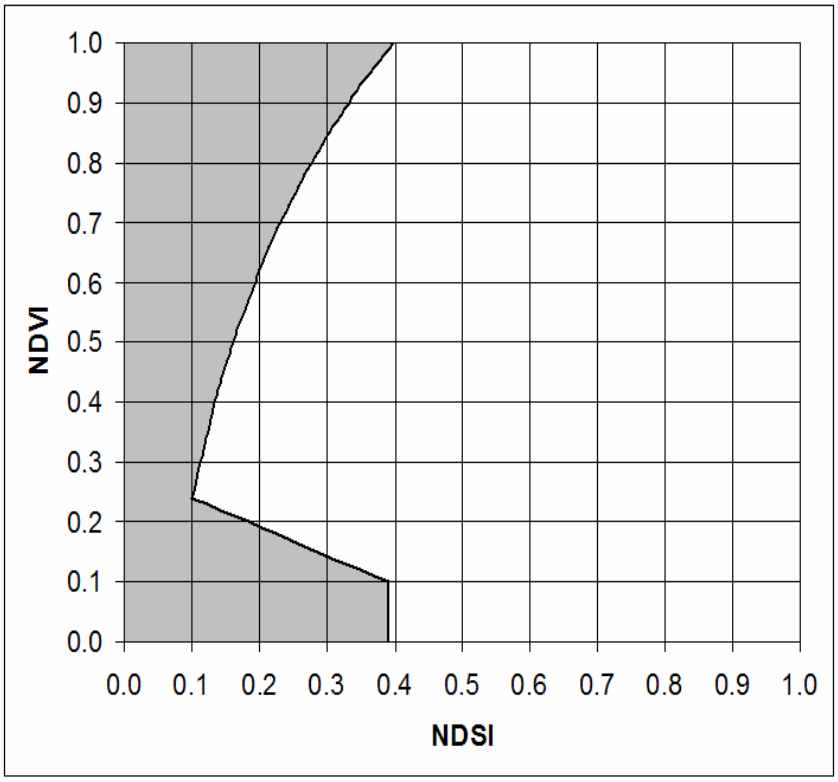

Figure 2.6 NDVI-NDSI Classification Space (Masuoka, 2003)

Figure 2.6 shows the NDVI-NDSI classification space which is also known as the NDSI-NDVI field. Values fall into the white area of this image are mapped as snow. This figure provides greater details regarding how the NDSI-NDVI field works as compared to Figure 2.4. The Version 4 algorithm uses the thermal mask and land/water mask mentioned above. Products at Level 2 use the liberal cloud-mask, while products at Level 3 continue to use the standard cloud-mask. A pixel that is more than 50% snow-covered (of the 500m resolution pixels) will be mapped as snow from the binary MODIS snow-mapping algorithm. MODIS data products used as input for the Version 4 snow-mapping algorithm are listed in Table 2.5.

Table 2.5 Data Product Inputs to MODIS Snow Algorithm (Riggs *et al*., 2003)

ESDT	Long Name	Data Used
MOD02HKM	MODIS Level 1B Calibrated and Geolocated Radiances 5-Min Swath 500m	Reflectances for MODIS bands: 1 (0.645 µm) 2 (0.865 µm) 4 (0.555 µm) 6 (1.640 µm)
MOD021KM	MODIS Level 1B Calibrated Radiance 5-Min Swath 1km	31 (11.28 µm) 32 (12.27 µm)
MOD03	MODIS Level 1A Geolocation Fields 5-Min Swath 1km	Land/Water Mask Solar Zenith Angles Sensor Zenith Angles Latitude Longitude
MOD35_L2	MODIS Level 2 Cloud Mask and Spectral Test Results 5-Min Swath 250m and 1km	Cloud Mask Flag Unobstructed Field of View Flag Various cloud test results Day/Night Flag

In the snow-mapping algorithm, at-satellite reflectances converted from usable level 1B products will be used. When missing data or unusable data from unacceptable quality is present in the level 1B product, it will be noted in the MOD10_L2 product (Riggs *et al.,* 2003). If the reflectance of the data is outside of its theoretical range of 0-100% or the NDSI ratio is outside its theoretical range of -1.0 to +1.0, it will not disqualify these pixels from being tested for snow but will be noted in the MODIS snow products. Despite the wide view angle of ±55º of the MODIS sensor, for the production of snow maps, only data from ±45° will be used (Hall *et al.,* 1995). This is due to the distortion in pixel geometry at angles greater than ±45°.

2.6 Previous Evaluation of MODIS Snowmap Algorithm in Literature

As MODIS was expected to offer improvements for snow-mapping compared to past methods, several studies were performed to determine if differences existed and to quantify improvements. In the study of Gomez-Landesa *et al.* (2001), two snow-mapping methods were compared: a linear combination of visible and near infrared channels and the MODIS Snowmap algorithm based on NDSI and NDVI. The linear combination approach used visible and near infrared albedos. A digital value proportional to the snow cover percent in each pixel of the snow map (Im) is given by the linear combination:

$$\mathrm{Im} = a_1 C_1 + a_2 C_2 \qquad [2.7]$$

where C_1 and C_2 are albedos for channels 1 and 2. The combination coefficients a_1 and a_2 are derived by the following equation:

$$a_1 \begin{pmatrix} S_1 \\ G_1 \end{pmatrix} + a_2 \begin{pmatrix} S_2 \\ G_2 \end{pmatrix} = \begin{pmatrix} 255 \\ 0 \end{pmatrix} \qquad [2.8]$$

where S_1 and S_2 are the snow threshold for channel 1 and channel 2, and G_1 and G_2 are the ground threshold for channel 1 and channel 2. The snow threshold is the minimum value of a pixel to be considered as fully covered by snow, while the ground threshold is the maximum value of a pixel to be considered as bare ground. The snow threshold can be obtained by using snow classification or snow histograms. The ground threshold is obtained through ground classification.

Equation [2.8] imposes 255 as the maximum possible value for pixels fully covered with snow and a minimum possible value of 0 for bare ground pixels. Mixed snow and ground pixels have a grey level proportional to their snow cover ratio, given by:

$$a_1 = 255\left(\frac{G_2}{S_1G_2 - S_2G_1}\right)$$

$$a_2 = 255\left(\frac{G_1}{S_1G_2 - S_2G_1}\right)$$

$$\mathrm{Im} = C_1a_1 + C_2a_2 = 255\left(\frac{C_1G_2 - C_2G_1}{S_1G_2 - S_2G_1}\right) \qquad [2.9]$$

In this study, the same groups of tests mentioned in the Snowmap Version 4 session are used as the MODIS snow-mapping algorithm. In forested areas, the MODIS algorithm has proven to be more accurate than the linear combination approach. It is due to: (1) the normalization of the spectral response of the target associated with NDSI and NDVI indices, and (2) not confusing forest pixels (having low visible albedo) with snow pixels (which have high visible albedo) by the use of a minimum visible albedo for snow.

Bitner *et al.* (2002) compared National Weather Service's National Operational Hydrologic Remote Sensing Center (NOHRSC) determined snow cover maps with MODIS snow products. NOHRSC used optical data only plus a supervised classification technique that required substantial manual interpretation, while the MODIS algorithm is an automated classification technique. The US Department of Agriculture forest canopy density map was also used for NOHRSC. As forest coverage increased, agreement between the two maps decreased. The number of pixels classified by MODIS as snow and classified by NOHRSC as snow-free increased, while the number of pixels classified by MODIS as snow-free but NOHRSC classified as snow, decreased. Bitner *et al.* (2002),

found that MODIS is better at mapping snow edge in forested areas, but NOHRSC produces a more continuous snowpack. This is due to the fact that the NDVI information allows the MODIS algorithm to adjust its threshold for snow-mapping based on the vegetation levels. NOHRSC can produce a more continuous snowpack because human judgment is needed to find the edge of snowpack and adjust the snow threshold level to create a more continuous snowpack. Bitner *et al.* (2002) also believed that for mid-winter conditions, NOHRSC and MODIS should agree.

Maurer *et al.* (2003) also did a comparison of NOHRSC and MODIS, but with an attempt to quantify the improvements offered by MODIS. Maurer looked at a study area in the United States Missouri River and the Columbia River basins over a 32 day and 46 day period, respectively. The Missouri area was primarily grassland, while the Columbia area was mainly forested. Both areas featured high numbers of ground observations. Maurer found that both case study snow cover maps generally agreed with ground observations but MODIS tended to classify fewer pixels as cloud and offered better snowpack edges at higher elevations. For Missouri, MODIS classified 10-13% fewer pixels as cloud while in the more heavily forested Columbia area, MODIS classified 14-17% fewer pixels as clouds. MODIS was also clearly better in classifying snow and snow-free pixels than NOHRSC on both cloudy and clear days.

2.7 Gaps and Limitations in Effectiveness and Implementation of the MODIS Snow Algorithm

Some of the literature reviews have stated drawbacks of the MODIS snow-mapping algorithm from different perspectives as presented in this section. Klein *et al.* (1998a) stated that the MODIS snow-mapping algorithm was developed using Landsat TM. Landsat TM was used to approximate some of the MODIS spectral bands, which will lead to inaccuracies as Landsat TM spectral bands cannot perfectly approximate MODIS spectral bands. The MODIS snow-mapping algorithm uses at-satellite reflectances as

input (Riggs *et al.,* 2003). At-satellite reflectances are also known as top of the atmosphere (TOA) reflectances. Personal communication with Dr. Isabelle Couloigner (University of Calgary) indicated that without atmospheric corrections, reflectances are highly affected by atmosphere components. When low bright clouds and areas with high aerosol contamination occur, the diffuse scattering from these features will lead to false snow detection. Analysis indicates that this is related to atmospheric contamination of band 1 and 4 in top of the atmosphere reflectance data (Masuoka, 2003). In the snow-mapping algorithm TOA reflectance data, these data are not atmospherically corrected. Difficulties in obtaining reliable aerosol characterization over extensive snow and ice surfaces are one of the many reasons why TOA reflectance data is used. TOA reflectances are reduced in all wavelengths in shadowed regions. However, from bright adjacent features such as clouds, the atmospheric scattering will increase reflectance. At shorter wavelengths, atmospheric scattering increases. Hence, this impacts the data from band 1 and 4, increasing NDSI value while reducing NDVI values. This event is most evident over surfaces with high NDVI values, when the NDVI-NDSI classification space is used (Masuoka, 2003).

MODIS is an optical sensor. Therefore, it has inherent limitations in observing snow and sea ice. The visible bands are only useful in daytime when reflectance is significant. The thermal bands are primarily used in the nighttime, when emittance becomes important. The MODIS snow-mapping algorithm in the study of Tait *et al*. (2001), used data from the visible to near-infrared part of the spectrum (0.545-1.652μm). During darkness or when clouds obscure the surface, no snow cover information could be obtained.

A serious limitation in the snow-mapping algorithm occurs in the spring (Klein et al., 1998b). In this period of time, snow lasts longer under canopy compared to clear areas. The algorithm cannot map snow in dense canopy areas or where there is significant amount of leaves on the ground. This results in the largest snow-mapping errors occurring during the spring snowmelt. Another fact the algorithm did not take into

account is the aging of snow. Snow reflectivity is highly sensitive to contaminants in the visible range of the spectrum (Singh and Singh, 2001). As snow ages, the contaminants on the snow increase and this decreases the reflectivity of snow. Another limitation of the MODIS snow-mapping algorithm is that it is a binary algorithm (snow or no snow) with 500m spatial resolution (Hall *et al.,* 2002). This is a major disadvantage to map snow in mountainous areas. This algorithm will map snow cover if approximately 50% of the 500m resolution pixels are snow-covered (Hall *et al.,* 2002).

In the MODIS snow products, rivers are often labeled as snow (Masuoka, 2003). It has been found that at times where the land/water mask does not correctly map inland water bodies, especially the small ones, the snow-mapping algorithm labels water as snow. This is often the case if the water bodies are shallow and contain a lot of sediment. The cloud mask currently used in the MODIS snow and ice algorithms tends to overestimate cloud cover (Hall *et al.,* 2002). In the study of Hall *et al,* (2002), 18% more snow cover is detected when the cloud mask was not employed. The same study also stated that in high elevation ranges, like the Sierra Nevada in California and the Southern Alps of New Zealand, confusion in the classification of cloud over snow has been observed. The use of a thermal mask eliminates most of these falsely detected snow pixels, especially in areas with high NDVI values. However, from Jensen (2000), the split window technique used in the thermal mask is not reliable over land.

2.8 Detailed Thesis Objectives

The first objective of this study is to determine the effectiveness of daily MODIS data for determining snow covered area (SCA) and areal snow depletion in the Canada northern Boreal Forest. With MODIS's fast repeat coverage time, relatively high spatial resolution, and the large selections of snow products, there is interest in determining how much more information can be obtained from this sensor to model snow hydrology. Precise snowmelt periods of each studied year will be determined using different MODIS

snow products. These periods are compared with the periods observed from meteorological data. Snow depletion curves (SDCs) computed using MODIS snow product will also be evaluated against meteorological and streamflow data.

Snow accumulation and melt are significantly affected by differences in landcover. The ideal case for global snow-mapping is to have two different criteria tests for dense and non-densely forested areas. However, due to the fact that a continuous high resolution global landcover data does not exist at this time, the ideal case may be only possible at a local scale. The MODIS snow-mapping algorithm, Snowmap, uses NDSI (Normalized Difference Snow Index) and NDVI (Normalized Difference Vegetation Index) information to determine snow cover in dense forest areas. One of the objectives of this study is to evaluate the MODIS snow-mapping algorithm using 100m resolution landcover data in conjunction with NDSI values. Instead of relying on computed NDVI values to identify vegetation cover for the snow-mapping algorithm, actual landcover data of the study area is used. It is assumed that the landcover distribution of the study area does not change dramatically from year to year.

The last objective of this study is to use the MODIS data in a conventional model of snowmelt to see if modelling is improved. In most conventional models of snowmelt, there is an assumption that the snow cover was uniform with constant depth and continuous areal coverage through out the melting period, until one day when all the snow is gone. However, in reality this is not the case. The aim of using MODIS data is to determine that specific amount of snow present on ground during each melting day. With this information, snowmelt modelling can be improved.

Chapter 3
Study Area and Methodology

3.1 Study Area Description

To test the snow-mapping algorithms, a study area near Thompson, Manitoba was chosen. The presence of boreal forest in this study area offers a large coverage of different vegetation types. Forest canopies in this area represent a challenge for snow-mapping algorithms in detecting snow within the forest. As can be seen in Figure 3.1, the study area is shown by the display of the rivers and lakes present in the area. Due to the irregular shape of the available landcover data, the study area is of the same shape. The outer corners shown on Figure 3.1 are the outer boundary of this study area. The coordinates of this boundary are listed in Table 3.1.

Table 3.1 Outer Boundary Coordinates of the Study Area

Boundary	UTM (zone 14)	Latitude Longitude
Northern	6195825.667N	55º 53’ 7.26”
Southern	6058125.667N	54º 39’ 56.08”
Western	352725.365E	-101º 21’ 16.8”
Eastern	570425.365E	-97º 54’ 29.17”

The total area enclosed by the outer boundary is 29,977.29km^2. The irregular shape study area is 18,308.81km^2. The area outside of the irregular shape study area and inside the outer boundary is 11,668.48km^2. The sum area of rivers and lakes present in this area is 1,857.06km^2. Without considering water bodies, lakes and rivers in this study, the actual study area is 16,451.75km^2. The study area is quite flat, as the study area’s elevation ranges from 186.8m to 366.8m above sea level over a distance of 184km. The largest grade change in this area is 0.3%.

There are two watersheds in this study area: the Upper Burntwood River watershed and the Taylor River watershed. In Figure 3.1 the Upper Burntwood River watershed is highlighted in pink, while the Taylor River watershed is highlighted in green. These two watersheds are located west of the City of Thompson in northern Manitoba.

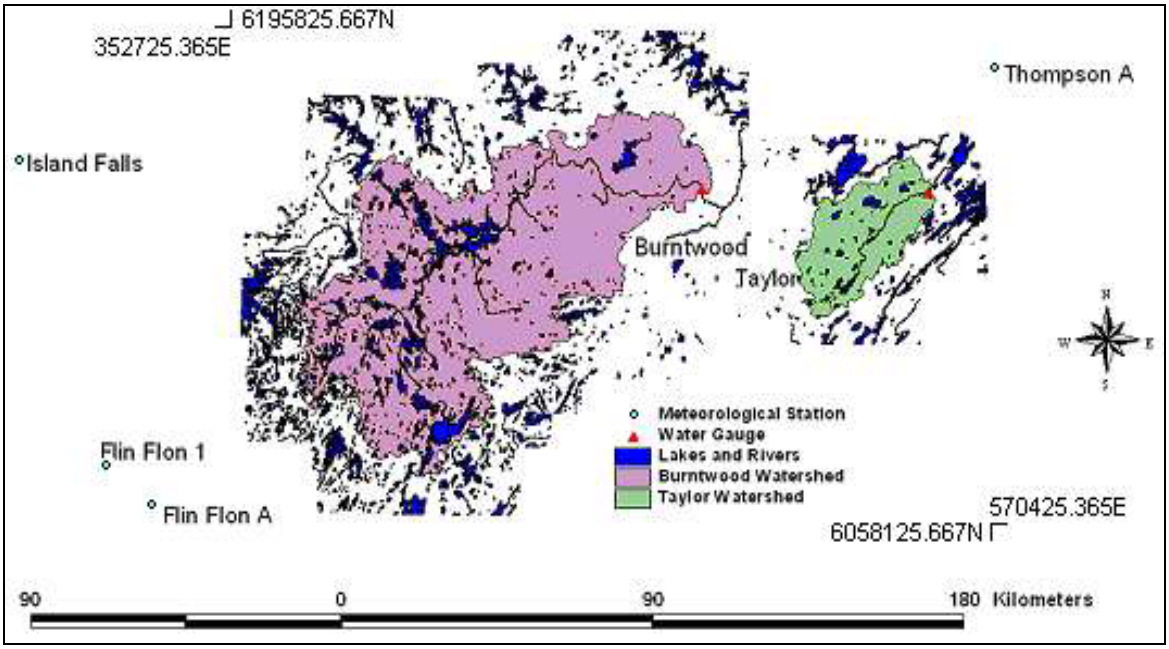

Figure 3.1 The Study Area with Water Gauges and Metrological Stations

The Burntwood River watershed has a computed area of 5,821km^2, with elevation ranging from 251.2m to 366.7m above sea level and with grade change less than 1%. The water gauge that measures the streamflow rates of this watershed is called the "Burntwood River Above Leaf Rapids". The Taylor River watershed has a computed area of 936km^2. The elevation in this area ranges between 191.2m to 271.2m above sea level, with grade change less than 1%. The water gauge that measures the streamflow rate of this watershed is called the "Taylor River Near Thompson". As can been seen in Figure 3.1, the Upper Burntwood River watershed contains a large amount of lake storage as compared to the Taylor River watershed.

3.2 Methodology

In order to evaluate the MODIS snow-mapping algorithm, three different test algorithms have been set up. Results were compared against each other and with the MODIS snow products. Meteorological and streamflow data have been obtained to evaluate the effectiveness of daily MODIS data for determining SCA and areal snow depletion in the northern Boreal Forest.

3.2.1 Development of Test Algorithms

Three algorithms were developed in relation to the Snowmap algorithm. These all are developed using the MODIS daily surface reflectance data (MOD09) as input. The first algorithm was developed using the generic Snowmap algorithm. The same thresholds of the Snowmap algorithm stated from literature reviews were applied, and calculated NDSI and NDVI values were used to determine snow cover in a dense forested area. This algorithm is henceforth called the "*Simulated Snowmap*" algorithm. The second algorithm uses the same thresholds as the original Snowmap algorithm but substitutes landcover data for the NDVI values used in the Simulated Snowmap algorithm. This algorithm is called the "*LandSnow*" algorithm. The third algorithm uses new arbitrary thresholds of the Snowmap algorithm with NDSI values and landcover data. This algorithm is called the "*Land-based Snow-mapping*" algorithm (LBSM). All test algorithm derived SDCs are compared against each other and with the MODIS Version 4 daily snow product (MOD10A1).

3.2.2 Case Study Analysis

Case study comparisons between MOD10A1 Version 3 and Version 4 products have been carried out for year 2001 and 2002 to evaluate the differences that exist between the two versions. With the MODIS daily snow cover data, snow depletion curves (SDCs) of

the boreal forest area in northern Manitoba have been produced and compared with the SDCs produced from the different test algorithms. Spatial agreement between the snow cover detected by the MOD10A1 product and the test algorithms were analyzed

Local watershed SDCs were produced using the LBSM algorithm and MOD10A1 products. The derived SCAs values were applied in the Temperature Index Method to determine if runoff modelling is improved. Analyses between the meteorological and the generated SCAs have also been carried out to evaluate the accuracy of the results. The derived SCAs and accumulated degree-days were plotted against each other to determine the degree of correlation. Elevation analysis has been carried out to discover the SCA and accumulated degree-days relationship at different elevation ranges.

3.3 Database Construction and Data Pre-processing

A database has been constructed containing MODIS imagery. Imagery includes the MODIS surface reflectance (MOD09) products, and MODIS snow (MOD10) products. MODIS snow data products are used to verify the three test algorithms. Other spatial data stored in the database are landcover and elevation data. Temporal data collected for this study included meteorological and streamflow data. These data were used to verify SDCs calculated using the MODIS snow products and results of the test algorithms.

3.3.1 MODIS Imagery

In this study, four types of MODIS imagery products are obtained. MODIS products can be assessed and obtained through the use of the Earth Observing System Data Gateway, also referred as EOS Data Gateway (EDG). There are a total of 44 standard MODIS data products, which are separated by type, spatial resolution and temporal resolution. These products are distributed through the Distributed Active Archive Centers (DAACs). These centers are part of the Earth Observation System Data and Information System

(EOSDIS), which utilizes the EOSDIS Core System (ECS) for data management across the DAACs and EDG (Hall *et al.,* 2002).

There is a total of eight NASA DAACs (Hall *et al.*, 2002). The following DAACs were accessed in order to obtain the MODIS data products for this study: National Snow and Ice Data Center DAAC (NSIDC DAAC), Land Processes DAAC (LP DAAC), and Goddard Earth Sciences DAAC (GES DAAC). All DAACs are part of the NASA's Earth Observing System Data and Information System (EOSDIS). All MODIS data within the EOSDIS can be searched and ordered through the EDG.

Table 3.2 MODIS Products Used in This Study

Granule Shortname	Long Name
MOD09GQK	MODIS/TERRA Surface Reflectance Daily L2G Global 250m SIN Grid V004
MOD09GHK	MODIS/TERRA Surface Reflectance Daily L2G Global 500m SIN Grid V004
MOD10A1	MODIS/TERRA Snow Cover Daily L3 Global 500m ISIN Grid V003 and MODIS/TERRA Snow Cover Daily L3 Global 500m SIN Grid V004
MOD10A2	MODIS/TERRA Snow Cover 8-Day L3 Global 500m SIN Grid V004

MODIS 250m daily surface reflectance product, MOD09GQK, is a two band product. Data from bands 3 to 7 are not included in this product. It is computed using MODIS level 1B band 1 and 2. MODIS 500m daily surface reflectance product, MOD09GHK, is a seven band product. It is computed using MODIS level 1B land bands 1 to 7. In both products, all bands are stored in 16-bit integer with a scale factor of 10000. These two products are also known as the MODIS level 2 land surface reflectance product, MOD09L2. They are selected as inputs for the criteria set algorithms because they are atmospherically corrected surface reflectance estimates. The scattering or absorption

effects of atmospheric gases (water, vapour, and ozone), aerosols and thin cirrus clouds have been corrected.

Starting with Version 3, the MOD09L2 product generates its own aerosol optical depth product, and uses this product for aerosol correction. Besides thin cirrus clouds, other types of cloud correction are not performed so cloudy pixels are not eliminated. The MOD09L2 products have quality assurance data at three different levels of detail: at the level of the individual pixel, at the level of each band and each resolution, and at the level of the whole file. MODIS channel 1 and 2 surface reflectances were extracted from MOD09GQK products. And channel 4 and 6 surface reflectances were extracted from MOD09GHK products. In this study, only Version 4 MOD09 products were used.

As mentioned before in Chapter 2, the MOD10A1 product contains tiles of daily snow cover at a 500m spatial resolution. It uses the MOD10L2G product as its basis, selecting the best data based on a scoring algorithm to produce the tile. MOD10A1 products are used to verify the results from the test snow-mapping algorithms. MOD10A1 Version 3 and Version 4 products during the study periods have been downloaded for this study. Daily tile snow cover data were extracted from MOD10A1 products.

The MOD10A2 product is an eight-day snow cover composite, created by compositing anywhere from two to eight days worth of the MOD10A1 product. In this study the MOD10A2 product is used to determine the snowmelt period in each year. Images from this product for year 2001 and 2002 are presented in Appendix A. For unknown reasons, the lake areas are classified as land in some of the MOD10A2 products. Only Version 4 MOD10A2 products were used in this study. Maximum snow extent data were extracted from MOD10A2 products. The key codes for the MOD10A1 and MOD10A2 products are presented in Table 3.3.

Table 3.3 MOD10A1 and MOD10A2 Product Key Code

Code	Description	MOD10A1	MOD10A2
254	non-production mask	**X**	
200	snow	**X**	**X**
100	lake ice	**X**	**X**
50	cloud obscured	**X**	**X**
39	ocean	**X**	**X**
37	inland water	**X**	**X**
25	land	**X**	**X**
11	night	**X**	**X**
4	erroneous data		**X**
3	beyond 45deg scan		**X**
1	no decision	**X**	**X**
0	missing data	**X**	**X**

3.3.2 Landcover Data

In order to evaluate the MODIS snow-mapping algorithm in dense forested areas in this thesis, landcover data were been obtained to replace the use of the NDSI-NDVI field from Snowmap. The landcover data used in this study has a total of 36 vegetation classes, without considering the vegetation site, cutting class and crown closure conditions. These classes are separated by the vegetation species and the ratio between different species in the considered amount of area. Overall the vegetation classes can be aggregated into five different types: coniferous trees, deciduous trees, mixed trees, muskeg and treed rock.

Table 3.4 and Table 3.5 present the different vegetation and non-vegetation classes along with their cover class codes for this study. All these classes are shown in Figure 3.2 separated into general types: coniferous forest, deciduous forest, mixed forest, muskeg, treek rock/impervious, lakes/river, and marsh/beaver flood. The percent coverage of each vegetation and non-vegetation class for the study area and the two watersheds are presented in Table 3.6 and Table 3.7, respectively. Table 3.8 presents the percentage coverage of specific vegetation types.

As can been seen from Figure 3.2, muskeg is the most common type of vegetation coverage in the northern Manitoba Boreal forest. Muskeg is also referred to as bogland, organic terrain, or peatland (St. Laurent, 2003). Explanation from the landcover data catalogue has stated muskeg areas in this data are at least ten percent covered by trees. Figure 3.3 shows a spruce bog sample plot located in the Ontario's northern Boreal Forest.

From Table 3.6, Black Spruce is the predominant tree species in the study area. This kind of tree grows in muskeg, bogs, covered sites with drier lichen, and rock outcrops (St. Laurent, 2003). The Boreal forest in Manitoba is characterized by well distributed homogenous stands of Black Spruce, Jack Pine, White Birch and Trembling Aspen (McKnight, 1993). These forest tree heights vary from stunted Black Spruce in bog areas to as tall as 15m. The undergrowth of the forest consists of a layer of deciduous shrubs overtop of a thick later of sphagnum moss and lichens (McKnight, 1993). As can been seen in Table 3.8, the study area has mainly coniferous trees and a small amount of deciduous trees. Vegetation coverage in the study area and in the two watersheds exceeds 80% of the total land coverage.

Table 3.4 Landcover Vegetation Classes

Cover Class Code	Subtype	Vegetation Type
4	Jack Pine 71-100%	Coniferous
6	Jack Pine 40-70% / Spruce	Coniferous
10	White Spruce 71-100%	Coniferous
11	White Spruce 40-70% / Jack Pine	Coniferous
13	Black Spruce 71-100%	Coniferous
14	Black Spruce 40-70% / Jack Pine	Coniferous
15	Black Spruce 40-70% / Balsam Fir	Coniferous
16	Black Spruce 40-70% / Tamarack Larch	Coniferous
21	Balsam Fir 40-70% / Spruce	Coniferous
30	Tamarack Larch 71-100%	Deciduous
31	Tamarack Larch 40-70% / Spruce	Deciduous
44	Jack Pine 51% / Hardwood	Coniferous
46	Jack Pine 50%or less / Spruce / Hardwood	Coniferous
50	White Spruce 51%+ / Hardwood	Coniferous
51	White Spruce 50%or less / Balsam Fir	Coniferous
53	Black Spruce 51%+ / Hardwood	Coniferous
54	Black Spruce 50%or less / Jack Pine / Hardwood	Coniferous
58	Black Spruce 50%or less / White Spruce / Hardwood	Coniferous
60	Balsam Fir 51%+ / Hardwood	Coniferous
61	Balsam Fir 50%or less / Spruce / Hardwood	Coniferous
81	Trembling Aspen / Jack Pine	Mixed
82	Trembline Aspen / Spruce or Balsam Fir	Mixed
86	White Birch / Jack Pine	Mixed
87	White Birch / Spruce or Balsam Fir	Mixed
88	Balsam Poplar / Softwood	Deciduous
90	Trembling Aspen	Deciduous
91	Trembling Aspen less than 50% / White Birch	Deciduous
92	White Birch	Deciduous
98	Balsam Poplar	Deciduous
701	Black Spruce Treed Muskeg	Muskeg
702	Tamarack Larch Treed Muskeg	Muskeg
711	Jack Pine Treed Rock	Treed Rock
712	Black Spruce Treed Rock	Treed Rock
713	Hardwood Treed Rock	Deciduous
721	Willow	Deciduous
722	Alder	Deciduous

Table 3.5 Landcover Non-Vegetation Classes

Cover Class Code	Subtype
731	Recreational sites
732	Small Islands
801	Barrens - Tundra
802	Bare Rock - Igneous
815	Land clearing in progress
816	Abandoned cultivated land
821	Dry Upland Ridge Prairie
822	Moist Pairie
823	Wet Meadow
830	Marsh - Muskeg
831	Muskeg
832	String Bogs
835	Marsh
838	Mud / Salt Flats
839	Sand Beaches
841	Townsites / Residental Sites
842	Airstrips
843	Roads / Railroads
844	Transmission lines / Piplines
845	Gravel Pits / Mine sites
847	Drainage Ditches
848	Beaver Flood
849	Dugouts / Water holes
900	Water
901	Rivers

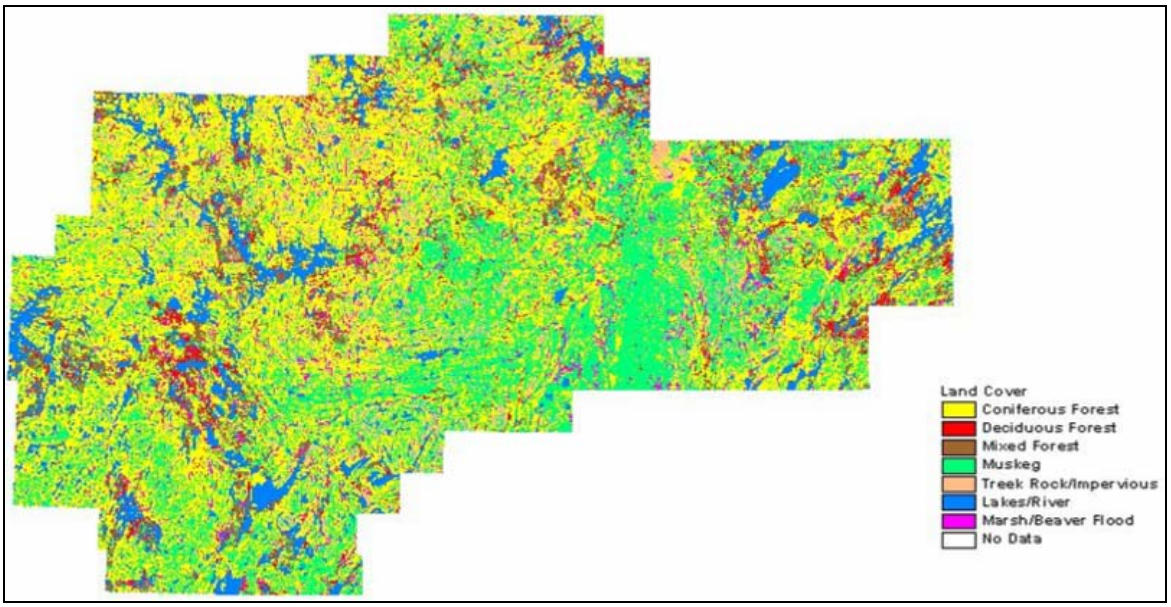

Figure 3.2 Landcover in the Study Area

Figure 3.3 Spruce Bog Sample Plot (Wildlands League, 2002)

Table 3.6 Percent Coverage of Vegetation Classes

Cover Class Code	Percent Coverage (%)		
	Study Area	Burntwood River Watershed	Taylor River Watershed
4	3.6438	4.8162	1.7110
6	12.8857	16.3629	5.9199
10	0.0066	0.0084	0.0000
11	0.2300	0.2211	0.0687
13	11.5926	9.6639	18.6422
14	13.2681	13.7767	10.9135
15	0.9966	1.2546	0.0885
16	0.4644	0.4084	0.2134
21	0.0028	0.0086	0.0000
30	0.0084	0.0028	0.0000
31	0.0562	0.0384	0.0989
44	1.0767	1.7180	1.2968
46	1.5141	1.7938	2.1596
50	0.0288	0.0279	0.0021
51	0.1637	0.1711	0.0760
53	0.6965	0.6258	0.6401
54	0.9601	0.7880	1.3259
58	0.2039	0.1650	0.0448
60	0.0021	0.0016	0.0000
61	0.0056	0.0036	0.0000
81	1.4834	1.9752	2.1325
82	1.9122	2.1471	2.3292
86	0.0042	0.0000	0.0000
87	0.0037	0.0008	0.0062
88	0.0109	0.0016	0.0000
90	0.8444	0.8175	0.4121
91	0.0022	0.0008	0.0000
92	0.0140	0.0008	0.0052
98	0.0016	0.0013	0.0031
701	22.3362	18.7133	27.5189
702	3.1086	2.4242	3.7155
711	5.4653	5.7490	4.4295
712	0.1075	0.1314	0.0000
713	0.0041	0.0124	0.0000
721	0.4562	0.4489	1.2562
722	0.0022	0.0000	0.0427

.

Table 3.7 Percent Coverage of Non-Vegetation Classes

Cover Class Code	Percent Coverage (%)		
	Overall Study Area	Burntwood River Watershed	Taylor River Watershed
731	0.0001	0.0000	0.0000
732	0.0569	0.0453	0.0156
801	0.0005	0.0000	0.0000
802	0.0187	0.0000	0.0510
815	0.0026	0.0007	0.0052
816	0.0003	0.0000	0.0000
821	0.0005	0.0010	0.0000
822	0.0035	0.0000	0.0000
823	0.0086	0.0000	0.0000
830	0.0042	0.0000	0.0000
831	1.3904	1.3167	1.0886
832	0.0171	0.0000	0.0146
835	0.1819	0.1469	0.1072
838	0.0015	0.0000	0.0000
839	0.0009	0.0000	0.0000
841	0.0302	0.0021	0.0000
842	0.0001	0.0000	0.0000
843	0.0877	0.0167	0.2040
844	0.0517	0.0445	0.0905
845	0.0942	0.0036	0.5724
847	0.0047	0.0000	0.0229
848	4.3356	4.5328	7.4977
849	0.0009	0.0000	0.0000
900	9.4893	9.0240	5.0810
901	0.6537	0.5843	0.1967

Table 3.8 Percent Coverage of Vegetation Type

Vegetation Type	Percent Coverage (%)		
	Overall Study Area	Burntwood River Watershed	Taylor River Watershed
Coniferous	47.7	51.8	43.1
Deciduous	1.4	1.3	1.8
Mixed	3.4	4.1	4.5
Muskeg	25.4	21.1	31.2
Treed Rock	5.6	5.9	4.4

3.3.3 Elevation

Besides vegetation coverage, the elevation range of an area will also affect the snowmelt rate. As mentioned before, the study area is relatively flat, with grade changes of less than 1%. The elevation ranges from 186.8m to 366.8m. The Burntwood River watershed elevation ranges from 251.2m to 366.7m above sea level. The Taylor River watershed has elevations that range between 191.2m and 271.2m above sea level.

The elevation data set is obtained by stitching the Burntwood River and Taylor River watersheds DEM (digital Elevation Model) data file together. As shown in the following image, the area and shape of the elevation data is different from the study area and landcover area. When the elevation data was applied in the analysis, only areas that overlap with the study area were considered.

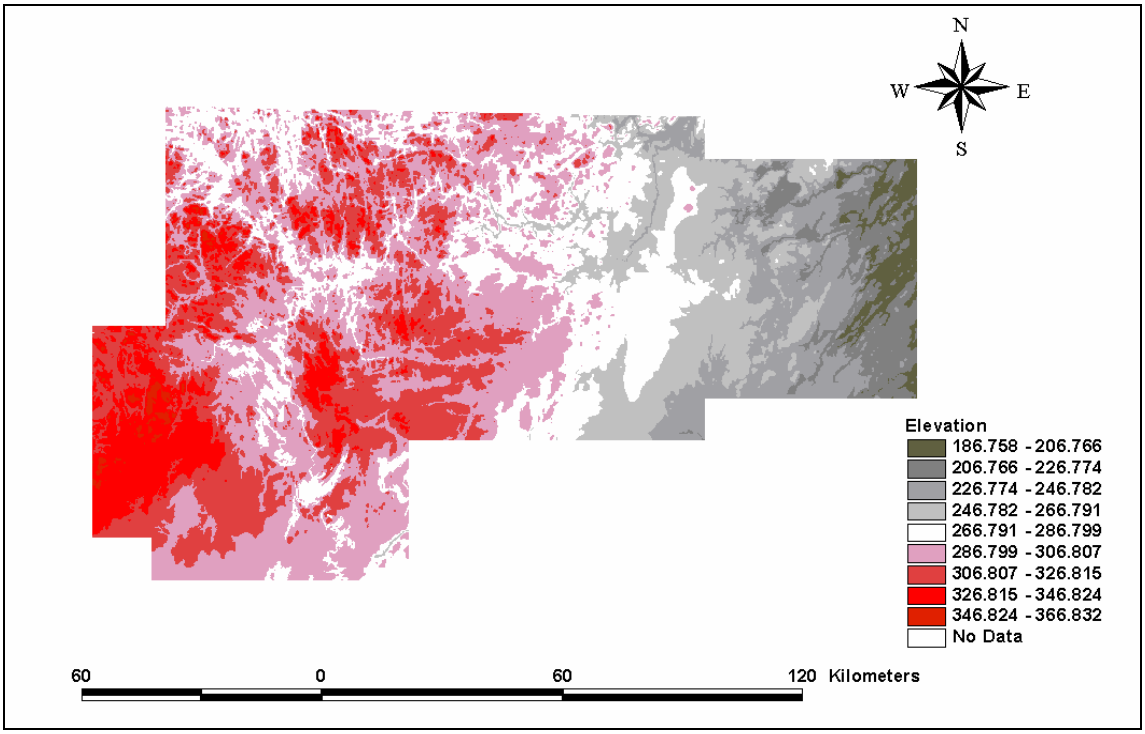

Figure 3.4 Elevation Range in the Study Area

3.3.4 Meteorological Data

In the study of Buttle *et al.* (2000), the climate in northern Manitoba is classified as typical subarctic. A brief description of this climate is summers with very high temperatures followed by long winters with very low temperatures. Meteorological data have been recorded at the Thompson Airport meteorological gauge (55º48' N; 97º52'W) and normal climate attributes from this gauge have been published from year 1961 to year 1990 (St. Laurent, 2003). January was selected as the coolest month of the year, while July is the warmest month of the year from this 30-year period data set. January experiences daily maximums of –19.5ºC, an average daily temperature of -25ºC, and daily minimum of –30.6ºC. While July experiences maximum daily temperatures of 22.6ºC, an average daily temperature of 15.7ºC, and daily minimum temperatures of 8.8ºC (Environment Canada, 1993).

The driest month of the year is February and the wettest month of the year is July. Normal precipitation data shows that February experiences on average only 13.9mm of total precipitation, typically in the form of snow. On the other hand, July experiences an average monthly rainfall of 84.3mm and no snowfall (Environment Canada, 1993). On an annual basis, the study area experiences an average precipitation total of 535.6mm, with snowfall accounting for 200.9cm and a rainfall total of 351.6mm (Environment Canada, 1993). Snow accounts for 33% of the total annual precipitation, while approximately 44% of the annual precipitation occurs during the summer months (June, July and August). Relative to other months, November on average receives the most snowfall (Environment Canada, 1993).

Environment Canada meteorological data will be used to verify results obtained from the MODIS data in this thesis. These data include: daily maximum, mean and minimum temperature, daily precipitation, rain and some with snow survey measurements. Four

meteorological stations near the study area have been selected. These stations with their station ID and coordinate information are presented in Table 3.9.

Table 3.9 Meteorological Stations (Environmental Canada, 2003)

Station	ID	Latitude	Longitude
Flin Flon 1	5050919	54º 46’	-101º 53’
Flin Flon A	5050960	54º 41’	-101º 41’
Island Falls	4063560	55º 32’	-102º 21’
Thompson A	5062922	55º 48’	-97º 52

In order to obtain average meteorological values to represent the whole study area, meteorological values from the four selected stations were averaged. The averaged results of September 21st 2000 to May 8th 2001 have been plotted in Figure 3.5, and results of September 21st 2001 to June 2nd 2002 are presented in and Figure 3.6. For year 2003, only three meteorological stations were available. They are the Flin Flon A, Island Falls and Thompson A stations. Averaged meteorological values from these three stations from September 26th 2002 to May 21st 2003 have been plotted in Figure 3.7.

As shown in Figure 3.5, the daily minimum of -38.8ºC for the plotted period was experienced on February 10th 2001. This period experienced a total of 140.45cm of snow and 28.85mm of rain. In Figure 3.6, a daily minimum of -42.65ºC was experienced on January 28th 2002. A total of 150.46cm snow and 53.13mm rain was calculated during the plotted time frame. During the plotted period of September 26th 2002 to May 21st 2003, the daily minimum of -41.3ºC was experienced on March 2nd 2003. The amount of accumulated snow and rain during this period was 100.23cm and 33.77mm, respectively.

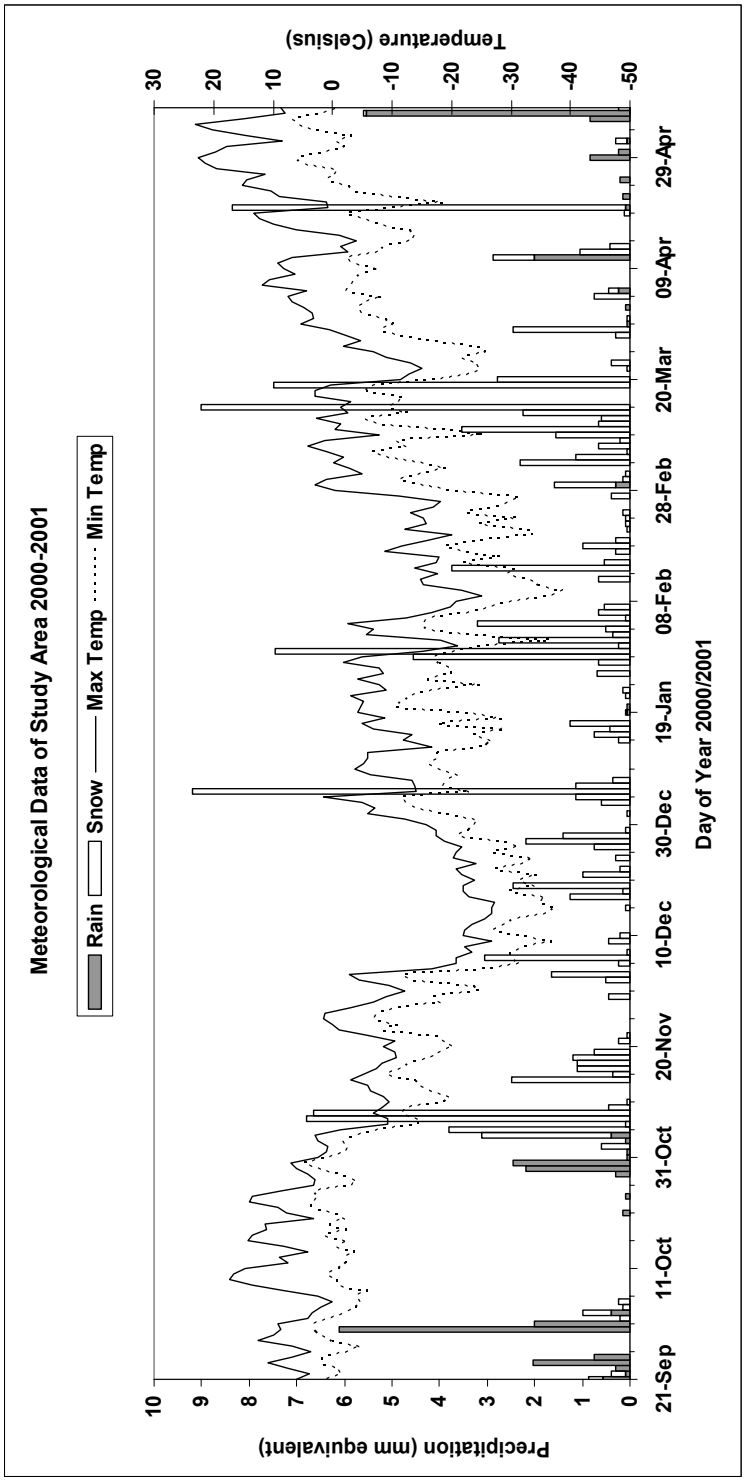

Figure 3.5 Meteorological Data of Year 2000-2001

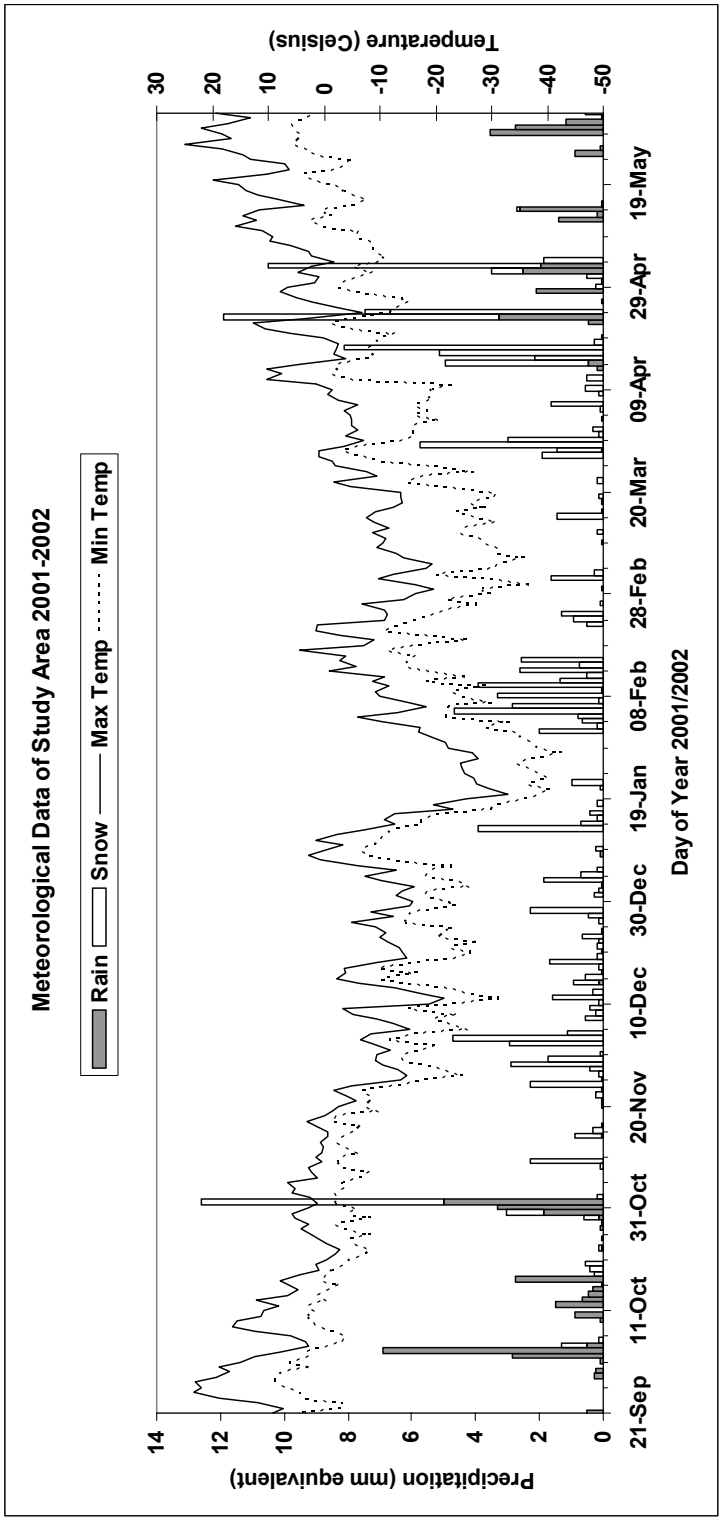

Figure 3.6 Meteorological Data of Year 2001-2002

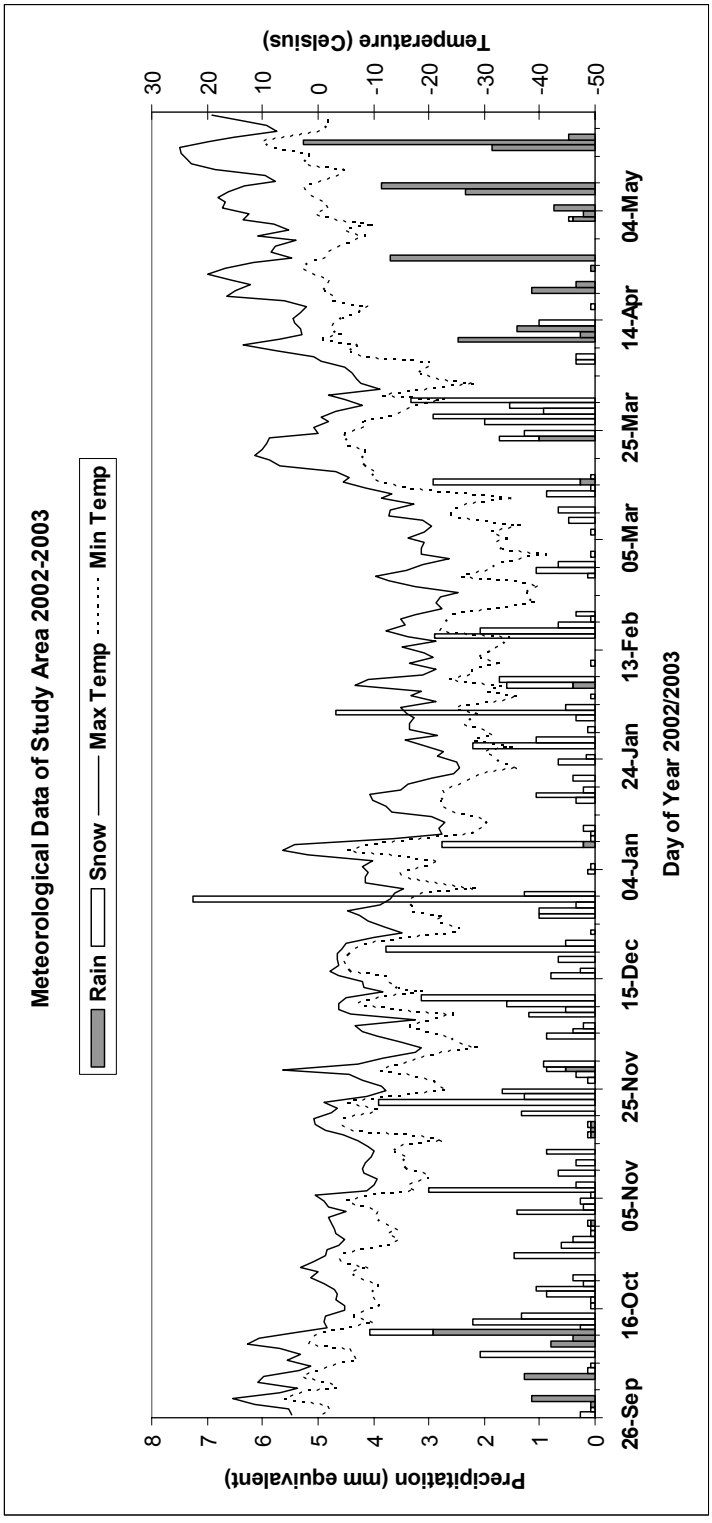

Figure 3.7 Meteorological Data of Year 2002-2003

3.3.5 Stream Flow Data

Streamflow data for year 2000 to 2002 have been obtained from the Water Survey of Canada (WSC). Two water gauges, Burntwood River Above Leaf Rapids and Taylor River Near Thompson, in the study area have been selected to provide streamflow rates for the Burntwood River and Taylor River watersheds, respectively. The station number for the Burntwood River Above Leaf Rapids water gauge is 05TE002. As indicated by the WSC, this instrument gauges an area of 5260km^2, and is located at 55º 30' 0" latitude and -99º 13' 20" longitude. The station number for the Taylor River Near Thompson water gauge is 05TG002. This instrument gauges an area of 883km^2, and is located 55º 29' 20" latitude and -98º 11'10" longitude.

The Burntwood River and Taylor River watersheds daily mean discharge and cumulated discharge from September 21st to August 31st of year 2000 to 2001, and year 2001 to 2002 have been plotted in Figure 3.8 and Figure 3.9, respectively. As shown in these figures, in year 2001 the daily mean discharge of the Burntwood River watershed started to increase on April 22nd while the Taylor River watershed started increasing on April 25th. In year 2002, the daily discharge of the Burntwood River watershed started to increase on May 8th and the Taylor River watershed started on May 11th.

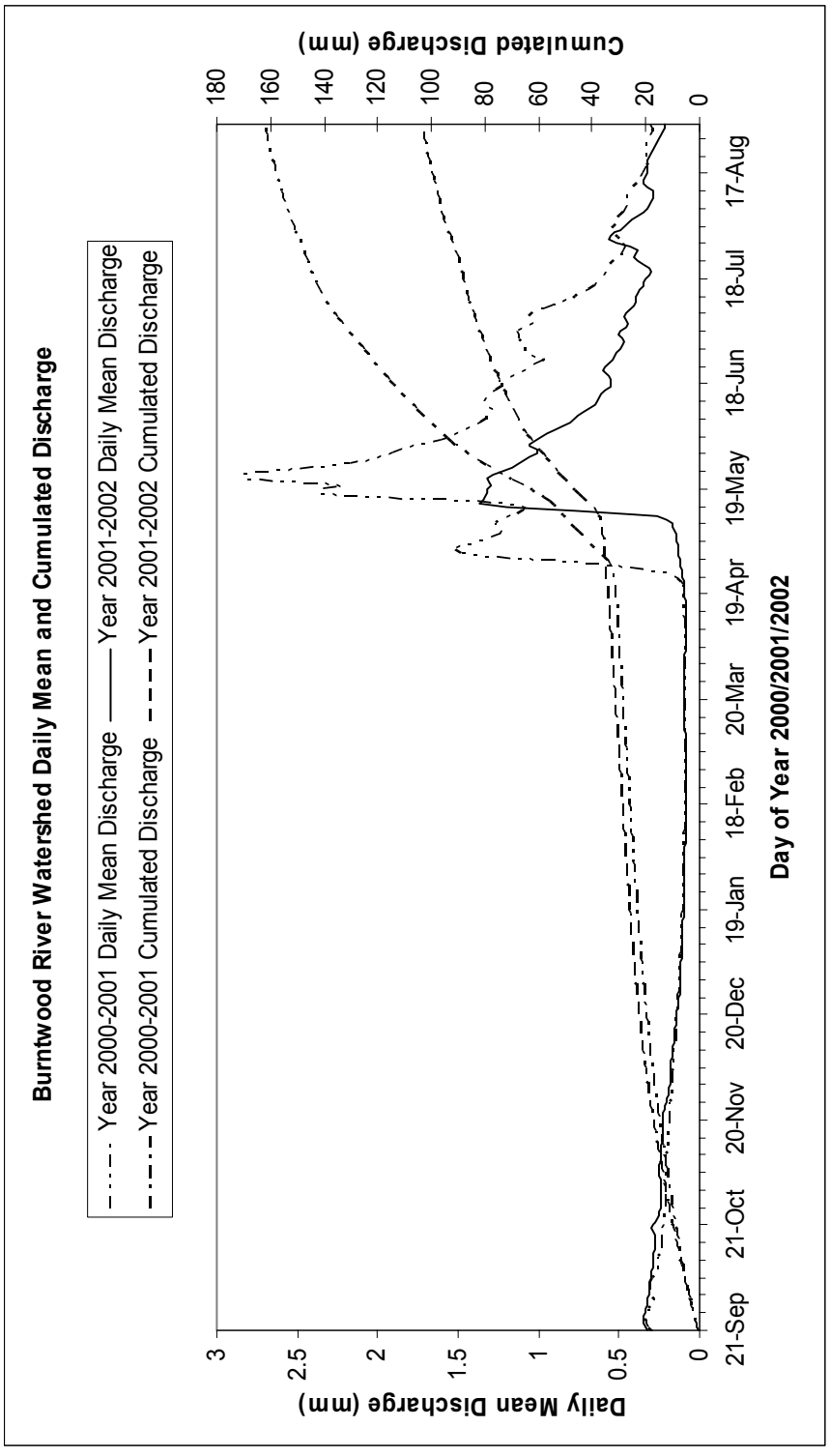

Figure 3.8 Burntwood River Watershed Daily Mean and Cumulated Discharge

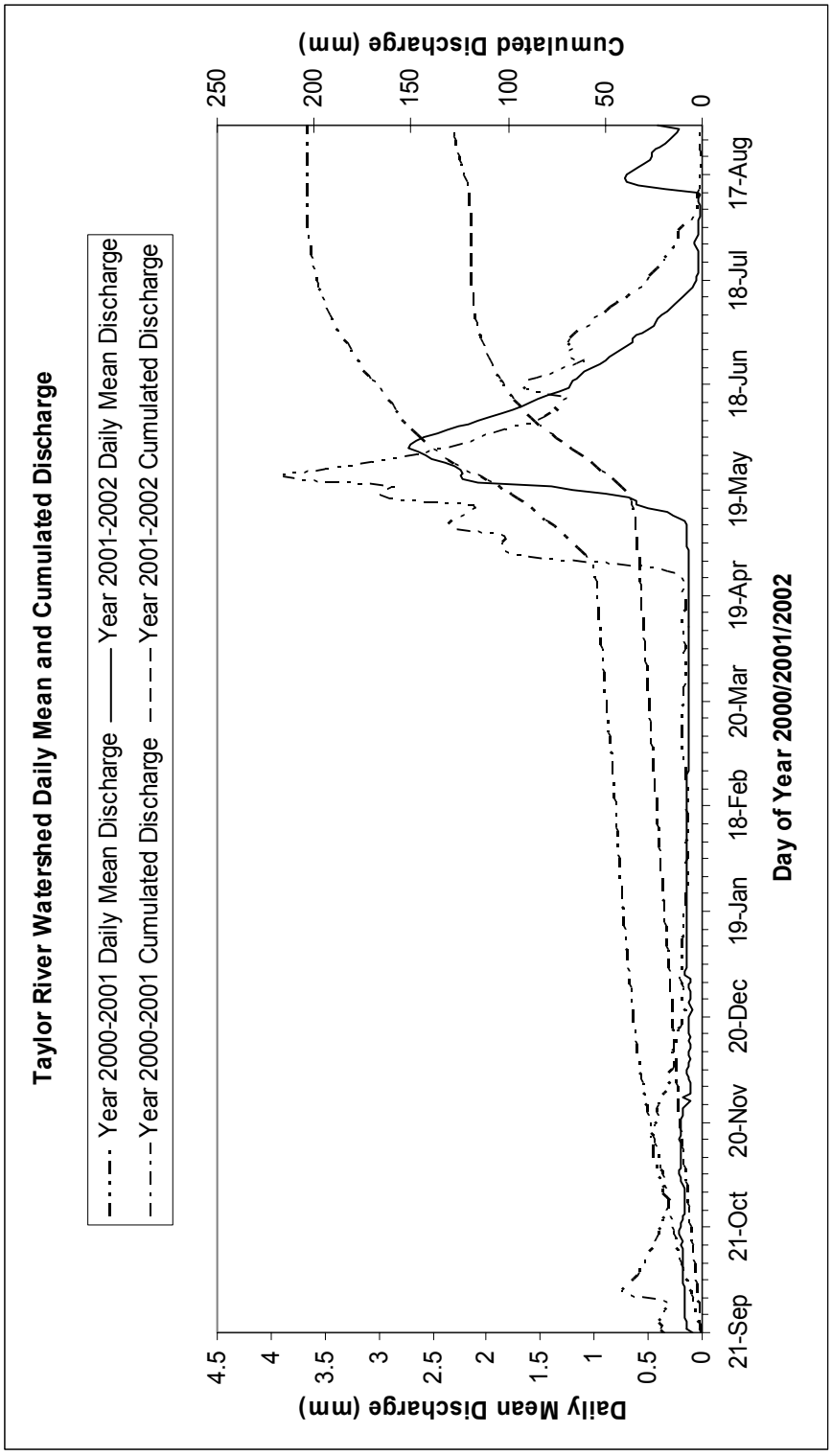

Figure 3.9 Taylor River Watershed Daily Mean and Cumulated Discharge

3.3.6 Verification Data and Data Quality Assurance

The product quality level for Version 4 MOD10A1 and MOD10A2 products used in this study are Validated stage 2. While the Version 4 MOD09GHK and MOD09GQK products are Validated stage 1, with L1B aerosols and cloud mask products still being refined. The Version 3 MOD10A1 data has a quality level of Provisional. No quality assurance was conducted on the non-imagery products used in this study

3.3.7 Software Tools

In this study the Geomatica PCI v8.2 software, was selected to view and process all imagery. Two programs of this software used in this study included "*ImageWorks*" and "*Xpace*". ImageWorks (ImageWorks Data Browser or PCI Image Handler) is an image display and manipulation program. It is part of the PCI's image analysis software. Depending on the number of channels and the image size of a database, the ImageWorks Configuration Panel allows the user to set up the configuration of an ImageWorks session. A user can display an image with the appropriate size containing a specific numbers of image/graphic planes in an ImageWorks session. There are four kinds of image planes types: 8-bits, 16-bits signed, 16-bits unsigned and 32-bits. In order to view or manipulate the data stored in a database, data channels in the database have to be loaded into appropriate image planes. For example, when working with floating point numbers, 32-bit image planes are required.

In the PCI ImageWorks, every operation works with image planes. Values in an image channel from a database file will not be modified by any operation used in ImageWorks until an in-memory image plane was saved into that specific channel. The image saving panel in ImageWorks, allows the user to save one image plane at a time from in-memory to an image channel in a database file. Another tool in ImageWorks heavily used in this

study is the EASI Modelling command window. This tool is used to enter modelling equations to be applied to the ImageWorks session image planes. Each ImageWorks session can be saved as a PIX file. A PIX file contains every saved database channel. A user can add more channels to a PIX file either by creating new channels, or by transferring layers to the database.

After different plane operations, results are saved into separate database channels. HISDUMP (Image Histogram Export) located in the PCI Xpace program was used to extract data from the channels. The HISDUMP program was used to generate histogram reports of image channels to text files.

All downloaded MODIS data are stored in the Hierarchical Data Format - Earth Observing System (HDF-EOS) format. HDF-EOS is a multi-object file format, and it is the standard data format for all EOS data products. However this format is not supported by the Geomatica PCI Imageworks v8.2 software. In order to view the MODIS products graphically or be able to import product data into Geomatica PCI Imageworks v8.2 software, the best way is to covert the HDF files to GeoTIFF files. PCI programs can read GeoTIFF format files and store the data into 16-bits unsigned channels.

HDF-EOS to GeoTIFF Converter, HEG v1.0, was used in this study to convert the data stored as HDF-EOS files into GeoTIFF. It was also used to re-project the data from the MODIS Integerized Sinusoidal or Sinusoidal projection to Universal Transverse Mercator (UTM) coordinates, and subset the download images to the outer boundary of the study area. This tool has the capability to re-project, resample, stitch (mosaic), and create metadata for HDF-EOS data. While another software HDF Explorer v1.2 was used to view the header files, and metadata of the downloaded HDF-EOS files.

3.3.8 Pre-Processing

A quick verification was conducted of the conversion from HDF-EOS files to GeoTIFF files. The author wanted to ensure that both file formats contained the same values after conversion. One downloaded HDF-EOS file was selected, and the desired subset of this HDF-EOS file was re-projected into UTM coordinates for both HDF-EOS and GeoTIFF file format. By using the HDF Explorer, the re-projected HDF file numeric values can be viewed. While for the re-projected GeoTIFF file, its numerical values can be viewed by loading into the PCI ImageWorks. The result came out that both re-projected files contained the same numerical value for the according pixel. Hence, the downloaded HDF-EOS files can be converted to GeoTIFF files for use in the PCI ImageWorks program.

Since the study focus is on the snowmelt period, the easiest way to determine the snowmelt period in each of the study years is by using the MODIS 8-day composite snow product, MOD10A2. Using the EOS Data Gateway, the MOD10A2 products from the beginning of each study year to early July have been obtained through FTP (File Transfer Protocol client). The HEG software was used to convert these HDF-EOS file to GeoTIFF format, and subset these imagery to the outer boundary of the study area. With these 8-day composite snow maps, an approximate snowmelt time frame for each year was located. Some of these snow maps are shown in Appendix A. The approximate snowmelt period for year 2001 was found to be from April 23rd to May 8th. While the approximate snowmelt period found using the MOD10A2 products for year 2002 was from May 9th to June 1st.

After the approximate snowmelt periods for each year were determined, daily 250m and 500m resolution surface reflectance products (MOD09GQK and MOD09GHK) and daily snow cover products (MOD10A1) for these periods were downloaded. Before converting all the downloaded MODIS data into GeoTIFF format files, another issue was raised. All

data are in different spatial resolutions. The MOD09 surface reflectance products are in 250m and 500m resolutions, MOD10 products have spatial resolutions of 500m, and the landcover data is in 100m resolution. In order to prevent any loss in landcover information, all MODIS products have been converted to 100m resolution. Fortunately, HEG is capable of performing this operation and is done during the conversion to GeoTIFF format and reprojection into UTM coordinates.

When using the downloaded HEG software graphical interface, the user can only process one surface layer at a time. It became too time consuming to convert all downloaded MODIS data manually. A batch program has been developed to create batch files that will automatically run the HEG's command-line interface and make all the conversions in one operation. This batch program requires the input HDF-EOS file names, subset area coordinates, the amount of channels being extracted, extracted channel name, and the resampling method. The Nearest Neighbour resampling method was used in all conversions. The resampling spatial resolution of 100m has already been integrated into the batch program. As mentioned before, MODIS channel 1 and 2 surface reflectances were extracted from MOD09GQK products, and channel 4 and 6 surface reflectances were extracted from MOD09GHK products. Daily tile snow covers were extracted from MOD10A1 products. Maximum snow extents were extracted from MOD10A2 products. After all the conversions, each subset image contains 2177 columns and 1377 rows.

Landcover and elevation data were obtained in ASCII text file format. Both spatial data were loaded into ESRI ArcView GIS 3.2a and exported as GeoTIFF format files. PIX files for each spatial data were created after their GeoTIFF files were loaded into ImageWorks.

3.4 The Test Snow-Mapping Algorithms

In order to test the MODIS snow-mapping algorithm, landcover data was obtained to replace the use of the NDSI-NDVI field. Three algorithms were developed in relation to the Snowmap algorithm. After converting MODIS imagery data to be compatible with the landcover data spatial resolution of 100m, all data were loaded into the PCI ImageWorks program separately with respect to the day and saved into individual PIX files. A PCI code (Appendix B) has been developed to apply the test algorithms to the daily PIX files by using the EASI Modelling command window.

The first criteria set was developed using the generic Snowmap algorithm. The same thresholds of the Snowmap algorithm stated from literature reviews were applied, and the calculated NDSI and NDVI values were used to determine snow cover in a dense forested area. This algorithm is called the Simulated Snowmap algorithm. The first part of the PCI code applies this algorithm, which calculates the NDSI (from equation [2.5]) and NDVI (from equation [2.6]) values to assess if that pixel contains snow. As in the MODIS Version 4 snow-mapping algorithm, the Simulated Snowmap algorithm also has two test criteria groups. For the first group, a pixel in non-densely forested region will be mapped as snow:

a. if NDSI $\geq$ 0.4;

b. and MODIS band 2 > 11%;

c. and MODIS band 4 $\geq$ 10%.

In the second group, a pixel in dense forested regions will be mapped as snow:

d. if fit in NDSI-NDVI field;

e. and MODIS band 2 > 11%;

f. and MODIS band 4 ≥ 10%.

The NDSI-NDVI field (criterion d) is constructed by fitting an exponential curve to best-fit the grey shaded curve in Figure 2.4. In the literature reviews, there were no equations or criteria mentioned specifically on what the MODIS snow-mapping algorithm uses for the NDSI-NDVI field. This exponential curve fitting is based on what is described in Figure 2.4. That is the closest that readers can get from the literature reviews. The curve equation and criteria for the NDSI-NDVI field will be modelled as follows. A pixel in dense forested region will be mapped as snow:

g. if $NDSI \geq 0.0652e^{(1.8069 * NDVI)}$;

h. and NDSI > 0.1;

i. and NDVI > 0.2.

After empirical testing of the simulated NDSI-NDVI field, the included thresholds of NDSI > 0.1 (criterion h) and NDVI > 0.2 (criterion i) classified most of the pixels to be land. This effect did not appear in the snow maps from the MOD10A1 data. It turned out that even the exponential curve was too much of a constraint on the algorithm. The author also tried to change the NDSI-NDVI field to the lowest constraints, NDSI > 0 and NDVI > 0, but it was still impossible to match up to the same amount of snow-covered pixels as in the MODIS products. These tests have proved that the first attempted Simulated Snowmap algorithm does not truly reflect the MODIS snow-mapping algorithm used in the MODIS snow product processing. After personal communication with Dorothy K. Hall, the source of this problem was from the input data. As mentioned in the literature review, the MODIS snow-mapping algorithm uses at-satellite reflectances. The snow-mapping criteria thresholds and the curve shown on Figure 2.4 should be applied to non-atmospherically correction data. However, no one has ever tested if these thresholds will

still apply to atmospherically corrected data or not. And there were no available snow-mapping thresholds that apply the same technique as the Snowmap setup for use with atmospherically corrected data.

Later, the author found an image on the MODIS Land Quality Assessment (QA) Home Page (Masuoka, 2003), that provides more detail for the NDSI-NDVI field. Figure 2.6 is an imitation of that image. Instead of basing NDSI-NDVI field on Figure 2.4, the NDSI-NDVI field has been modified as mentioned in Chapter 2 based on Figure 2.6 which is using in the MODIS Version 4 snow products. The NDSI-NDVI field for the revised Simulated Snowmap algorithm will be as follow. A pixel in dense forested region will be mapped as snow:

j. if $NDVI \geq 0.25$

k. and $NDSI \geq 0.0652e^{(1.8069 * NDVI)}$

l. if $NDVI \geq 0.1$ and $NDVI < 0.25$

m. and $NDSI \geq ((NDVI - 0.2883) / -0.4828)$

In order to determine if the same thresholds for the Snowmap algorithm still apply for atmospherically corrected input data, criteria (a) to (f) still remain the same. Since the study area is located in the northern hemisphere with sub-arctic climate, the thermal mask will not be applied. From the literature, the thermal mask in the algorithm does not make much of a difference in snow-covered areas (Hall *et al.,* 2002). Also, the land/water mask will not be applied in the Simulated Snowmap algorithm. The study area has no access to the ocean; however there are large lakes, which can be excluded in the analysis using the landcover data. For the cloud-mask, a pixel will be classified as cloud cover if it is classified as cloud in the MOD10A1 product. This criterion does not require extra input data to the algorithm. With regard to non-production masks, no decision and

missing data pixels in the MOD10A1 product will be treated as no decision pixels in the Simulated Snowmap algorithm.

For the LandSnow algorithm, which uses the same thresholds as the original Snowmap algorithm but substituted landcover data for the NDVI values. The second part of the PCI code applies the second criteria set and it uses landcover data to replace the NDSI-NDVI field. When the landcover data indicates that a pixel contains dense vegetation, the pixel will still be assessed as snow-covered even when this pixel has a low calculated NDSI value. Similar to the Simulated Snowmap algorithm mentioned before, a pixel in non-densely forested region will be mapped as snow:

n. if NDSI $\geq$ 0.4;

o. and MODIS band 2 > 11%;

p. and MODIS band 4 $\geq$ 10%.

However, in this algorithm a pixel in a dense forested region will be mapped as snow:

q. if Land Cover Class Code is less or equal to 722 and NDSI is greater than 0;

r. and MODIS band 2 > 11%;

s. and MODIS band 4 $\geq$ 10%.

As in the Simulated Snowmap algorithm, the thermal and land/water mask will not be applied to the LandSnow algorithm. The same rules in the Simulated Snowmap apply for the LandSnow algorithm with regards to cloud-mask and no decision pixels.

The Land-based Snow-mapping algorithm (LBSM) uses new arbitrary thresholds of the Snowmap algorithm with NDSI values and landcover data. The third part of the PCI code

applies to this algorithm. Similar to the LandSnow algorithm, this algorithm has new arbitrary thresholds to account for the atmospheric effect corrected nature of the MOD09 product. The arbitrary threshold for water was obtained from Jensen (2002). A pixel in a non-densely forested region will be mapped as snow:

t. if NDSI $\geq$ 0.4;

u. and MODIS band 2 > 6%;

v. and MODIS band 4 $\geq$ 5%.

In a dense forested region, this algorithm will map a pixel as snow:

w. if Land Covertype Code is less or equal to 722 and NDSI is greater than 0;

x. and MODIS band 2 > 6%;

y. and MODIS band 4 $\geq$ 5%.

As in the Simulated Snowmap and LandSnow algorithms, the thermal and land/water masks will not be applied to the LBSM algorithm. The same rules in the Simulated Snowmap and LandSnow apply for the LBSM algorithm with regards to cloud-mask and no decision pixels.

It should be noted that the PCI code command lines for mapping water bodies' pixel (rivers and lakes) and boundary pixels used the landcover data. As mentioned earlier in this chapter, in this study area water bodies will not be considered. For the later case study analysis, command lines to determine spatial agreement between the algorithms are also included in the PCI code. At the end of the program, MOD10A1 product excluded water bodies' and boundary pixels from the landcover data, and MOD10A1 product excluded water and dark targets pixels from the LBSM algorithm, were saved into

separate image planes. The key codes for the three test algorithms have been listed in Table 3.10. The input data and thresholds used in all the snow-mapping algorithms are summarized in Table 3.11.

Table 3.10 Test Algorithms Key Code

Code	Description
255	no decision
102	lake or river
50	cloud obscured
48	water
42	dark target
1	snow
0	land

Table 3.11 Snow-Mapping Algorithms Criteria

	Snowmap	**Simulated Snowmap**	**LandSnow**	**LBSM**
Input Data	MOD 02	MOD 09	MOD 09	MOD 09
Snow Over General Pixels	NDSI > 0.4	NDSI > 0.4	NDSI > 0.4	NDSI > 0.4
Detect Dark Target	Band 4 > 10%	Band 4 > 10%	Band 4 > 10%	Band 4 > 5%
Detect Water	Band 2 > 11%	Band 2 > 11%	Band 2 > 11%	Band 2 > 6%
Snow Over Dense Forest Pixels	NDSI-NDVI field	NDSI-NDVI field	Landcover data NDSI > 0	Landcover data NDSI > 0

3.5 Case Study Comparisons

Case study comparisons were devised to test the snow-mapping algorithms against the MODIS product snow maps in order to assess the differences that exist between the algorithms. Snow depletion curves were computed. These curves are later compared with meteorological and streamflow data to assess the models' accuracy. The case study comparisons that were chosen are intended to provide as much information as possible for evaluating the algorithms in view of no ground truth cover data. There is no specific Basis of Comparison case (BOC). Instead, different comparisons will be made between different algorithm results, but the LBSM algorithm is essentially the BOC in final comparisons. The following table shows the general specification of different case study comparisons. The time periods indicated for case study 4.1.1 to 4.1.3 are the data time frames used in the statistical tests.

Table 3.12 Case Study Comparisons

Case Name and Results Section Number	Data Compared	Time Period
4.1.1	Compare the Three Test Algorithms	▪ April 21st to May 1st year 2001 ▪ May 8th to May 20th year 2002
4.1.2	MOD10A1 Version 3 vs Version 4	▪ April 23rd to May 1st year 2001 ▪ May 7th to May 21st year 2002
4.1.3	MOD10A1 Version 4 vs the Three Test Algorithms	▪ April 21st to May 1st year 2001 ▪ May 8th to May 20th year 2002
4.1.4	Spatial Agreement Analysis	▪ April 15th to May 5th year 2001 ▪ May 8th to May 30th year 2002

Chapter 4
Case Comparison Results

4.1 Cases

After converting MODIS imagery data to match the landcover data's resolution of 100m, all data were loaded into the PCI ImageWorks program, separated by date and saved as a daily PIX file. The PCI code listed in Appendix B has been applied to each daily PIX files. Besides input imagery, landcover and MOD10A1 products have also been loaded according to the right date. Due to the fact that the Geomatica PCI v8.2 software does not provide a user-friendly batch processing tool, each PIX file had to be processed manually. The whole procedure required to process one day of data included: (1) create a new PIX file, (2) transfer proper imagery data into the database channels, (3) load the database channels into the proper image planes, (4) enter the PCI code into the EASI Modelling command window, (5) Run the command window, (6) create new database channels, and (7) save the results in the image planes into the new channels. The results for the different algorithms were saved in separate channels.

After running the PCI code, histograms of the results saved in the database channels were extracted using the XPace HISDUMP program. As mentioned in Chapter 3, this program was used to generate histogram reports of image channels into text files. With this feature, the number of pixels for each algorithm key code feature was listed. In order to separate the results from different snow-mapping algorithms, results channels were run separately. Each channel has its own text file that contains the histogram report.

With these histogram reports, the percentages of SCA for each algorithm with respect to date were calculated. Besides the percentages of SCA, the percentages of other algorithm key code feature areas were also obtained. The boundary, lake and river pixels are not included in any key code area percentage calculations.

In this study, only days with less than 40% cloud coverage were used in the analysis. This is an arbitrary constraint set by the author. Days with distortion in the input imagery are also not considered in the analysis. Figure 4.1 is the converted image of MOD09GQK channel 1 taken on April 24th 2001. It was loaded into PCI ImageWorks and the adaptive enhancement was applied. Cloud coverage of 38.7% was present in the study area on this date.

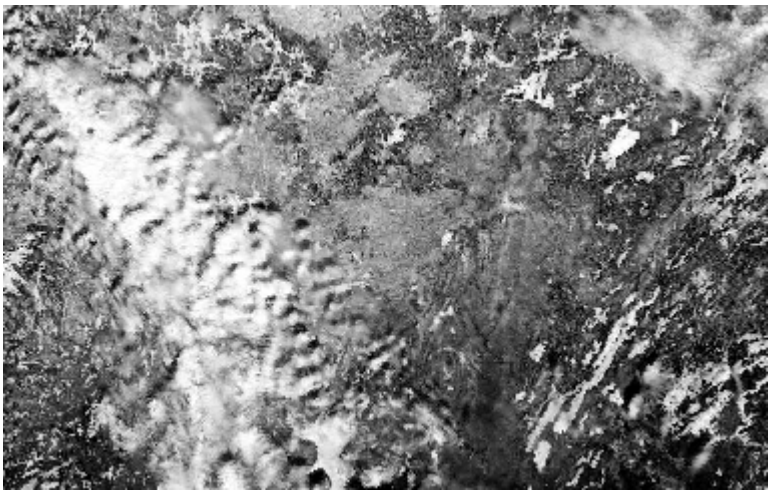

Figure 4.1 Cloud Obscured Image

A distorted image is shown in Figure 4.2. The left hand side of this image is clear while the right side across a line close to the middle of this image is fuzzy. Lake boundaries and rivers are clearly seen on the left hand side. This image is channel 1 of the MOD09GQK product and was taken on May 18th 2002. The same enhancement as Figure 4.1 in ImageWorks was applied.

Figure 4.2 Image with Distortion

Statistical tests comparing different algorithms and products have been conducted based on the snowmelt period indicated from the derived SDC. These snowmelt periods are summarized in Table 3.12. The statistical test used in the case studies is the Wilcoxon rank-sum test. Walpole *et al.* (1998), indicated this test is best used in testing equality of means of two continuous distributions that are non-normal and with samples that are independent (*i.e.,* no pairing of observations). Devore (1982), described this test as the best test in the sense of maximizing power for fixed α (significant) and still remain valid even if the underlying distributions are quite non-normal. In the following case studies, when the distributions sample sizes exceeded eight, the normal approximation for two-tail rank-sum test described in Devorem (1982) was used. On the other hand, when the distribution sample sizes are both less than eight, the general Wilcoxon two-tail rank-sum test was used. These statistical tests are only applied to calculated percentage values during the snowmelt period indicated by the snow depletion curves. Specification and numerical results of all case studies' statistical tests are listed in Appendix C.

4.1.1 Comparison of the Three Test Algorithms

As mentioned in Chapter 3, three test algorithms were developed in relation to the Snowmap algorithm in order to test if there are any differences caused by the changes in input data and the usage of landcover data instead of the NDSI-NDVI field. Full details of these criteria sets are presented in section 3.4. Figure 4.3 shows the percentage of SCA for the three test algorithms in year 2001. Figure 4.4 shows the accumulated amount of different feature areas percentage from April 15th to May 5th 2001.

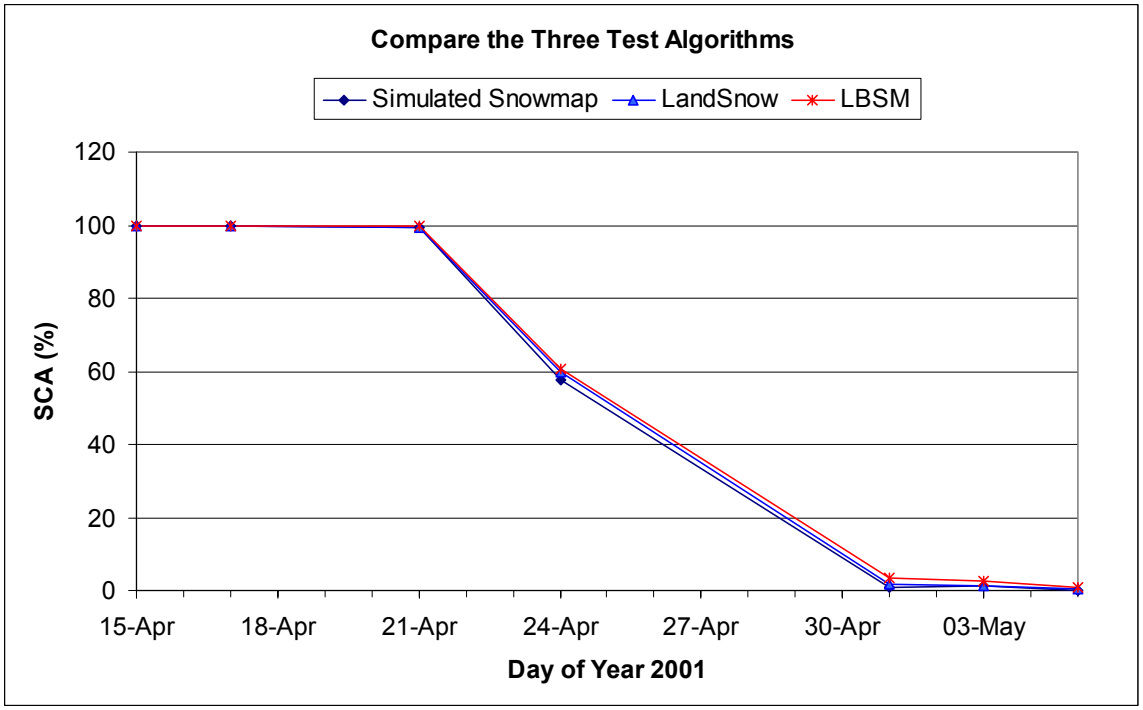

Figure 4.3 Year 2001 Percentage of SCA for the Test Algorithms

Figure 4.3 shows that during times of high snow coverage, all three test algorithms yield the same results. However, small differences in the amount of SCA detected by the algorithms exist during and after the snowmelt period. The snowmelt period of year 2001 indicated by the SDCs, is from April 21st to May 1st. In this period, the LBSM algorithm

detected more snow than the other two test algorithms. The LandSnow algorithm detected more snow than the Simulated Snowmap algorithm. As shown in Figure 4.3, the snowmelt period of year 2001 for the whole study lasted around 10 days. After eliminating the days that did not fulfill the cloud threshold and the no input imagery distortion requirement, only three days of data are left.

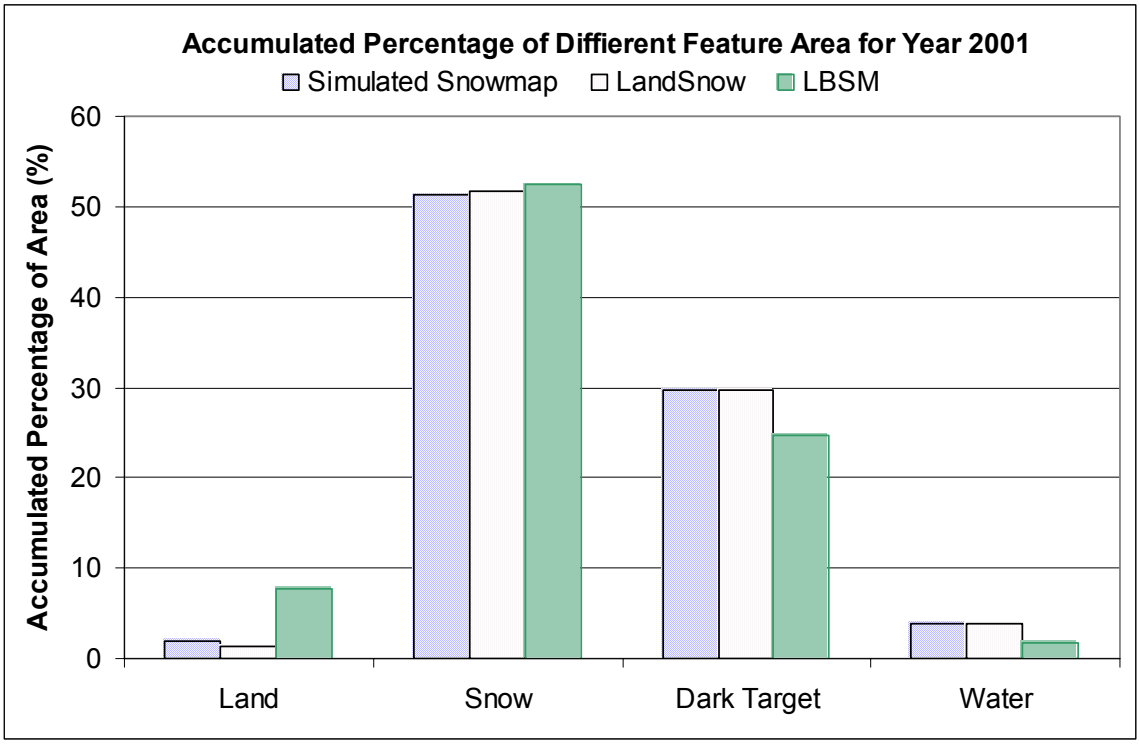

Figure 4.4 Year 2001 Accumulated Percentage of Different Feature Area for the Test Algorithms

As stated in Chapter 3, all three test algorithms used the same criteria to screen cloud cover and no decision pixels. Hence, the percentages of cloud cover and no decision pixel areas detected during this study period were not included in Figure 4.4. This figure shows the same result indicated in Figure 4.3. The amount of snow detected by the LBSM algorithm is higher than the other two test algorithms and mapped more land and snow

pixels, with less dark target and water pixels compared to the other algorithms. This effect can be explained from the thresholds used in the LBSM algorithm. As mentioned in Chapter 3, the thresholds used in the LBSM algorithm are thresholds chosen to account for the atmospheric effects corrected nature of the MOD09 product. These thresholds are half the amount required as the thresholds stated in the literature reviews, which lowered the constraints. These changes lead to the effect of fewer pixels being classified as dark target or water. On the other hand, more pixels can be classified as snow or land.

Due to the use of the same thresholds for dark target and water pixels, the Simulated Snowmap and LandSnow algorithm mapped the same amount of dark target and water pixels. As seen in Figure 4.4, the LandSnow algorithm mapped more snow cover than the Simulated Snowmap algorithm. However, it is reversed on the amount of land cover pixels being mapped. The only difference in these two algorithms is the thresholds for mapping snow in dense forested areas. The Simulated Snowmap algorithm used the NDSI-NDVI field; while the LandSnow algorithm used the landcover data. The results indicated that the use of landcover data mapped more snow than using the NDSI-NDVI field in year 2001. Figure 4.5 and Figure 4.6 show the percentage of SCA and the accumulated amount of different feature areas percentage, respectively, for the three test algorithms in year 2002. The accumulated amount of different feature areas percentage is computed from May 8th to May 30th 2002.

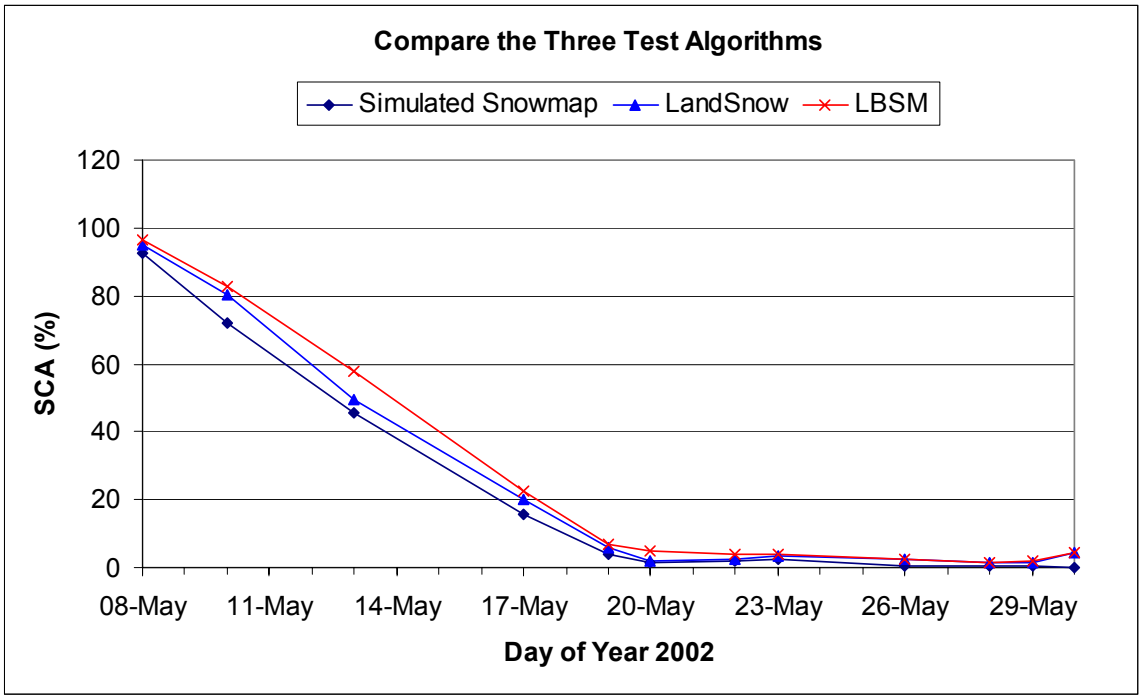

Figure 4.5 Year 2002 Percentage of SCA for the Test Algorithms

Similar results as in Figure 4.3 and Figure 4.4 are shown in Figure 4.5 and Figure 4.6. In year 2002 the same trends as in year 2001 can be seen. From Figure 4.5, the LBSM algorithm once again mapped more SCA than the other two algorithms. The LandSnow algorithm also mapped more SCA than the Simulated Snowmap algorithm. The snowmelt period of year 2002 indicated by the SDCs, is from May 8th to May 20th. The accumulated amount of different feature areas percentage shown in Figure 4.6 indicated that the LBSM algorithm mapped more snow and land pixels than the other two algorithms. On the other hand, it mapped less dark target and water pixels. The causes of these effects have been explained earlier and can also explain why the Simulated Snowmap and LandSnow mapped the same amount of dark target and water pixels. An interesting fact shown in Figure 4.6 is that the LBSM algorithm mapped more land pixels than snow pixels. This phenomenon is caused by the inclusion of after melt days. No significant differences between these three test algorithms for both years were found

using the statistical tests. Less than 5% difference existed in the amount of accumulated SCA percentage mapped over the whole period between the test algorithms each year.

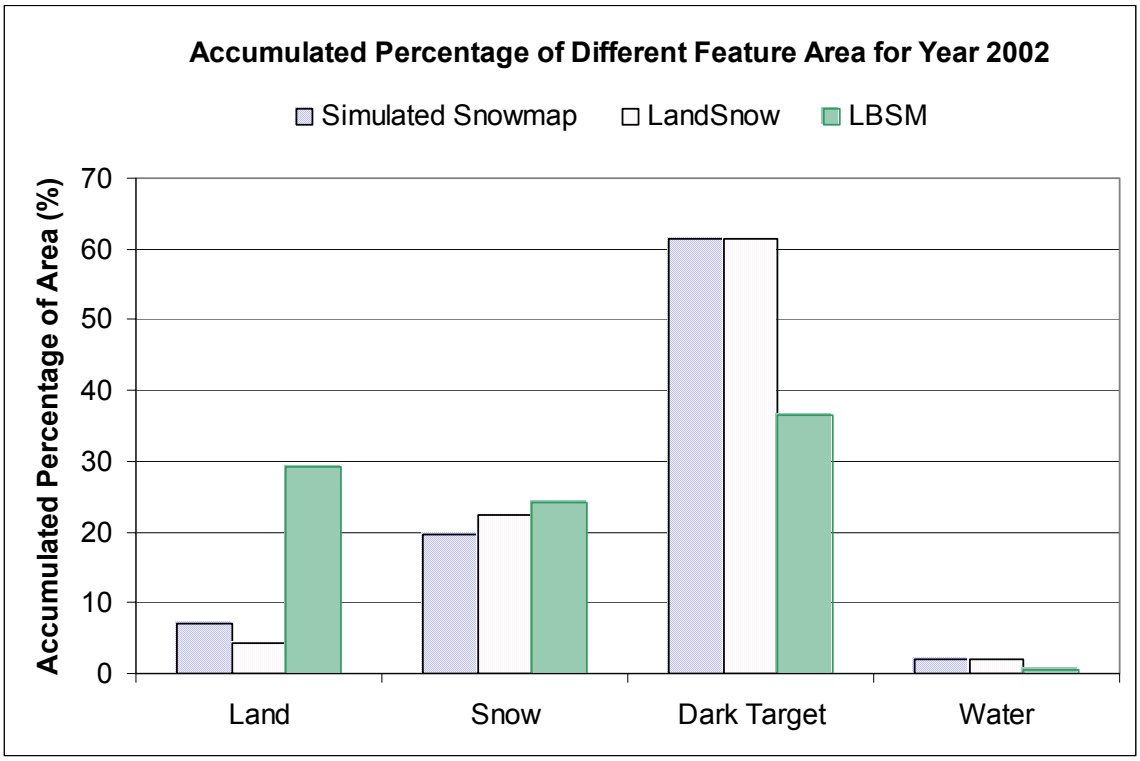

Figure 4.6 Year 2002 Accumulated Percentage of Different Feature Area for the Test Algorithms

4.1.2 MOD10A1 Snow Product Version 3 versus Version 4

There are several differences in the MODIS Version 3 and Version 4 snow products. The main difference is the projection. The grid projection used in Version 3 products is the Integerized Sinusoidal (ISIN), while the Version 4 products are stored in Sinusoidal (SIN) grid projection. Two different cloud masks are offered in the MOD10_L2 product. The thermal mask threshold in the snow-mapping algorithm has changed from 277K to 283K. In this case study, the results from the Version 3 and Version 4 MOD10A1

products are compared. Mentioned earlier in the chapter, the boundary, lake and river pixels are not included in this case study area percentage computation. However, days with cloud obscured over 40% of the study area were included in this case study. This is to show the connective results of the MOD10A1 products, and the different versions' reaction to cloud obscured effects. Both versions presented here used the standard conservative cloud mask. Figure 4.7 shows the daily percentage of SCA for year 2001 while Figure 4.8 shows the accumulated percentage of different feature area for year 2001. Daily area percentages of different features were accumulated from April 15th to May 8th 2001.

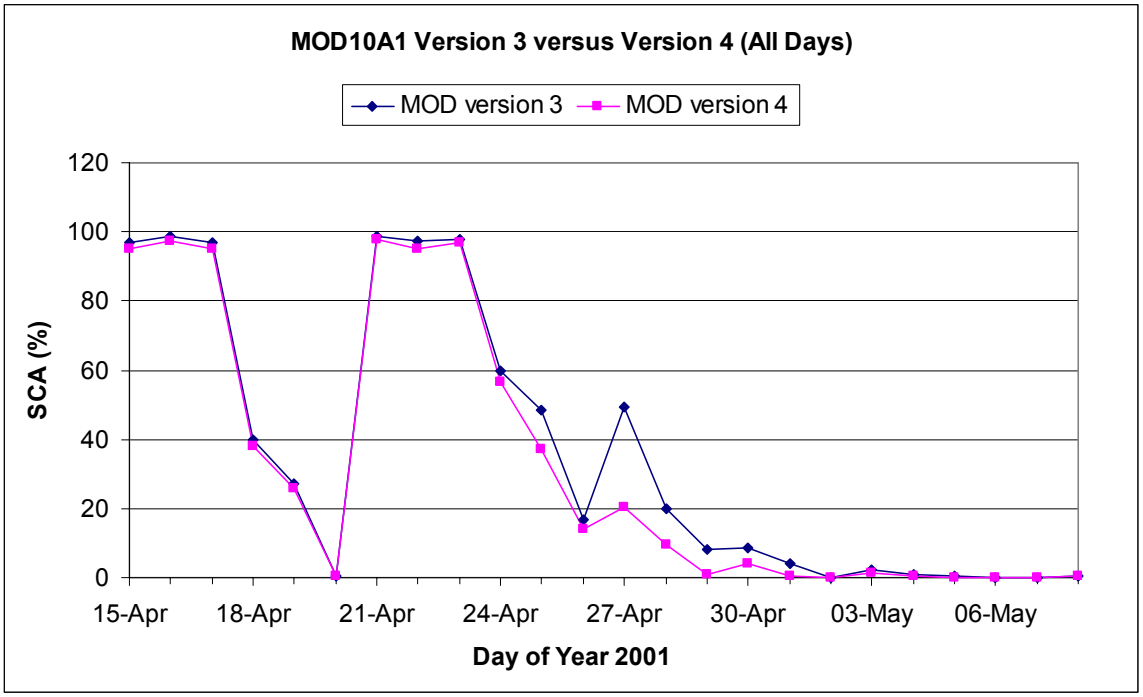

Figure 4.7 MOD10A1 Version 3 versus Version 4 for Year 2001

Figure 4.7 shows for year 2001 that Version 3 and 4 MOD10A1 products do not exhibit many differences before melt, which contained high amounts of daily snow cover. The amounts of snow detected during the snowmelt period, April 23rd to May 1st of year 2001,

from the two versions have shown some difference. Over the graphed period, the Version 3 products mapped more or the same amount of SCA as compared to Version 4 products. Figure 4.8 shows that Version 4 products mapped more lake ice, inland water, cloud, and land cover pixels than Version 3 during the melt period of this year. However, Version 3 products have mapped more snow cover pixels than Version 4. As seen in Figure 4.7 the snow depletion curve generated using Version 3 products is less steep than the one generated from Version 4 products. The inclusions of days from April 18th to April 20th have lead to large amounts of total cloud pixels detected during this period.

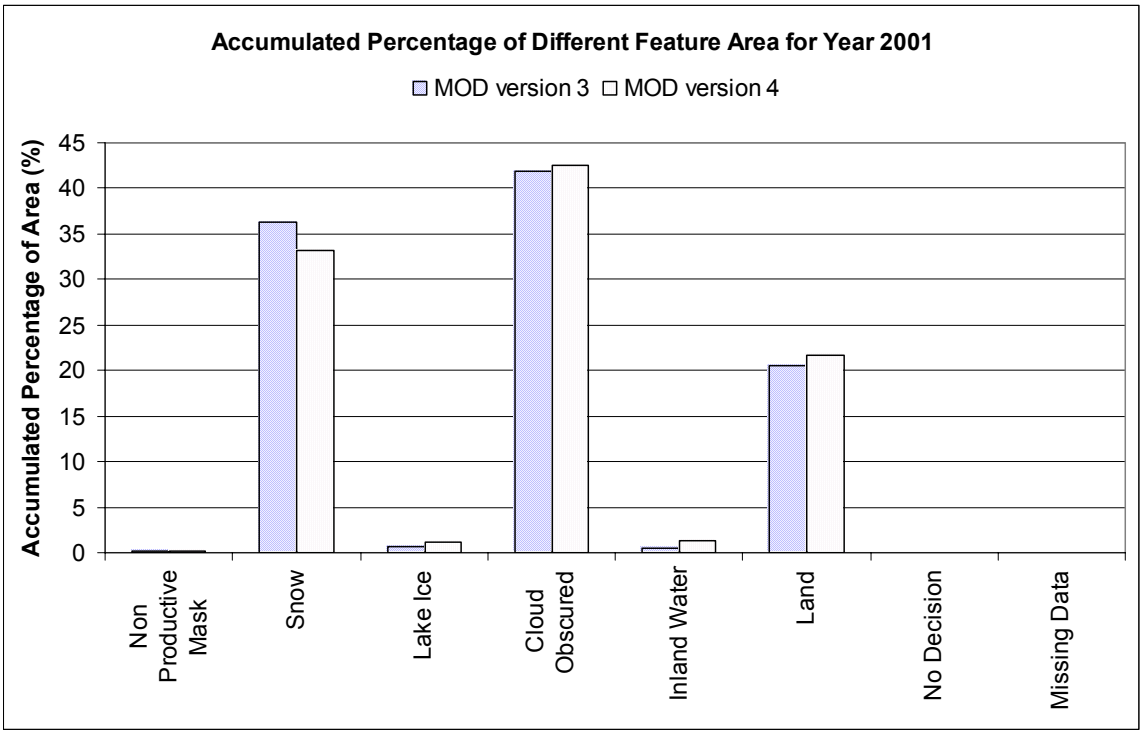

Figure 4.8 Year 2001 MOD10A1 Accumulated Percentage of Different Feature Area

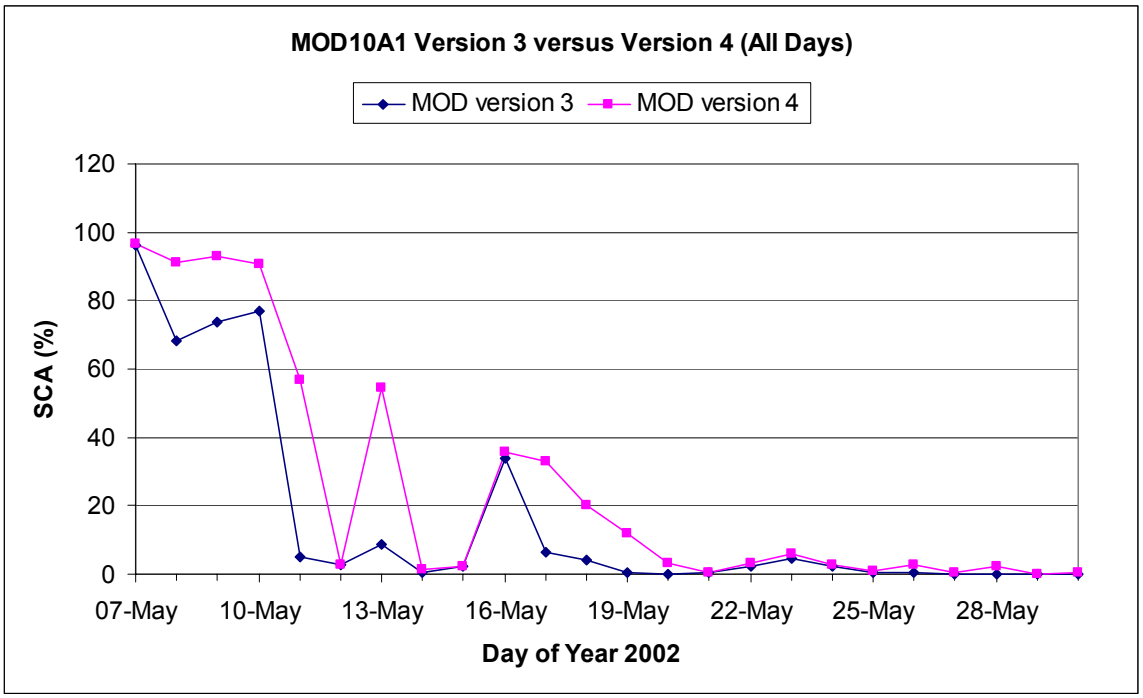

Figure 4.9 MOD10A1 Version 3 versus Version 4 for Year 2002

Figure 4.9 shows the daily percentage of snow coverage for year 2002. The snowmelt period of this year indicated from the SDCs is from May 7th to May 21st. Similar to Figure 4.7, differences between the two version products existed during the melt period. Compared to year 2001, this year has greater differences between the two products. Opposite to year 2001, Version 4 products mapped more or the same amount of snow cover compared to Version 3 products over the graphed period.

Figure 4.10 shows the accumulated area percentage of different features for year 2002. This figure indicated that both version products mapped similar amounts of lake ice, cloud and inland water cover pixels. Compare to Version 4, Version 3 products mapped more land and no production mask cover pixels. On the other hand, Version 4 products mapped more snow pixels. Statistical tests indicated that there are no significant differences between these two versions of MODIS snow products for both study years.

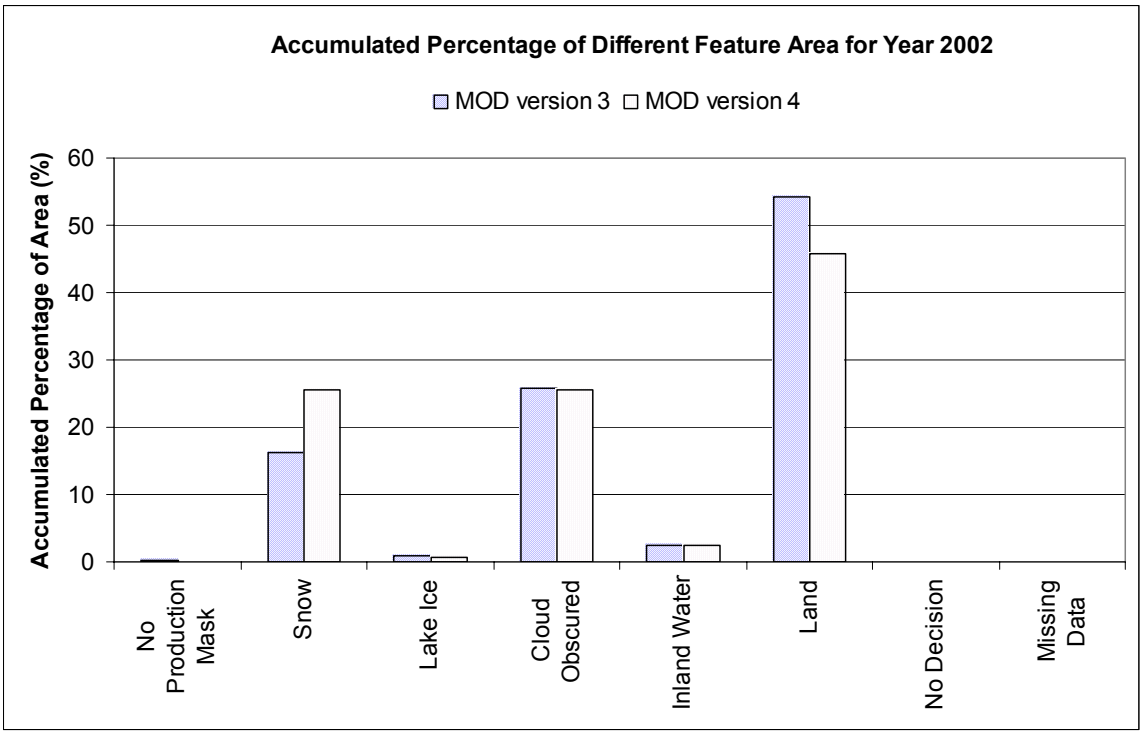

Figure 4.10 Year 2002 MOD10A1 Accumulated Percentage of Different Feature Area

The snow depletion curve generated using MOD10A1 Version 3 and Version 4 products are shown in Figure 4.11. Any days from either version product that exceeded the cloud obscured constraint of 40% were eliminated. After the cloudy days have been eliminated, the snow depletion curves generated from these two versions fluctuated less. The snowmelt periods indicated from these depletion curves are April 23rd to May 1st 2001 and May 7th to May 20th 2002. Statistical tests have indicated that these snow depletion curves generated using different version products have no significant differences.

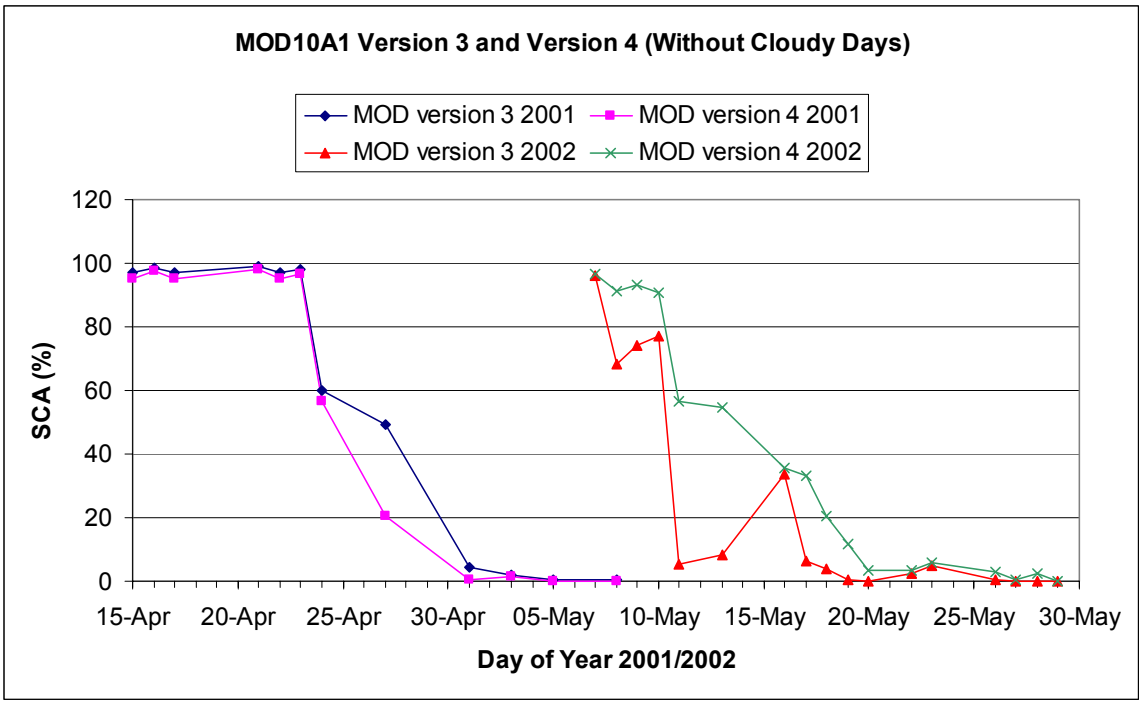

Figure 4.11 MOD10A1 Version 3 and Version 4 Without Cloudy Days

4.1.3 MOD10A1 Version 4 Snow Product versus the Test Algorithms

In this case study the newer MODIS snow products, Version 4 daily snow products, are compared to the results generated from the three test algorithms. The same amount of product dates used in the three test algorithms were applied to the Version 4 products. Hence the snowmelt period used in the statistical tests for this case study is the same as the case study in section 4.1.1. The computed percentage snow coverage of the test algorithms and MOD10A1 Version 4 products for year 2001 and year 2002 are presented in Figure 4.12 and Figure 4.13, respectively. Similar results from the case study in section 4.1.2 were observed. In year 2001 the MOD10A1 Version 4 products mapped less percentage of snow than all the test algorithms. In year 2002, the MOD10A1 Version 4 products mapped more snow than all the test algorithms. Statistical tests indicated no significant difference existed between all test algorithms and the MOD10A1 product results.

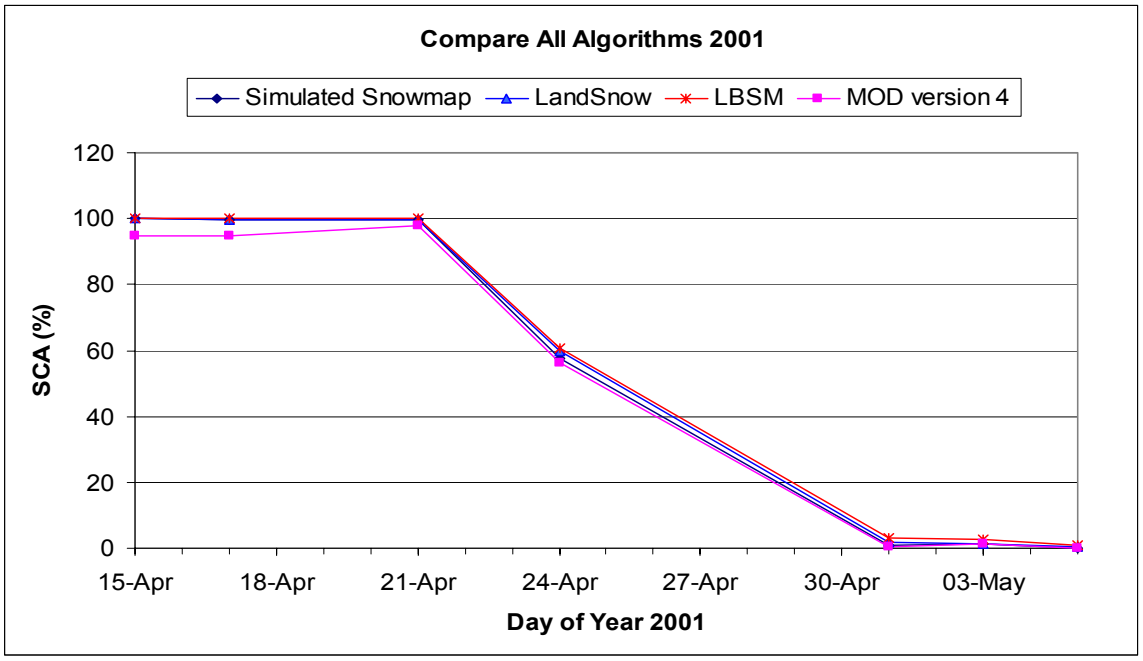

Figure 4.12 Test Algorithms versus MODIS Version 4 Product for Year 2001

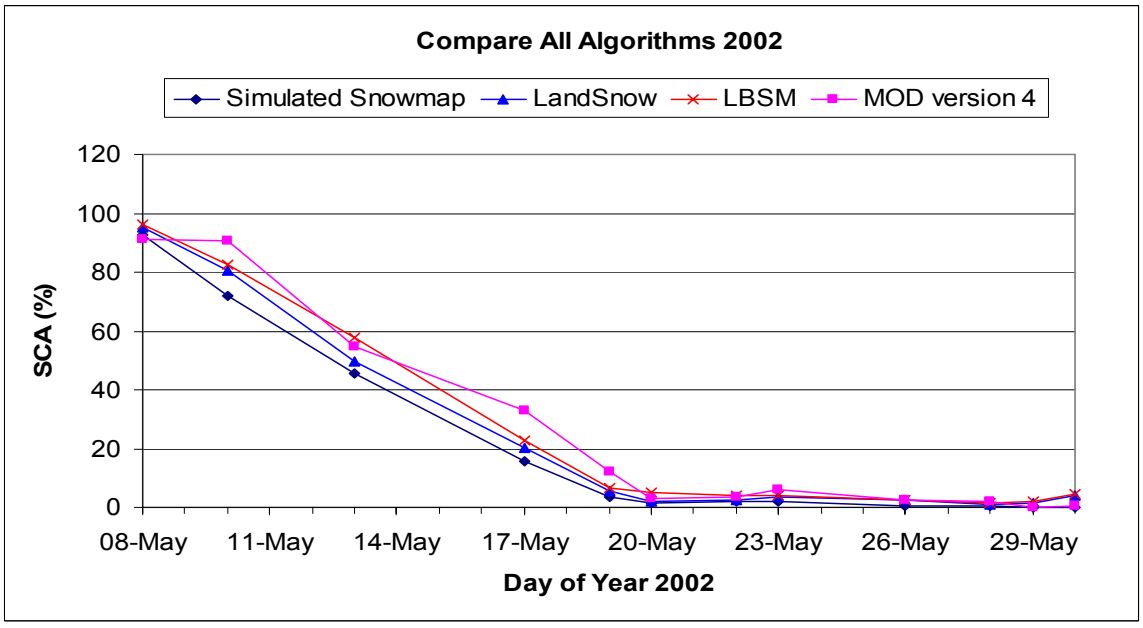

Figure 4.13 Test Algorithms versus MODIS Version 4 Product for Year 2002

4.1.4 Spatial Agreement

Besides the percentages of SCA, the percentages of spatial agreement for the snow cover pixels mapped from the different algorithms and MODIS snow products were used to assess the differences in the results. In this case study, the MOD10A1 product results were assumed to be the reference. The percentage of spatial agreement was computed using the amount of snow cover pixels mapped by both the test algorithm and MOD10A1 product divided by the total amount of snow cover pixels mapped using the MOD10A1 product. The daily snow cover spatial agreement between the MOD10A1 products and test algorithms are presented in Figure 4.14.

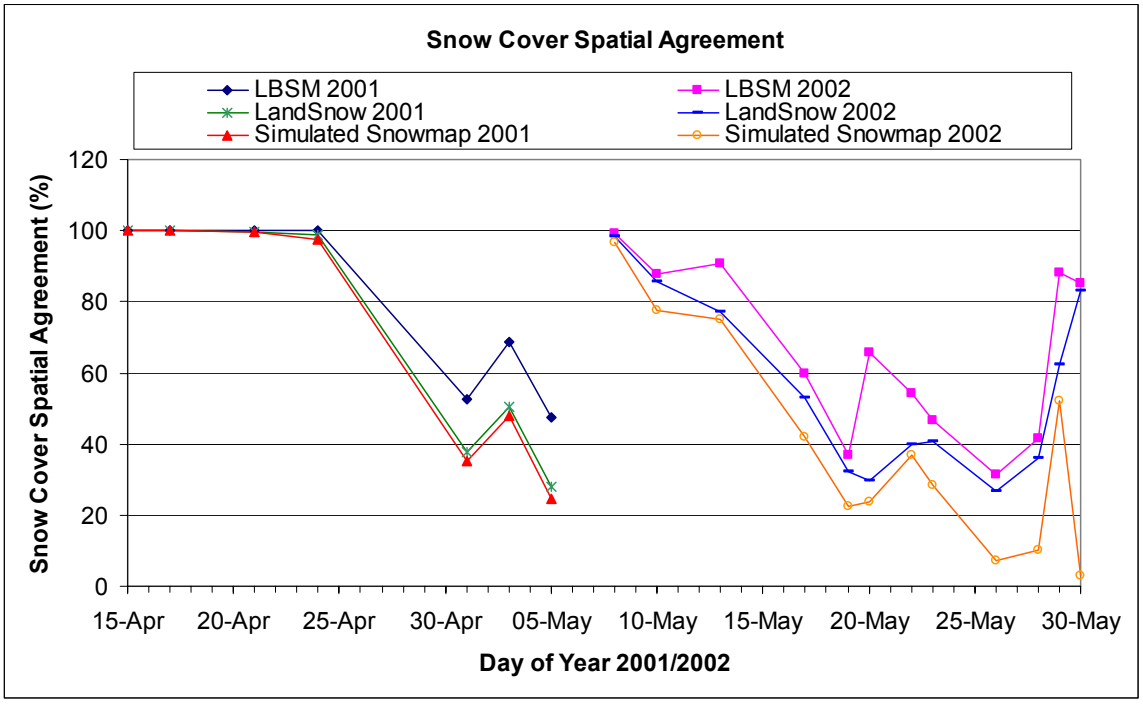

Figure 4.14 Snow Cover Spatial Agreement

In the year 2001, the snow cover pixels mapped by the test algorithms spatially agreed close to 100% of what the MOD10A1 products mapped before the melt period. The high

percentage of spatial agreement between the test algorithms and MOD10A1 products may due to the fact that in year 2001, the MOD10A1 products mapped less percentage of daily snow cover compared to the test algorithms. The spatial agreement started to decrease during the snowmelt period. In year 2002, the percentages of spatial agreement between the landcover based test algorithms and MOD10A1 products were high at the beginning and at the end of the snowmelt period. During the snowmelt period the percentages of spatial agreement decreases. The percentages of spatial agreement between the Simulated Snowmap and MOD10A1 products decease with respect to time. This case study has clearly shown that even though the test algorithms mapped close amounts of daily snow cover pixels as compared to the MOD10A1 products, the locations of these mapped snow covers may not agree, especially during the snowmelt periods.

Accumulated percentage of spatial agreement or disagreement for 2001 and 2002 are shown in Figure 4.15 and Figure 4.16, respectively. The percentage of spatial disagreement was computed using the amount of pixels mapped as non-snow cover by the test algorithm but mapped as snow cover by the MOD10A1 product divided by the total amount of snow cover pixels mapped using the MOD10A1 product. The accumulated period for year 2001 was from April 15th to May 5th. For year 2002, the accumulated period was from May 8th to May 30th.

As shown on both figures, the Simulated Snowmap has the least spatial agreement with the MOD10A1 products. Thus, one can conclude that the Snowmap algorithm thresholds are not appropriate to apply on atmospherically corrected data as is. The main feature that caused a high percentage of spatial disagreement is the dark target constraint, especially in year 2002. Despite this constraint, both landcover based algorithms worked well with NDSI values to map snow in atmospherically corrected data. The differences in the percentages of spatial agreement between the test algorithms and the MOD10A1 product may be caused by two factors. First, the different spatial resolution of the parameters

used in the algorithms. As mentioned in Chapter 2 and 3, the MOD10A1 product has spatial resolution of 500m, while the landcover data are in 100m resolution. The use of higher spatial resolution landcover data has enhanced the spatial accuracy of snow cover classification. The second factor is the difference in input data. The Snowmap algorithm uses at-satellite reflectance, which is not atmospherically corrected. Due to atmospheric scattering effects, the location of the snow cover detected by the satellite sensor may actually suffer a minor shift in location from atmospherically corrected data.

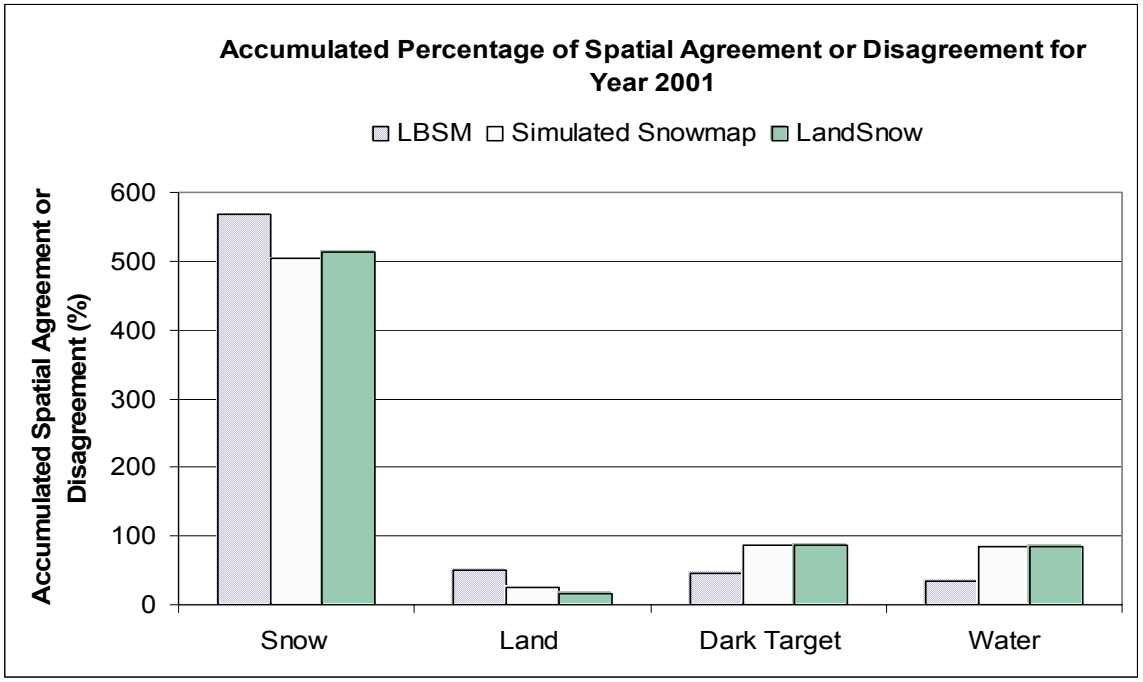

Figure 4.15 Accumulated Spatial Agreement or Disagreement for Year 2001

This case study has indicated that the results generated by applying the LBSM algorithm are more closely related to the MOD10A1 products as compared to the other two test algorithms. Only results from the LBSM algorithm and MOD10A1 products will be analyzed in the following chapter. Coloured MOD10A1 products and LBSM algorithm generated snow maps are located in Appendix D.

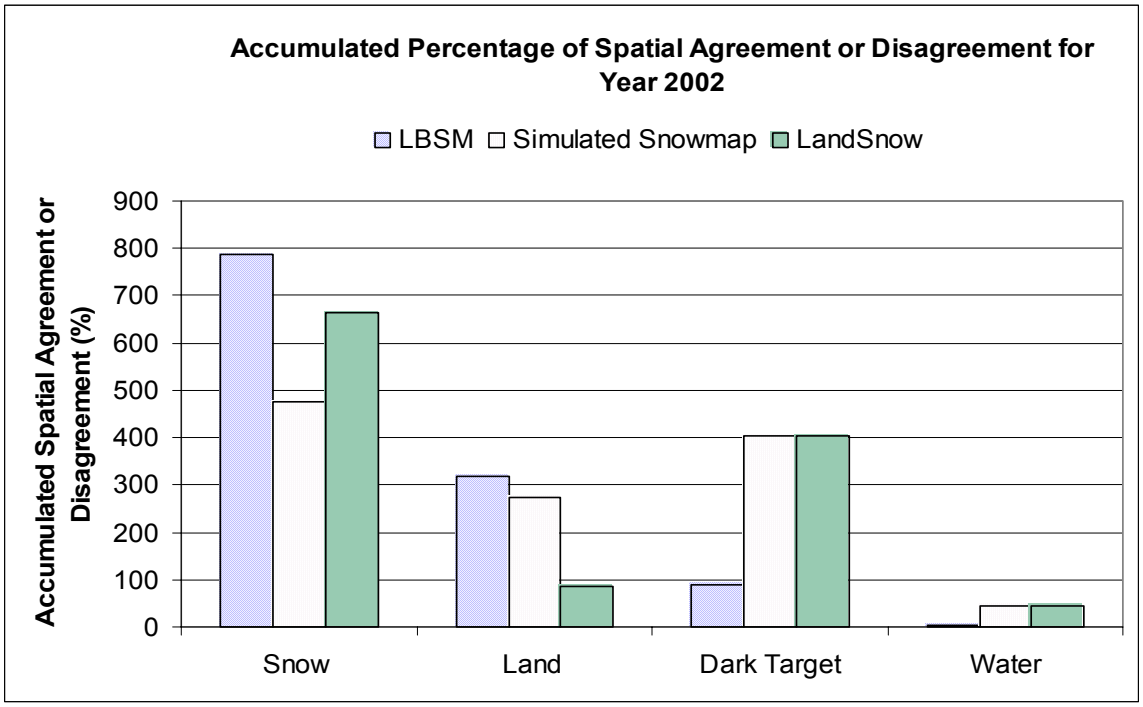

Figure 4.16 Accumulated Spatial Agreement or Disagreement for Year 2002

4.2 Case Study Summary

These case studies have shown that differences exist in the amount of SCA mapped by the different algorithms during the snowmelt periods. However, less than 5% difference of the accumulated SCA percentage resulted from the different algorithms. Statistical tests have indicated no major differences existed in the amount of SCA mapped between the test algorithms and the MOD10A1 products. Spatial agreement analysis has shown that despite the fact that the algorithms mapped similar amounts of SCA, the spatial agreement between the SCA locations are low during the melt period. It also indicated that it would not be appropriate to apply the Snowmap algorithm to atmospherically corrected data. The SCA mapped by the LBSM algorithm has a higher correlation to the SCA mapped by the MOD10A1 products as compared to the other two test algorithms.

Chapter 5
Snow Depletion Curves and Verification using Hydro-Meteorological Data

5.1 Introduction

In this chapter three different analyses were carried out to evaluate the derived SDCs' accuracy. Local watershed SDCs were produced using the LBSM algorithm and MOD10A1 products. Satellite data derived SCA values were applied with the Temperature Index Method at a daily time step to determine if runoff modelling is improved. The derived SCAs and accumulated degree-days were plotted against each other to see if any correlation existed. Elevation analysis has been carried out to discover the snow depletion behavior at different elevation ranges. The SCA and accumulated degree-days relationship at different elevation ranges are also presented in this chapter.

5.2 Runoff Analysis

Streamflow data for year 2000 to 2002 have been obtained from the Water Survey of Canada (WSC). Two streamflow gauges, Burntwood River Above Leaf Rapids and Taylor River Near Thompson, were selected to provide streamflow rates for the Burntwood River and Taylor River watersheds, respectively. Details of these water gauges are given in Chapter 3. With the use of the PCI code located in Appendix B, snow depletion curves for the two watersheds have been generated. These computed SCAs were used in the Temperature Index Method to estimate the amount of runoff from snowmelt. The estimated amount of runoff using SCAs were compared with estimated amount of runoff generated without using SCAs, and later compared with the streamflow data.

5.2.1 Watershed Snow Depletion Curves

The snow depletion curves shown in Chapter 4 were for the whole study area. In order to verify the satellite image derived results with streamflow data, the snow depletion curves for the selected watersheds have to be computed. As the daily percentage of cloud cover present over the watersheds is different from each other and also different from the whole study area, the amount of SCA used to generate the snow depletion curves for each watershed is different. The Snow Depletion Curves of the Burntwood River Watershed are shown in Figure 5.1.

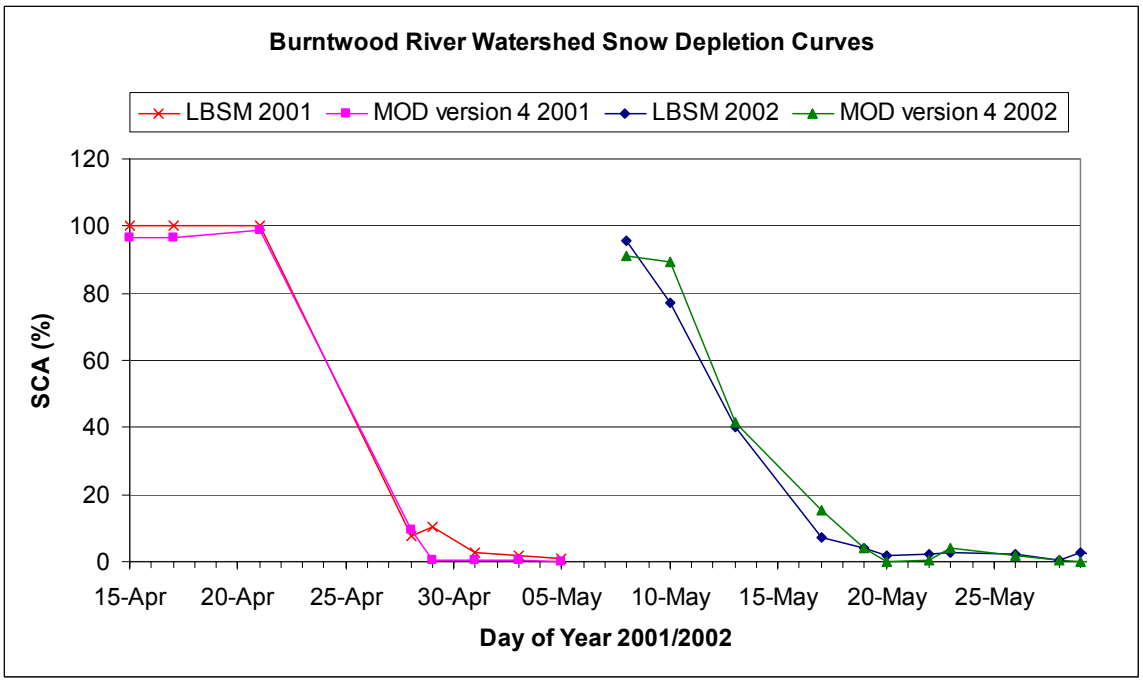

Figure 5.1 Burntwood River Watershed Snow Depletion Curves

The snowmelt period of year 2001 shown in the depletion curves is from April 21st to April 29th. The detected snowmelt period of year 2002 is from May 8th to May 20th. Similar snow depletion curves generated by the two different algorithms for this

watershed have been presented for both years. The snow depletion curves of the Taylor River watersheds generated from the MODIS products and the LBSM algorithm are shown Figure 5.2. This figure indicates that for the Taylor River watershed, the snowmelt period of year 2001 is from April 24th to May 1st, and for year 2002 the snowmelt period is from May 13th to May 29th. Both snow-mapping algorithms resulted in similar snow depletion curves. For this watershed, year 2002 shows a steeper depletion curve as compared to year 2001. This may due to the lack of calculated SCAs available in year 2001. Comparing Figure 5.1 and Figure 5.2, the Taylor River watershed has shown a delay in melt compared to the Burntwood River watershed by four to six days each year. This effect will be further investigated in the following elevation analysis section.

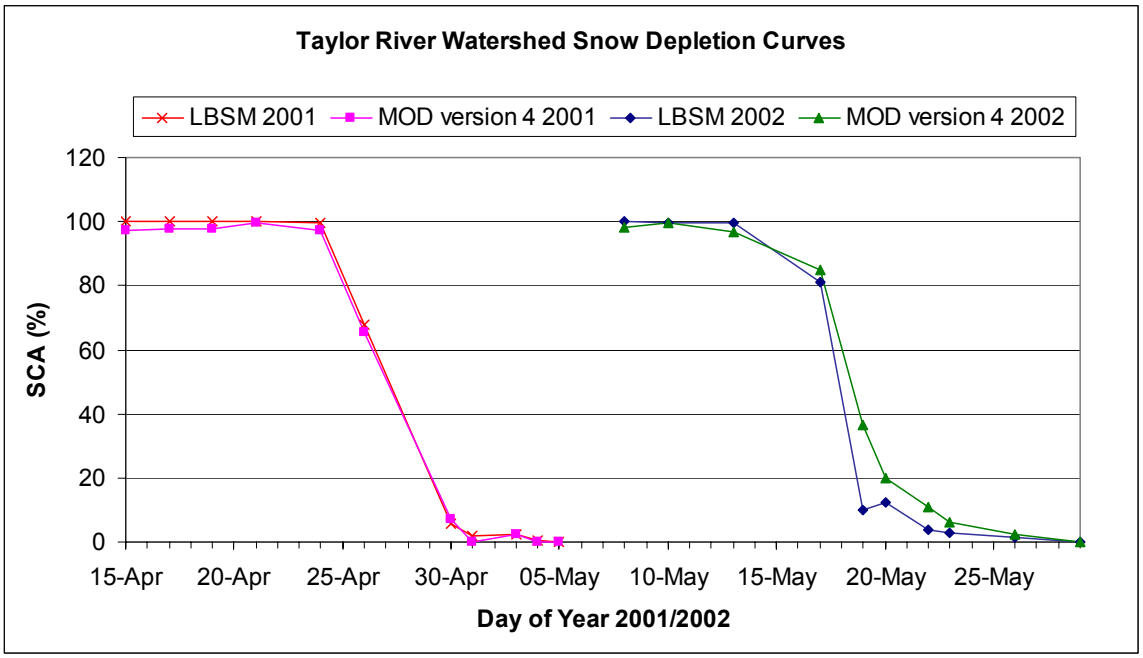

Figure 5.2 Taylor River Watershed Snow Depletion Curves

5.2.2 Temperature Index Method

An important determinant of snowmelt runoff is temperature. The Temperature Index Method employs the daily mean temperature as the fundamental prediction element for snowmelt. The U.S. Army Corps of Engineers (1956) has produced several general equations for different snowmelt rain and rain-free periods. Specific equations were available for open, partly forested and heavily forested areas. The modified snowmelt equations from this reference used in this study are listed below. Heavily forested areas are regions where over 80% of the area is covered by forest. For heavy forest with rainfall the general equation is:

$$M_i = (K + 0.007R_i)(T_i - 32) + 0.05 \quad [5.1]$$

where M is the daily snowmelt (inches/day), K is a proportional constant, R is the rainfall intensity (inches/day), T is the daily mean temperature (ºF) and i is the daily increment. Melt was set equal to zero when T is below 32ºF. For heavy forested areas during rain-free periods:

$$M_i = K(T_i - 32) \quad [5.2]$$

After the melt is computed, the amount of runoff is computed by:

$$Q_i = (M_i Fr_i + (1 - Fr_i)R_i)A \quad [5.3]$$

where Q is the amount of runoff (m^3/day), M and R are in (m/day), Fr is the fraction of SCA in the watershed, and A is the watershed area (m^2). Due to the sparse amount of calculated SCAs during the melt period of year 2001, the Temperature Index Method was only applied to the watersheds in year 2002. Linear interpolation was used to obtain daily

values of SCA in the watershed when data were missing. A linear relationship is the most conservative and in keeping with using as much of the observed data as possible instead of a fitted relationship curve. The snow depletion curves remained the same as those in Figure 5.1 and Figure 5.2. The runoff computation started on the first day the daily mean temperature is above zero degrees, which is April 11th 2002. The Burntwood River watershed size is 5821km^2, while the area for Taylor River watershed is 935.9km^2. Runoff computation for the Burntwood River watershed ended on May 20th, and it ended on May 29th for the Taylor River watershed. The *Fr* value was assumed equal to 1 before the snowmelt period. Along with runoff, the snow water equivalent is computed as follows:

$$SWE_i = SWE_{i-1} - (M_i Fr_i) + Sn_i \quad [5.4]$$

where *SWE* is the snow water equivalent (mm/day), *M* is in (mm/day), and *Sn* is the amount of snow (mm/day). The initial SWE value is usually the total amount of snow collected prior to the melt period. In this study, the initial SWE value for year 2002 is 150.46mm, with a general assumption of 1cm of snowfall is equivalent to 1mm of rainfall (Environment Canada, 2004). Traditionally, when daily SCA values were unavailable, users will assume that the *Fr* is equal to 1 at all times for all equations during the snowmelt period. This assumption has also been carried out and compared to results computed using SCAs. Results of all computations are shown in Appendix D. The *K* values were calibrated by ensuring that all snowcover was depleted for each algorithm according to the algorithm's SCA. The calibrated *K* values are also given in Appendix D. Calculated runoff for the Burntwood River and Taylor River watersheds with streamflow are shown in Figure 5.3 and Figure 5.4, respectively.

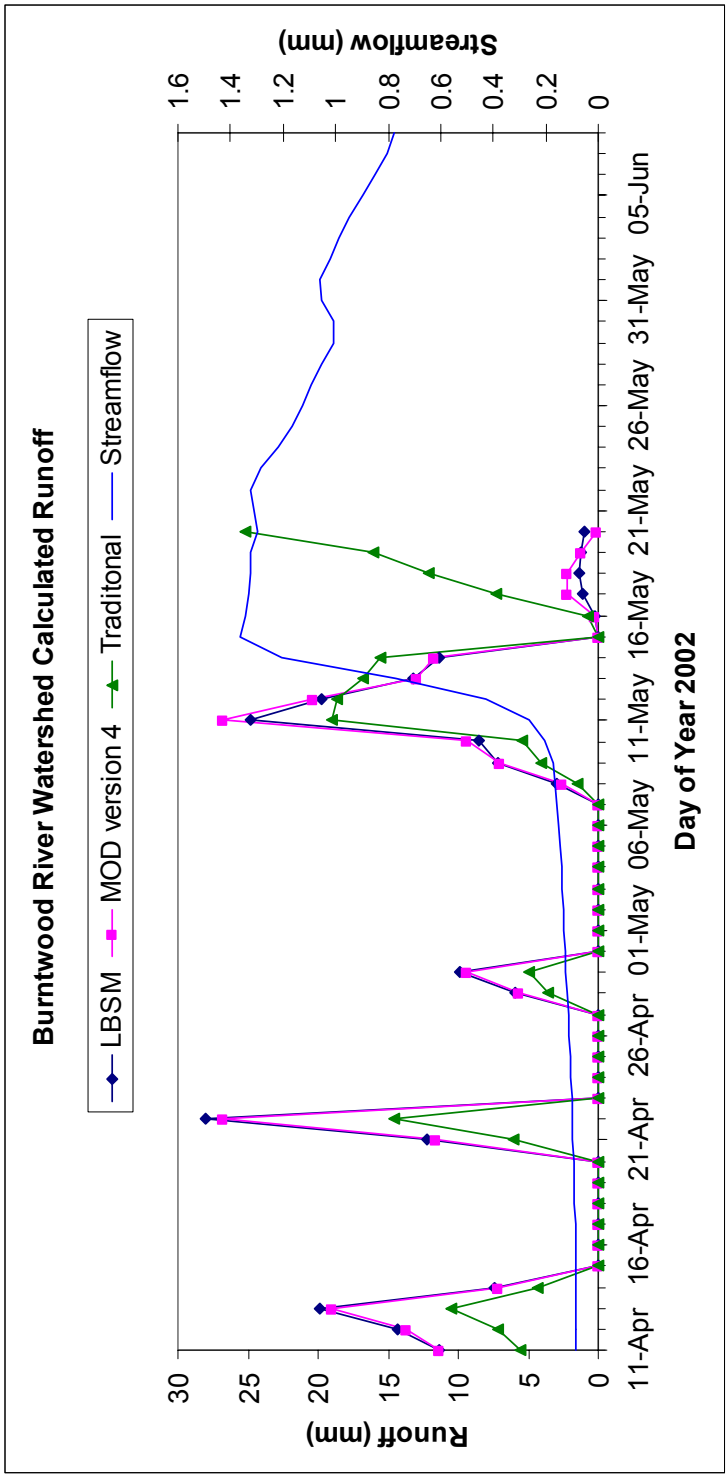

Figure 5.3 Burntwood River Watershed Calculated Runoff

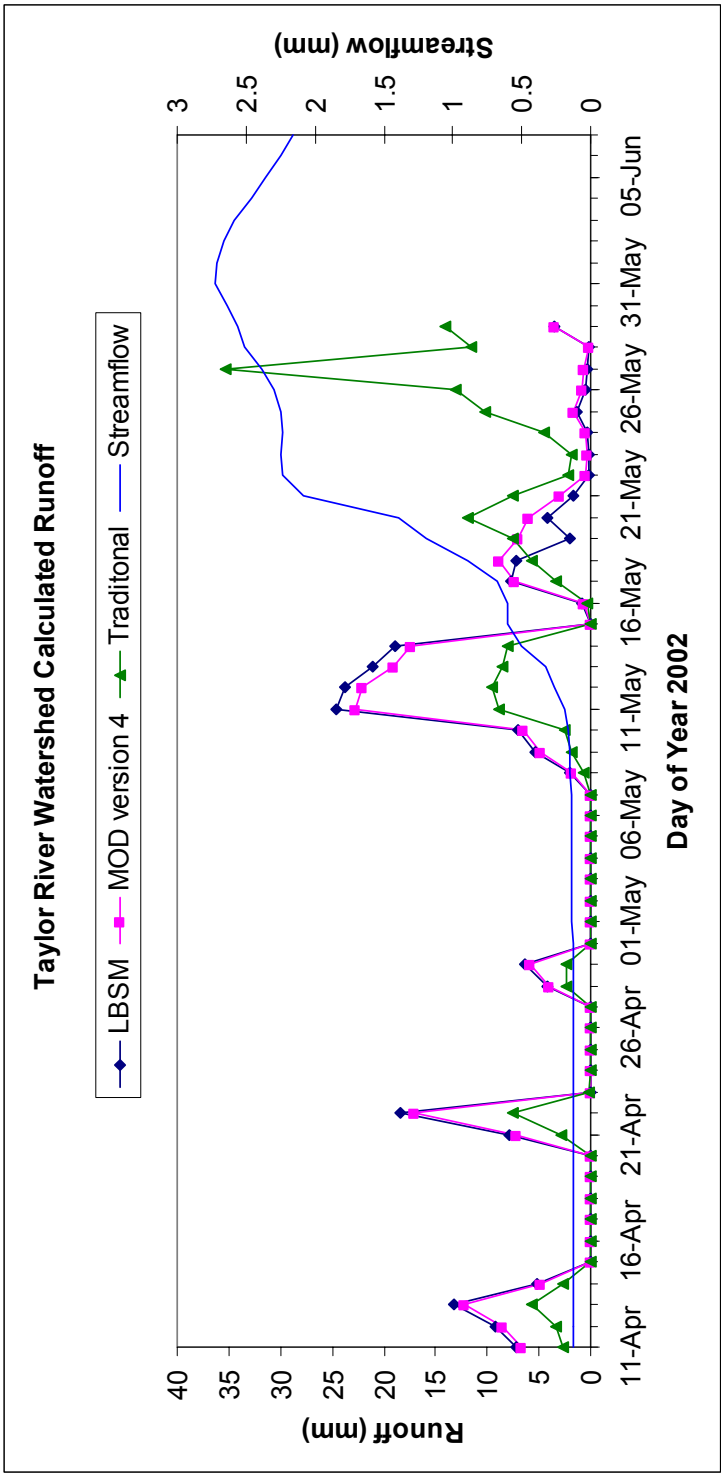

Figure 5.4 Taylor River Watershed Calculated Runoff

As seen in Figure 5.3, the Temperature Index Method has indicated there is some snowmelt occurring before the actual snowmelt period. Due to the assumption of *Fr* being equal to 1 before the melt period, the algorithms and traditional assumption yielded similar trends. The amount of runoff difference between the algorithms and traditional assumption during this period is due to the different assigned *K* constants. Differences between the three started at the beginning of the snowmelt period: May 8th to May 20th. With the use of SCAs, the computed runoff for the two algorithms reacted similarly. On the other hand, the traditional assumption of *Fr* equal to 1 for all days until SCA is zero over estimated the amount of runoff when the daily SCA is close to zero. During the melt period the traditional method yielded lower runoff peaks compared to the case when SCA values are applied. The total amount of runoff computed for the Burntwood River watershed during the snowmelt period using the LBSM SCAs is 92.65mm. Using the MOD10A1 product, the total amount of calculated runoff during the melt period is 97.06mm. The traditional assumption calculated 142.43mm of runoff during the melt period. The amount of streamflow measured during the months of May to August for 2002 from the Burntwood River Above Leaf Rapids water gauge was 61.40mm.

Similar behaviour to Figure 5.3 was also found in Figure 5.4. Differences between the algorithm and the traditional assumption exist during the snowmelt period. Snowmelt runoff in a basin requires time to travel to the water gauge. Hence from Figure 5.4, it can be seen that the traditional assumption calculated runoff completely missed the streamflow peak period. The total amount of runoff computed for the Taylor River watershed, during the snowmelt period of May 13th to May 29th, using the LBSM SCAs is 69.99mm. Using the MOD10A1 product, the total amount of calculated runoff during the melt period is 77.93mm. The traditional assumption calculated 145.75mm of runoff. The amount of streamflow measured, during the months of May to August for 2002 by the Taylor River Near Thompson water gauge was 90.27mm. As indicated from these figures, to accurately calculate the amount of runoff generated from snowmelt, SCA values since the first day that the mean temperature raised above zero should be obtained.

The Burntwood River watershed has many more lakes and rivers than the Taylor River watershed. Part of the snowmelt runoff may have been stored in the lakes and then lost to evaporation prior to reaching the water gauge. Streamflow volumes for the Taylor River watershed seem to be under estimated in comparison to the measured totals. This is due to rainfall in the summer period was not accounted for in the modelling process. Results in this analysis have shown that the use of SCA values in the Temperature Index Method could provide runoff estimates of high accuracy.

5.3 Degree-Days Analysis

Degree-days are the accumulated departures of temperature above or below a particular threshold value. The threshold values that are selected depend on each particular application that they are used for. For this study, a threshold value of 0ºC was used, with snowmelt considered to have occurred if the daily mean temperature was above 0ºC. Then the difference between the daily mean temperature and this threshold value was calculated as a degree-day. When the daily mean temperature is below 0ºC, the degree-day was set equal to 0ºC-days. As mentioned in Chapter 3, the meteorological data of four meteorological stations near the study area were obtained from Environment Canada. In order to obtain daily mean temperature values to represent the whole study area, daily mean temperature values from the four selected stations were averaged. In year 2001, the first day whose averaged daily mean temperature higher than 0ºC was on April 2nd. For year 2002, it was on April 11th. The accumulated degree-days (ADD) for year 2001 and year 2002 were calculated starting from these days and plotted on Figure 5.5 with corresponding snow depletion curves.

This figure shows the accumulated degree-days for year 2001 increases faster than year 2002. This is due to the daily mean temperature of year 2001 in this period increasing faster than in year 2002. The uses of ADD shows that the obtained meteorological data agreed with the snow depletion curves calculated from the two different algorithms. Both

years' ADD started to rise at the start of the snowmelt period detected using satellite imagery.

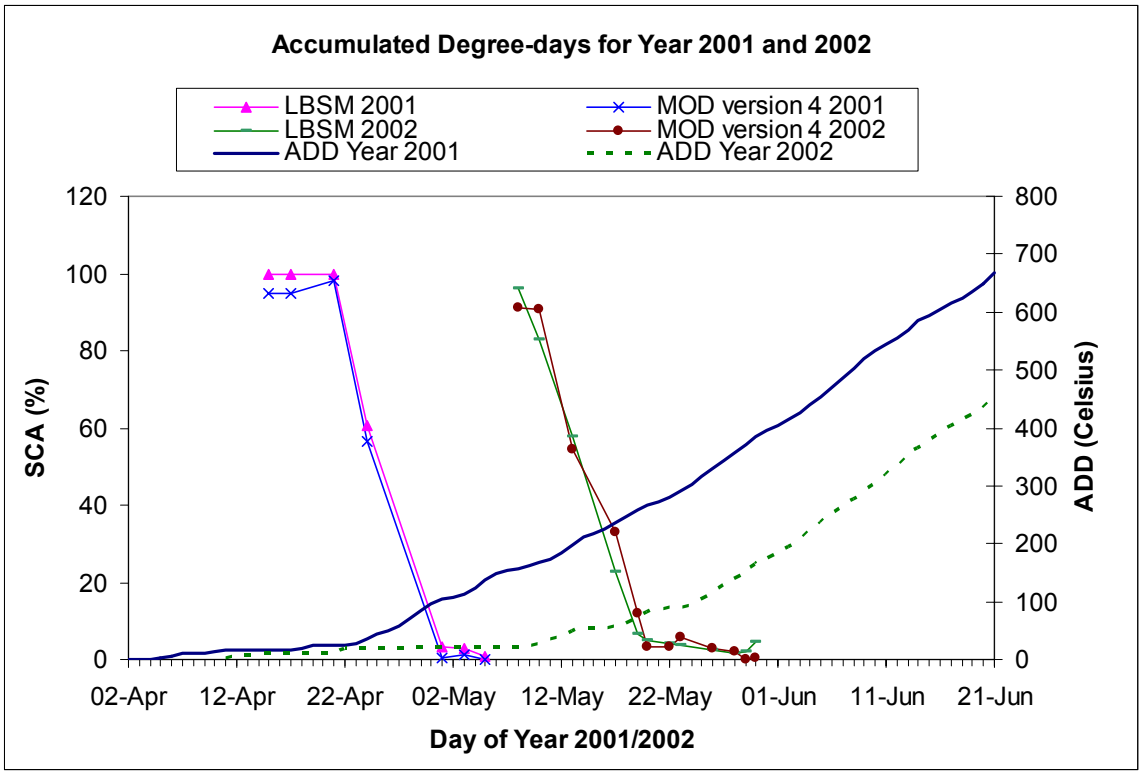

Figure 5.5 Accumulated Degree-Days for Year 2001 and 2002

In year 2003, the first day whose averaged daily mean temperature was higher than 0ºC was on March 19th. The ADD for year 2003 calculated starting from this day until May 18th was plotted on Figure 5.6 with a MOD10A1 product derived snow depletion curve. As shown again in this year, the ADD started to rise at the beginning of the melting period. In year 2003, the snowmelt period lasted for 25 days.

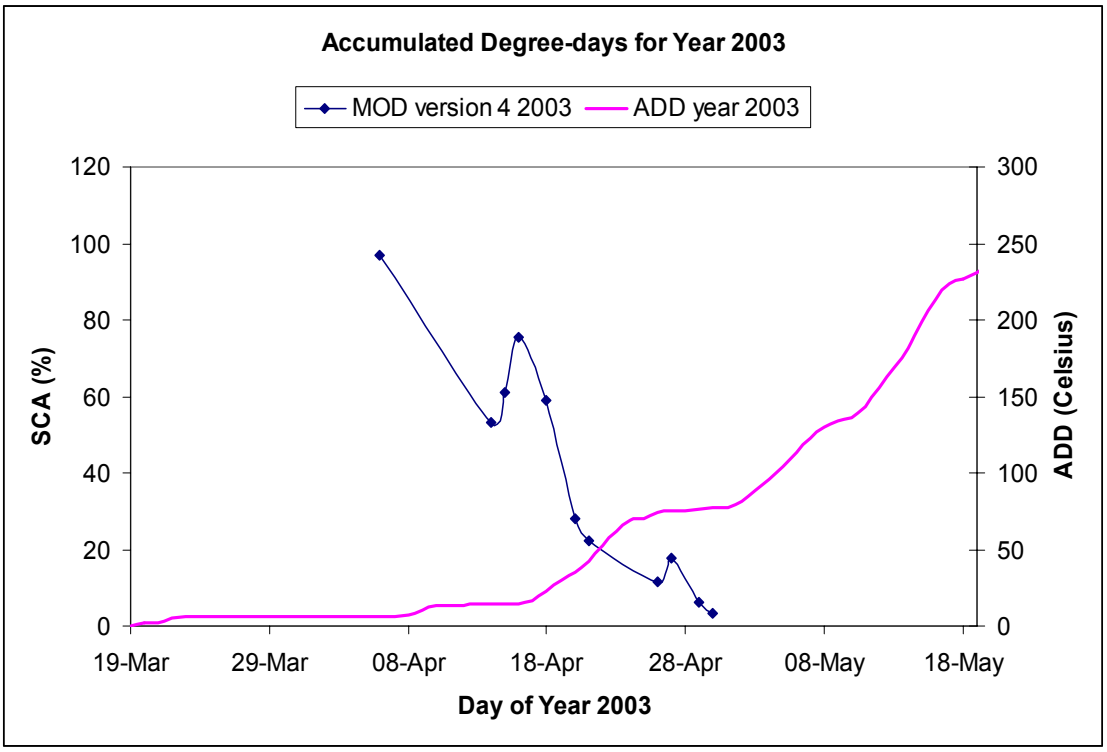

Figure 5.6 Accumulated Degree-Days for Year 2003

To take the degree-days analysis to another level, the relationship between the SCAs detected by the snow-mapping algorithms and the ADD have been plotted on Figure 5.7, Figure 5.8, and Figure 5.9 for year 2001 to 2003, respectively. Only SCAs during the snowmelt period were used. The reduction of the SCA is a cumulative effect of climatic conditions in and around the SCA with time. At each point in time, snowmelt can be related to air temperatures. These figures have shown that the SCA detected from the algorithms reduces exponentially with accumulated degree-days. This relationship can be expressed by equation [5.5].

$$SCA = a \cdot \exp(-b \cdot \mathrm{ADD}) \quad [5.5]$$

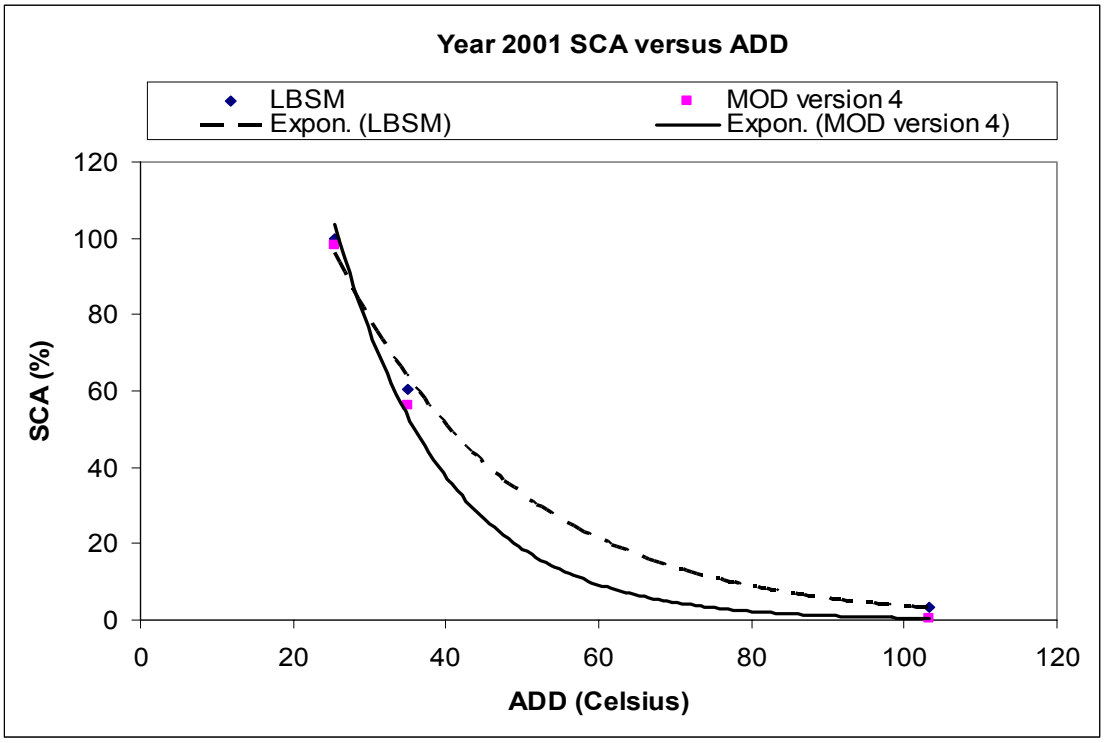

Figure 5.7 Year 2001 SCA versus ADD

With the same amount of temperature increase, the SCA in year 2001 and 2002 decreased more rapidly than in year 2003. This difference reflected the length of time of the melt period of each year. As mentioned previously, year 2001 and 2002 took approximately 10 days for snow depletion, while year 2003 took 25 days. Aside from the difference in the annual relationships, the fit of the curves between the SCAs detected from different snow-mapping algorithms were also different. In year 2001, the fit of the relationship suggested the MOD10A1 products resulted in a more rapid reduction of SCA as compared to the results calculated using the LBSM algorithm. This was opposite to year 2002.

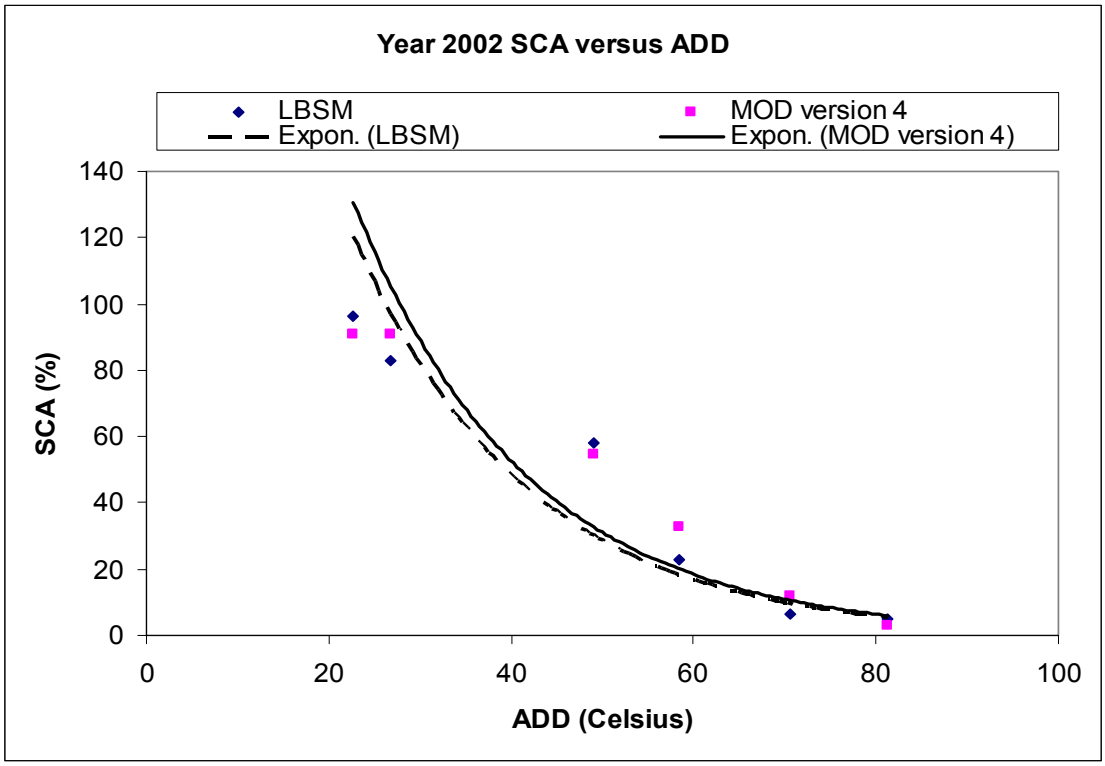

Figure 5.8 Year 2002 SCA versus ADD

Snow and rain events occurred during the snowmelt period of year 2002 and 2003, while only rain events occurred during the melt period of year 2001. Rain on snow events greatly alters the way snow melts and thus temperature is not the only factor.

As indicated by the Temperature Index method, the relationship between melt and temperature is purely linear. With degree-days being defined as (T - 0ºC), people might expect the relationship between the SCA and ADD to be linear. There are two reasons for the SCA and ADD relationship to be exponential. First, as shown in Figure 5.5 and Figure 5.6 the ADD increase is an exponential rise. Another more important reason is that as SCA depletes, ground is exposed and bare ground heats up faster than snow. The heat coming from the ground after daytime heating helps to accelerate melt. The Temperature Index method does not account for such effects, but the SCA does.

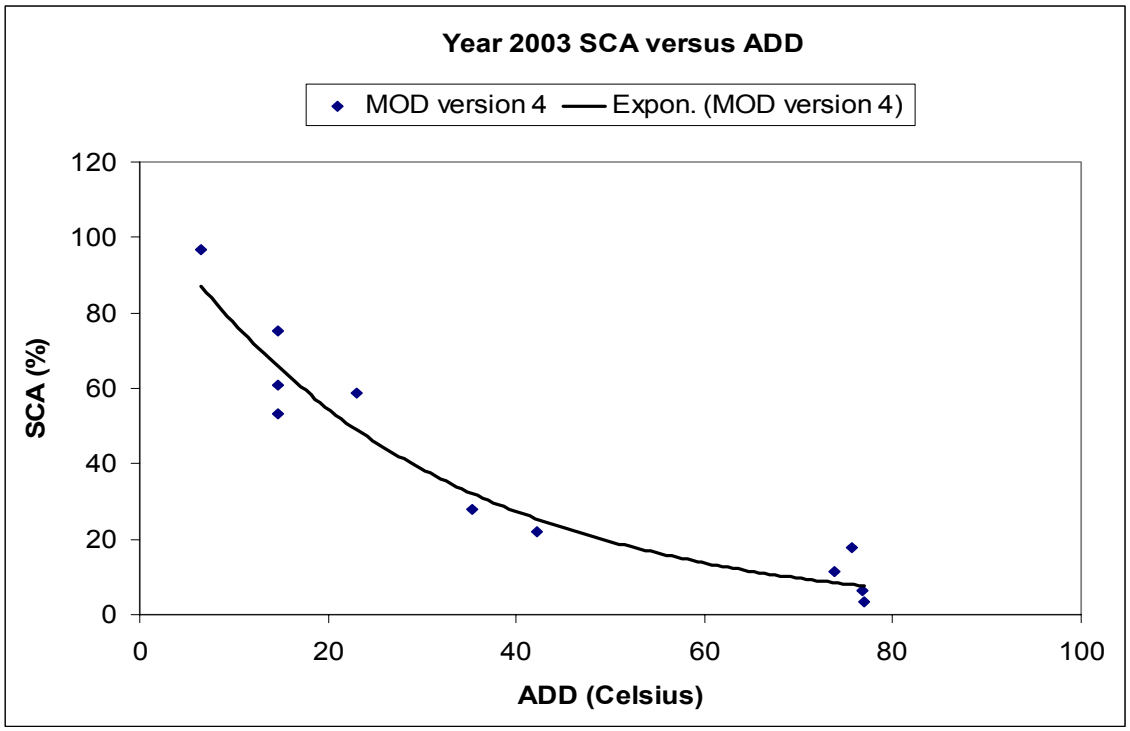

Figure 5.9 Year 2003 SCA versus ADD

The derived coefficient values *a* and *b* along with the coefficient of determination (R^2) for the different algorithms are given in Table 5.1. Adjusted R^2 values have also been evaluated, and minimum reduction was found. The computed high values of R^2 for all fitted trends show that the SCA and accumulated degree-days are highly correlated. However, while the R^2 values indicate high fit relationships, many of the data points are outside of the curves especially in year 2002 and 2003.

Table 5.1 Derived Coefficient Values

Algorithm	Year	*a*	*b*	R^2
LBSM	2001	292.66	0.0437	0.9995
MODIS version 4	2001	613.93	0.0698	0.9996
LBSM	2002	396.85	0.0526	0.9158
MODIS version 4	2002	431.49	0.0526	0.8768
MODIS version 4	2003	109.05	0.0346	0.867

5.4 Elevation Analysis

To further investigate the spatial agreement between the LBSM and Snowmap algorithms during snowmelt, an elevation analysis was carried out. As mentioned in Chapter 3, the elevation range in the study area is from 186.8m to 366.8m, with higher elevations located on the south-west boundary of the study area. A snow depletion trend with respect to the study area elevation range has been observed from the coloured snow maps in Appendix E. The coloured snow maps generated from the LBSM and MOD10A1 products show that snow depleted from higher elevation locations to lower elevation locations.

As stated in Chapter 2, elevation affects the amount of snowmelt in an area. To determine the correlation between elevation ranges and the snow depletion rate of an area, the snowmelt period in year 2002 has been chosen. After using the cloud obscured and distortion input image constraints, year 2002 provided a more detailed snowmelt period compared to year 2001. Five days of snow maps were available during the 12 days of melt. These five days are May 8^{th}, 10^{th}, 13^{th}, 17^{th} and 19^{th}.

The snow maps of these five days are saved into one PIX file. A simple EASI Modelling code has been developed to add the mapped snow cover pixels in each snow map together. The amount of days when a pixel in any snow map is classified as snow was counted. Five is the maximum amount of days a pixel can be classified as snow covered, while zero is the minimum. Another EASI Modelling code was developed to associate the amount of days a pixel can be snow covered with the height range. Since the duration of the year 2002 snowmelt period was not five days, the amount of days covered by snow for pixels in a specific elevation range was averaged out to a maximum of 12 days. Results are shown in Figure 5.10.

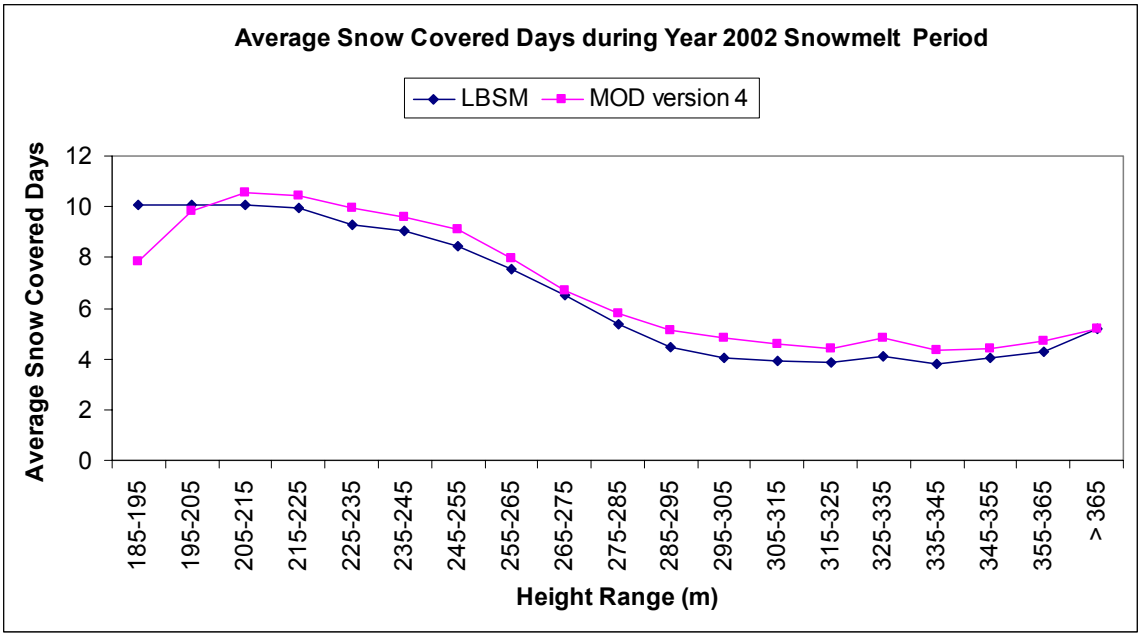

Figure 5.10 Average Snow Covered Day versus Height Range 2002

The LBSM curve in this figure shows that pixels located in lower elevations tend to have a higher than average number of snow covered days. For the curve generated using MOD10A1 Version 4 data, the pixels at the lowest elevations do not behave the same way. Another computation with regards to elevation height range has also been carried

out. In this computation, the average percentage of snow cover change per day in a specific elevation height ranges has been determined. With the elevation data, the number of pixels that fit in specific elevation height range was obtained. From the previous calculation, the maximum amount of pixels once covered by snow in that elevation height range can be determined. With this information the maximum percentage of snow cover for each elevation range was calculated. Then the percentage of snow cover for a specific elevation range per day was computed using the amount of pixels and their specific average snow cover days. After the percentage of snow cover per day was computed, the change in percentages of snow cover during the melt period was averaged for a specific elevation range. Results are shown in Figure 5.11.

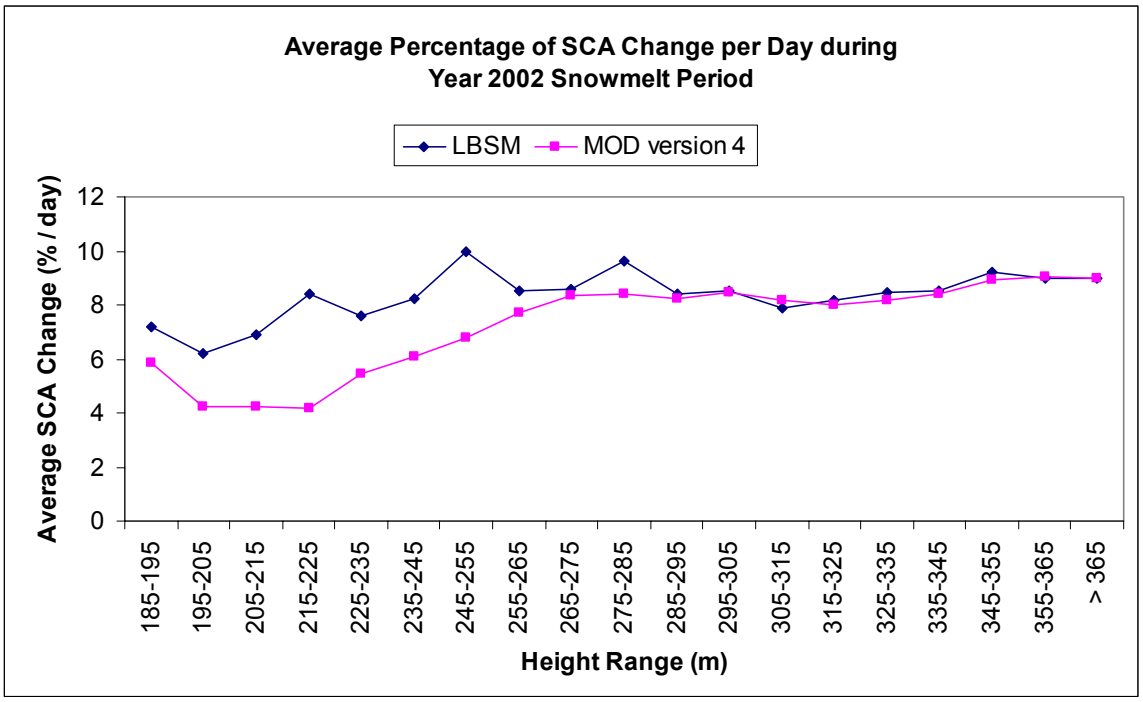

Figure 5.11 Average Percentage of SCA Change versus Height Range 2002

The curves generated from the two algorithms show that pixels located in high elevation areas experienced the most dramatic snow cover change in a day. The same analysis has

also been applied to the MOD10A1 version 2003 data. For year 2003, eleven days of snow maps were available during the 25 days of melt. These eleven days are April 6th, 14th, 15th, 16th, 18th, 20th, 21st, 26th, 27th, 29th and 30th. Average snow covered days at different elevation ranges in year 2003 is shown in Figure 5.12. Average SCA change per day at different elevation ranges in year 2003 is shown in Figure 5.13.

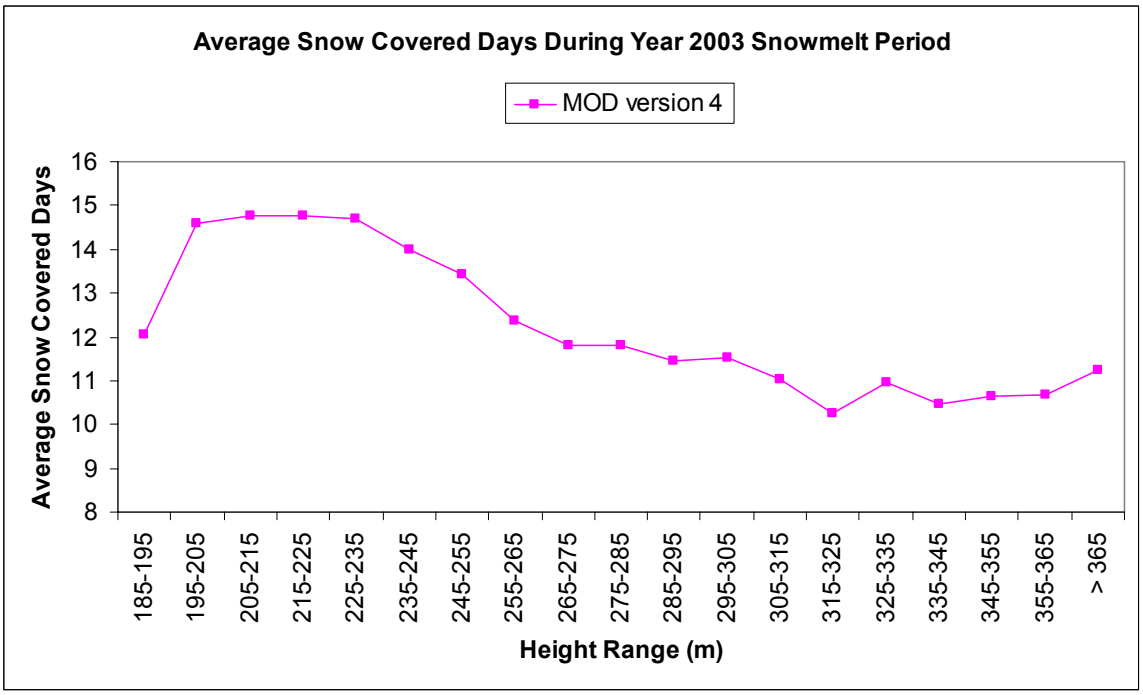

Figure 5.12 Average Snow Covered Days versus Height Range 2003

Figure 5.12 and Figure 5.13 show similar trends to the previous figures. The figure depicting the average snow covered days from year 2003 has again proved that snow cover lasts longer at lower elevations. Figure 5.13 also shows minor SCA changes for different elevations during long snowmelt periods. Comparing Figure 5.11 and Figure 5.13 shows that during a fast snowmelt period, the higher elevation ranges makes a greater difference.

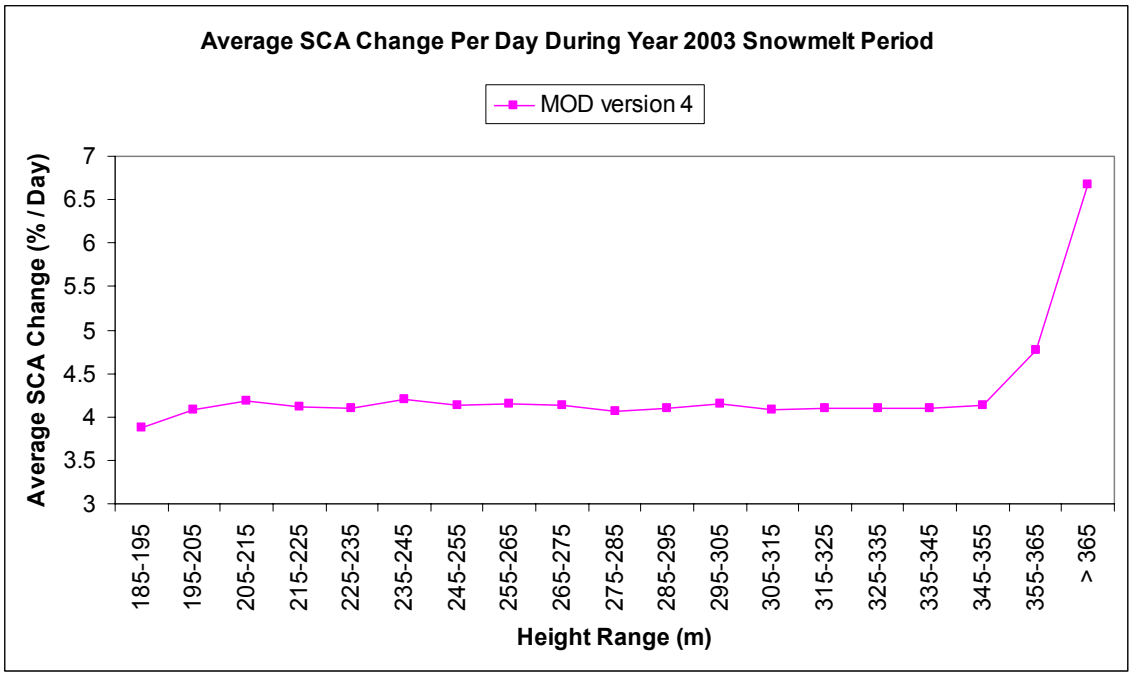

Figure 5.13 Average Percentage of SCA Change versus Height Range 2003

Figure 5.14 and Figure 5.15 show that the relationship between SCA values and ADD for seven different elevation ranges using LBSM and MOD10A1 results for year 2002, respectively. As seen in these figures, the SCA and ADD relationship at different elevation ranges act differently. At low elevations, the amount of SCA remained the same during low ADD, and dramatically decreased during high ADD. On the other hand, at mid to high elevations the relationship between SCA and ADD is more linear. The MODIS SCAs have a more linear relationship with ADD at mid to high elevations as compared to the SCAs derived using the LBSM algorithm. This effect can be explained by the spatial disagreement between the two algorithms, which is due to the different spatial resolution of the input data. The MOD10A1 was originally at 500m spatial resolution, and in this study it was resampled to 100m resolution to match the landcover data.

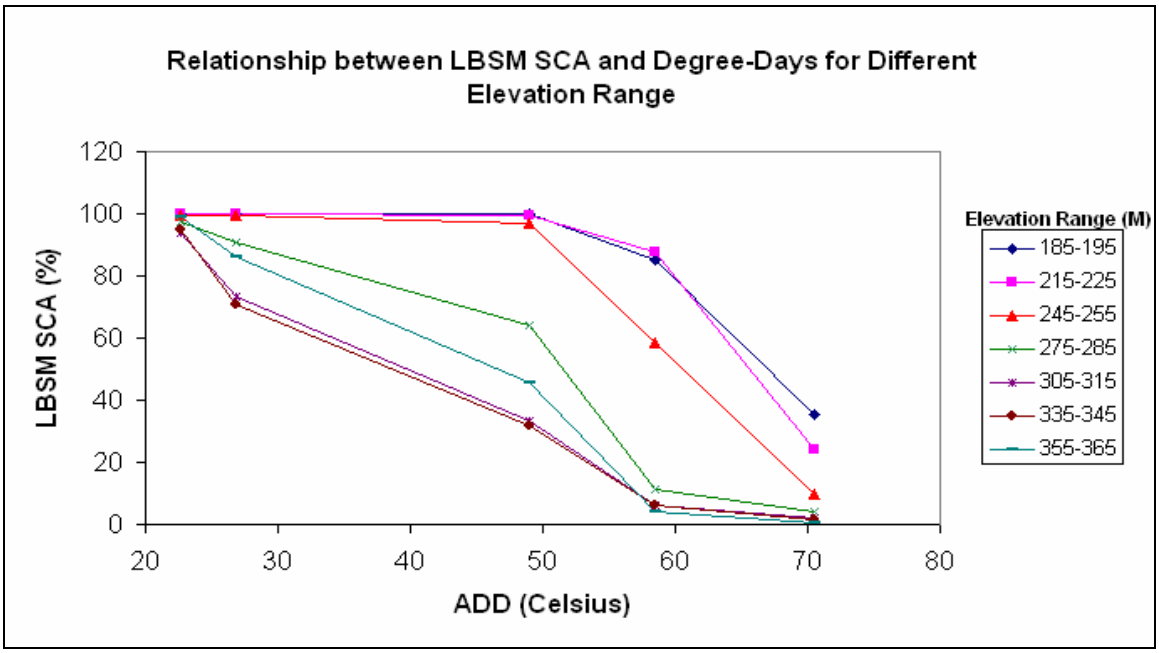

Figure 5.14 LBSM SCA and Degree-Days for Different Elevation Range 2002

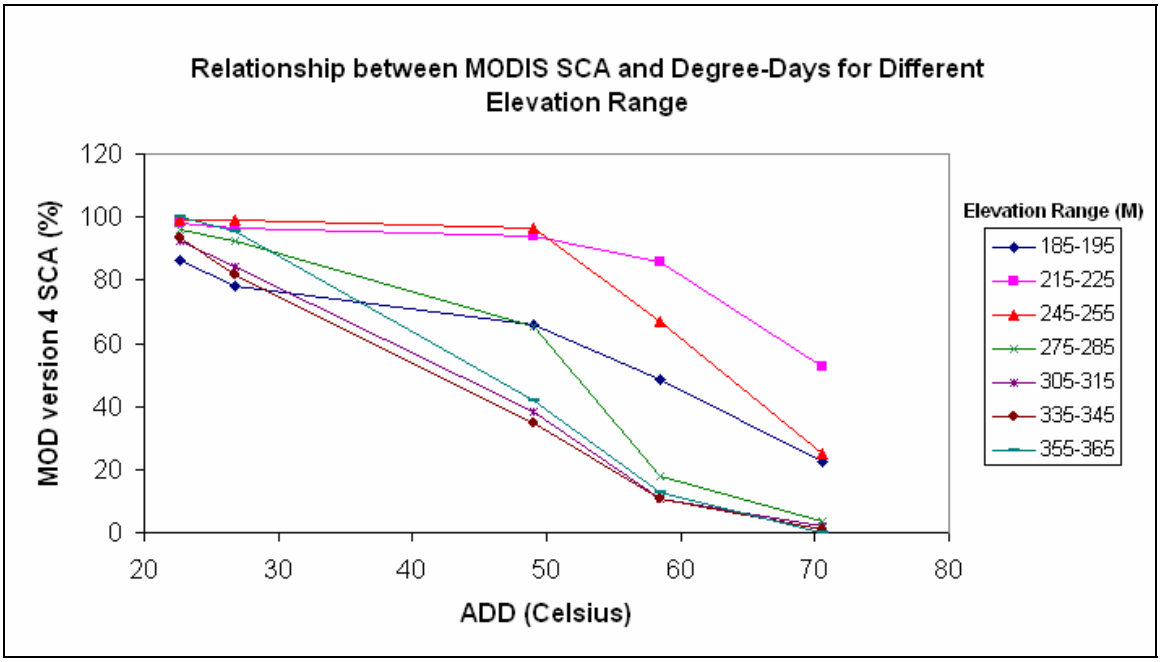

Figure 5.15 MODIS SCA and Degree-Days for Different Elevation Range 2002

Figure 5.16 shows that the relationship between SCA values and ADD with respect to seven different elevation ranges using MOD10A1 results for year 2003. The SCA and ADD relationship at different elevation ranges act differently. At low elevations, the SCA and ADD relationship is more linear. At high elevations, the SCA and ADD relationship is more exponential. The main cause of the difference between the year 2002 and year 2003 SCA and ADD relationship is the duration of melt period.

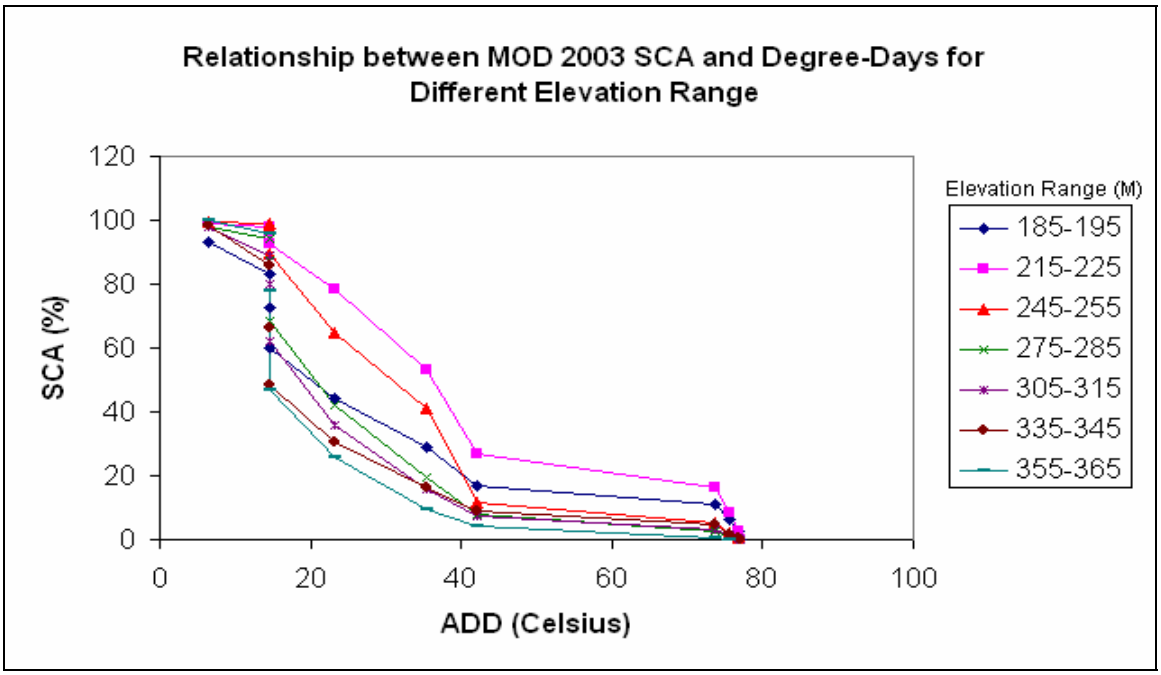

Figure 5.16 MODIS SCA and Degree-Days for Different Elevation Range 2003

The SCAs and degree-days relationship for every elevation range have also been plotted and are shown in Appendix F. The number of pixels per elevation range is also listed. In this elevation analysis, it was shown that for the study area the snow cover at mid to high elevations melted faster than snow cover at low elevations. This also explains why the onsets of Taylor River Watershed snowmelt periods were delayed, in both years as compared to the snowmelt periods of the Burntwood River Watershed.

Chapter 6
Conclusions and Recommendations

In this study, the MODIS snow-mapping algorithm "*Snowmap*" and its ability to map snow cover in forested areas has been investigated. Focus was placed on applying the derived snow cover area (SCA) into runoff models, and discovering the relationship between SCA and accumulated degree-days along with land elevation.

6.1 Snow-Mapping Algorithms

A major limitation of current SCA modelling using optical satellite sensors is snow-mapping in forested areas. The most ideal case for snow-mapping in dense forested areas is to have a landcover data that indicates the location of the forested area and have separate classification criteria for forested and non-forested areas. This study has investigated Snowmap's capabilities in mapping snow in the Northern Boreal Forest of Manitoba. This algorithm uses the NDSI-NDVI field to detect if snow is present in dense forested areas. Three test algorithms have been set up and tested against the publicly available MOD10A1 products. The first algorithm is a simulation of the MODIS Snowmap algorithm called "*Simulated Snowmap*". The second algorithm used the same threshold as in Snowmap, but replaced the NDVI data with landcover data. This algorithm is called "*LandSnow*". The third algorithm used thresholds to adjust the characteristics of the atmospherically corrected input data. This algorithm also used the landcover data with NDSI data instead of the NDSI-NDVI field in the Snowmap algorithm. This algorithm is known as the "*Land-Based Snow-Mapping*" (LBSM) algorithm.

During the study period, both Version 3 and 4 MODIS data were available. Comparisons between the two versions during the study's snowmelt periods indicated minor differences between the computed SCAs. Statistical tests also showed no significant differences between the two product versions. Comparisons among the three test algorithms have shown that both landcover based algorithms mapped more snow in the study periods compared to the Simulated Snowmap algorithm for both years, with the LBSM algorithm mapping the most snow cover for both years. These algorithms all exhibit similar snow depletion trends and statistical tests between the algorithms have resulted in no significant differences. Comparison between the MODIS Version 4 snow products and the results from the test algorithms have also shown minor differences during the melt periods. Statistical tests using all algorithm results for both study years have indicated there are no significant differences among the amounts of SCA mapped by the algorithms. The landcover based algorithms only differ from the Snowmap algorithm greatly during the melt period and this could only be observed in year 2002. It was difficult to determine which type of vegetation caused the difference between landcover based algorithms and MOD10A1 snow products. The MOD10A1 snow products originated in the lower spatial resolution of 500m as compared to the 100m resolution of landcover data hence is difficult to pinpoint any specific vegetation type.

Even though all algorithms mapped similar amounts of SCA during the snowmelt period, the spatial agreement between different algorithms during these periods is low. This effect may be due to the different spatial resolutions of the imagery component used in the algorithms. It may also be caused by the atmospheric scattering effect of non-atmospherically corrected data. An interesting fact that was discovered in the course of the study was that the MODIS snow product does not correct for atmospheric effects. This analysis has shown that the Snowmap algorithm thresholds used in the Simulated Snowmap algorithm are not suitable for application with atmospherically corrected data. This case study has indicated the results generated by applying the LBSM algorithm are

more closely related to the MOD10A1 products as compared to the other two tested algorithms.

6.2 Runoff Model and SCA Relationships

Satellite derived snow cover area (SCA) is an important input parameter for snowmelt modelling, and is used for many hydrological and climatic studies. The variation in SCA also relates to the amount and rate of runoff introduced by the snowmelt process in a watershed. Snowmelt runoff computation in year 2002 using the derived SCA data at a daily time scale was conducted in the Burntwood River and Taylor River watersheds, both of which were located in the study area. A quick verification with streamflow data has indicated the inclusion of these derived SCA data in the runoff computation yielded accurate runoff estimates. LBSM and MODIS snow products derived SCA data have shown to have an exponential relationship with accumulated degree-days. Snow depletion also been investigated in this study. Results have shown that snow located at higher elevation ranges melt faster as compared to snow located at lower elevation ranges. This study also provides the relationship between SCA data and accumulated degree-days at different elevation ranges.

6.3 Difficulties Faced in This Study

During the time of this study, the MODIS sensor is a relatively new sensor. References regarding the new sensor and applied product algorithms were not widely available in literature. Commonly used image processing software did not support the new MODIS EOS-HDF file format. Each downloaded MODIS product file size varies from 11MB to 380MB, therefore taking many hours to download even just one data set. Subsetting options were not available for ordering data from the provider, so it was not possible to reduce the download size. The amount of cloud obscured statistic for the imagery as a

whole or locally were also not available prior to ordering, forcing the download of data sets that proved to be unsuitable for the study.

Since the launch of the satellite and during the time of this study, the MODIS data has gone through three different product versions as researchers become more familiar with the characteristics of the sensor. Even the Version 4 data which was used in this study is not the finalized product version. In the near future, Version 5 data will be available, with changes to the algorithms that are used to generate data. However, the evaluations between the different versions and applied algorithms are difficult to find. Different version products are only available for a certain time frame. Newly acquired data may take weeks to months of processing before there is a release to the public, making it unfeasible for realtime analysis or making relevant SCA predictions for use in hydrological modelling.

At the time of the study, only a few years of data were available for study. As shown in the snowmelt period of year 2001, numerous cloudy days existed and resulted in only a limited number of images that were suitable for analysis. The number of useful images was further reduced because analysis had to take place in the time periods corresponding with rain and snow events during the melt period.

6.4 Recommendations

Due to the fact that optical-based sensors cannot be used to determine the snow depth, which is a useful parameter for determining accurate runoff modelling, snow depth measurements should be included to properly estimate the snow water equivalent values. Different thresholds of the Snowmap snow-mapping algorithm should be tested with the use of atmospherically corrected input. Over time, as more years of data become available, they should be evaluated. With the used of landcover data, a more optimal snow depletion curve should be fitted locally.

References

1. American Society of Civil Engineers. 1996. "Hydrology Handbook," *American Society of Civil Engineers*, 2nd ed., 471 pages.

2. Archer, D. R., Bailey, J. O., Barrett, E. C. and Greenhill, D. 1994. "The Potential of Satellite Remote Sensing of Snow over Great Britain in Relation to Cloud Cover," *Nordic Hydrology,* 25, pages 39-52.

3. Bitner, D., Carroll, T., Cline, D. and Romanov, P. 2002. "An assessment of the differences between three satellite snow cover mapping techniques," *Hydrological Processes.* no. 16, pages 3723-3733.

4. Burkard, M. B., Whiteley, H. R., Schroeter, H. O. and Donald, J. R. 1991. "Snow Depth/Area Relationships for Various Landscape Units in Southwestern Ontario," *Proceedings of 48th Annual Eastern Snow Conference*, Guelph, Ont., Canada, pages 51-65.

5. Buttle, J. M., Creed, I. F., and Pomeroy, J. W. 2000. "Advances in Canadian Forest Hydrology, 1995-1998," *Hydrological Processes*, no. 14, pages 1551-1578.

6. Caves, R., Turpin, O., Clark, C., Ferguson, R. and Quegan, S. 1999. "Comparison of SCA derived from different satellites sensors: implications for hydrological modelling," *Earth Observations: From Data to Information: Proceedings of the 25th Annual Conference and Exhibition of the Remote Sensing Society (Proc. of RSS '99)*, UK, pages 545-552.

7. Colombo, A., Binaghi, E., Lechi, G. and Rampini, A. 1999. "Subpixel estimation of areal extent of snow cover*," Proceedings of The International Society for Optical Engineering (SPIE)*, vol. 3868, pages 434-444.

8. Conboy, B. 2003. *MODIS Home Page*. Last visited December 15, 2003. http://modis.gsfc.nasa.gov/

9. Devore, J. L. 1982. "Probability and statistics for engineering," *Brooks/Cole Publishing Company,* 631 pages.

10. Engeset, R. V., Udnæs, H-C., Guneriussen, T., Koren, H., Malnes, E., Solberg, R. and Alfnes, E. 2003. "Improving Runoff Simulations using Satellite-observed Time-series of Snow Covered Area," *Nordic Hydrology*, 34, no. 4, pages 281-294.

11. Donald, J. R., Soulis, E. D., Kouwen, N. and Pietroniro, A. 1995. "A landcover-based snow cover representation for distributed hydrologic models," *Water Resources Research*, 31, no. 4, pages 995-1009.

12. Environment Canada. 1993. "Canadian Climate Normals 1960-1990," *Canadian Communication Group*, 266 pages.

13. Environment Canada. 2003. "Climate Station Catalogue," *Environmental Canada Website*. Last viewed December 17, 2003. http://www.msc-smc.ec.gc.ca/climate/station_catalogue/index_e.cfm

14. Environment Canada. 2004. "Canadian Climate Normals 1961-1990 – Climate Information – Canadian Climate and Water Information," *Meteorological Service of Canada.* Last viewed January 21, 2004. http://www.msc.ec.gc.ca/climate/climate_normals_1990/climate_info_e.cfm

15. Gomez-Landesa, E., Rango, A. and Hall, D. K. 2001. "Improved snow cover remote sensing for snowmelt runoff forecasting,"*Proceedings symposium of Remote Sensing and Hydrological 2000*, Santa Fe, New Mexico, USA. IAHS Publ. no. 267, pages 61-65.

16. Hall, D. K., Riggs, G. A. and Salomonson, V. V. 1995. "Development of methods for mapping global snow-cover using moderate resolution imaging spectroradiometer data," *Remote Sensing of Environment*, no. 54, pages 127-140.

17. Hall, D. K., Riggs, G. A., Salomonson, V. V. and Scharfen, G. R. 2001a. "Earth Observing System (EOS) Moderate Resolution Imaging Spectroradiometer (MODIS) global snow-cover maps," *Proceedings symposium of Remote Sensing and Hydrological 2000*, Santa Fe, New Mexico, USA. IAHS Publ. no. 267, pages 55-60.

18. Hall, D. K., Riggs, G. A. and Salomonson, V. V. 2001b. "Algorithm Theoretical Basis Document (ATBD) for MODIS Snow and Sea Ice-Mapping Algorithms," *The MODIS Snow/Ice Global Mapping Project Website*. Last visited December 15, 2003. http://modis-snow-ice.gsfc.nasa.gov/atbd.html

19. Hall, D. K., Riggs, G. A., Salomonson, V. V. DiGirolamo, N. E. and Bayr, K. J. 2002. "MODIS Snow-Cover Products," *Remote Sensing of Environment*, no. 83, pages 181-194.

20. Jensen, J. R. 2000. "Remote sensing of the environment: an earth resource perspective," *Prentice-Hall, Inc.,* 544 pages.

21. Johansson, B., Caves, R., Ferguson, R. and Turpin, O. 2001. "Using remote sensing data to update the simulated snowpack of the HBV runoff model," *Proceedings symposium of Remote Sensing and Hydrological 2000*, Santa Fe, New Mexico, USA. IAHS Publ. no. 267, pages 595-597.

22. Klein, A. G., Hall, D. K. and Riggs, G. 1997. "Improving the MODIS global snow-mapping algorithm," *Proceedings of International Geoscience and Remote Sensing Seminar (IGARSS '97)*, Noordwijk, The Netherlands: ESA Publications, pages 619-621

23. Klein, A. G., Hall, D. K. and Seidel, K. 1998a. "Algorithm intercomparison for accuracy assessment of the MODIS snow-mapping algorithm," *Proceedings of the 55th Eastern Snow Conference*, 3-5 June 1998, Jackson, New Hampshire. ESC.

24. Klein, A. G., Hall, D. K. and Riggs, G. A. 1998b. "Improving snow cover mapping in forests through the use of a canopy reflectance model." *Hydrological Processes*, no. 12, pages 1723-1744.

25. Klein, A. G., Hall, D. K. and Riggs, G. A. 1998c. "Global Snow Cover Monitoring Using MODIS," *27th International Symposium on Remote Sensing of Environment*, 8-12 June 1998, Tromsø, pages 363-366.

26. Lindström, G., Johansson, B., Persson, M., Gardelin, M. and Bergström, S. 1997. "Development and test of the distributed HBV-96 hydrological model," *Journal of hydrology*, vol. 201, pages 272-288.

27. Macie, M. 2003. *EOS Data Gateway at redhook.gsfc.nasa.gov Website*. Last visited December 15, 2003. http://redhook.gsfc.nasa.gov/~imswww/pub/imswelcome/

28. Marks, D., Winstral, A., Vactor, S. S. V., Robertson, D. and Davis, R. E. 2001. "Topographic and canopy controls on snow deposition, snow-cover energy balance and snowmelt," *Proceedings symposium of Remote Sensing and Hydrological 2000*, Santa Fe, New Mexico, USA. IAHS Publ. no. 267, pages 129-135.

29. Master, G. M. 1997. "Introduction to Environmental Science and Engineering," *Prentice Hall Inc.*, 2nd ed., 651 pages.

30. Masuoka, E. 2003. *MODIS Land Quality Assessment (QA) Home Page*. Last visited December 15, 2003. http://landdb1.nascom.nasa.gov/QA_WWW/newPage.cgi

31. Maurer, E. P., Rhoads, J. D., Dubayah, R. O. and Lettenmaier, D. P. 2003. "Evaluation of the SCA data product from MODIS," *Hydrological Processes*. no. 17, pages 59-71.

32. McCuen, R. H. 1998. "Hydrologic Analysis and Design," *Prentice-Hall, Inc.*, 2nd ed., 814 pages.

33. McKnight, T. L. 1993. "Physical Geography: A Landscape Appreciation," *Prentice-Hall Inc.*, New Jersey, 626 pages.

34. Metcalfe, R. A. and Buttle, J. M. 1998. "A statistical model of spatially distributed snowmelt rates in a boreal forest basin," *Hydrological Processes*. no. 12, pages 701-1722.

35. Metcalfe, R. A. and Buttle, J. M. 1999. "Semi-Distributed Water Balance Dynamics in a Small Boreal Forest Basin," *Journal of Hydrology*, vol. 226, pages 66-87.

36. Murray, C. D. and Buttle, J. M. 2003. "Impacts of clearcut harvesting on snow accumulation and melt in a northern hardwood forest," *Journal of Hydrology*, vol. 271, pages 197-212.

37. NSIDC. 2003. *The National Snow and Ice Data Center Website.* Last Visited December 15, 2003.
http://nsidc.org/

38. Riggs, G. A. and Hall, D. K. 2002. "Reduction of Cloud Obscuration in the MODIS Snow Data Product." *Presentated at the 59th Easthern Snow Conference*, 5-7 June 2002, Stowe, VT.

39. Riggs, G. A., Hall, D. K. and Salomonson, V. V. 2003. "MODIS Snow Products User Guide for Collection 4 Data Products," *The MODIS Snow/Ice Global Mapping Project Website*. Last visited December 15, 2003.
http://modis-snow-ice.gsfc.nasa.gov/sugkc2.html

40. Rosenthal, W. and Dozier, J. 1996. "Automated mapping of montane snow-cover at subpixel resolution from the Landsat Thematic Mapper," *Water Resources Research*, no. 32, pages 115-130.

41. Schaper, J., Seidel, K. and Martinec, J. 2001. "Precision snow cover and glacier mapping for runoff modelling in a high alpine basin," *Proceedings symposium of Remote Sensing and Hydrological 2000*, Santa Fe, New Mexico, USA. IAHS Publ. no. 267, pages 105-111.

42. Simpson, J. J., Stitt, J. R. and Sienko, M. 1998. "Improved estimates of the areal extent of snow cover from AVHRR data," *Journal of Hydrology*, vol. 204, pages 1-23.

43. Singh, V. P. 1992. "To Hydrologists and Water Scientists Around the Globe," *Prentice-Hall, Inc.,* 973 pages.

44. Singh, P. and Singh, V. P. 2001. "Snow and Glacier Hydrology," *Kluwer Academic Publishers*, 742 pages.

45. Singh, P. 2003. "Relating Air Temperature to the Depletion of Snow Covered Area in a Himalayan Basin," *Nordic Hydrology*, 34, no. 4, pages 267-280.

46. St. Laurent. 2003. "GIS Assisted Distributed Hydrological Modelling in the High Boreal Forest of Northern Manitoba," *MSc Thesis, Department of Civil Engineering, University of Manitoba, Winnipeg*, MB, 241 pages and appendix.

47. Strabala, K. 2003. "MODIS Cloud Mask User's Guide," *Cooperative Institute for Meteorological Satellite Studies Website*. Last Viewed December 15, 2003. http://cimss.ssec.wisc.edu/modis1/pdf/CMUSERSGUIDE.PDF

48. Tait, A., Barton, J. and Hall, F. 2001. "A prototype MODIS-SSM/I snow-mapping method," *Proceedings symposium of Remote Sensing and Hydrological 2000*, Santa Fe, New Mexico, USA. IAHS Publ, no. 267, pages 139-140.

49. U.S. Army Corps of Engineers. 1956. "Snow Hydrology," *North Pacific Division*, U.S. Army Corps of Engineers, Portland, Ore., June 30.

50. Viessman, W., Knapp, J. W., Lewis, G. L. and Harbaugh, T. E. 1977. "Introduction to Hydrology," *Harper & Row, Publishers, Inc.,* 2nd ed., 704 pages.

51. Walpole, R. E., Myers, R. H. and Myers, S. L. 1998. "Probability and statistics for engineers and scientists," *Prentice Hall, Inc.,* 6th ed., 739 pages.

52. Ward, A. D. and Elliot, W. J. 1995. "Environmental Hydrology," *Lewis Publishers*, 462 pages.

53. Wildlands League. 2002. "2002 Boreal Expedition Slideshow," *Wildlands League Website*. Last visited December 17, 2003. http://www.wildlandsleague.org/slideshow.html

54. Winther, J-G. and Hall, D. K. 1999. "Satellite-derived snow coverage related to hydropower production in Norway: present and future," *International Journal of Remote Sensing*, vol. 20, no. 15&16, pages 2991-3008.

Appendix A – MOD10A2 Products

Year 2001

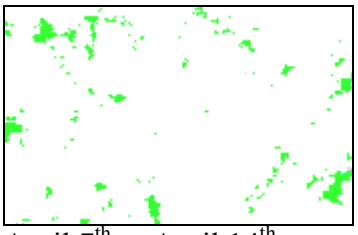

April 7th to April 14th

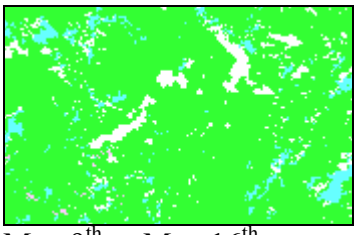

May 9th to May 16th

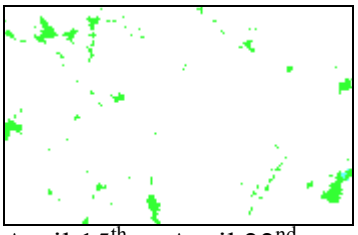

April 15th to April 22nd

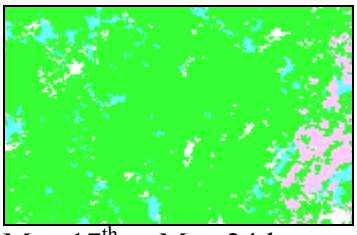

May 17th to May 24th

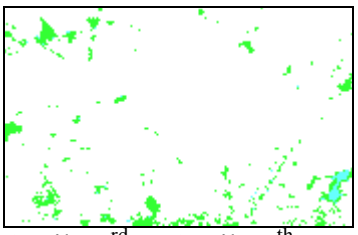

April 23rd to April 30th

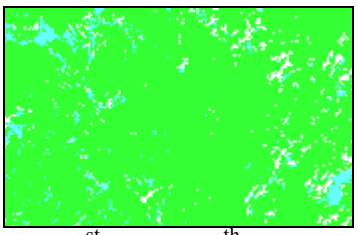

May 1st to May 8th

Year 2002

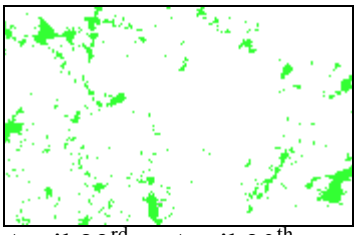

April 23rd to April 30th

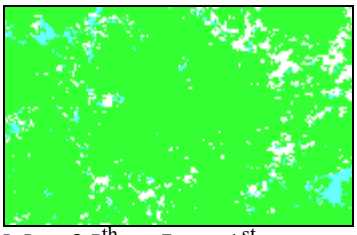

May 25th to June 1st

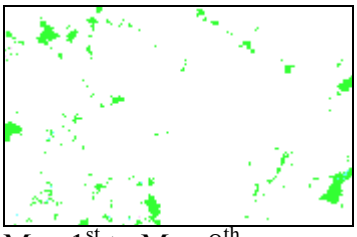

May 1st to May 8th

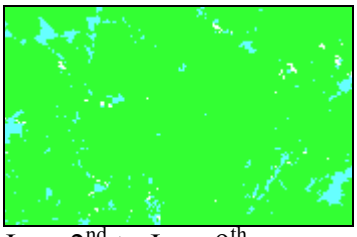

June 2nd to June 9th

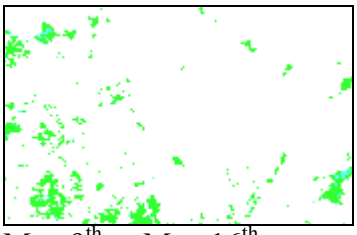

May 9th to May 16th

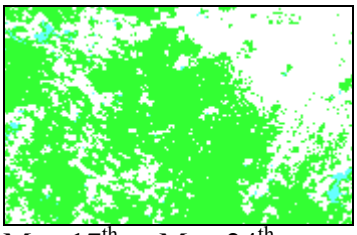

May 17th to May 24th

Appendix B – PCI Code

```
REM %1=MODISch1 %2=MODISch2 %3=MODISch4 %4=MODISch6
REM %5 = landcover data
REM %6 = MOD10A1 version 4 data

REM %7 = NDSI
REM %8 = NDVI
REM %9 = Simulated Snowmap
REM %10 = LBSM

REM %11 = MOD10A1 vs Simulated Snowmap
REM %12 = MOD10A1 vs LBSM

REM %13 = Simulated Snowmap exclude MOD10A1 water pixels
REM %14 = LBSM exclude MOD10A1 water pixels
REM %15 = MOD10A1 exclude landcover rivers, lakes and border pixels
REM %16 = MOD10A1 exclude LBSM water and dark target pixels

REM %17 = LandSnow
REM %18 = MOD10A1 vs LandSnow
REM %19 = LandSnow exclude MOD10A1 water pixels


REM calculate NDSI values
%7=(%3-%4)/(%3+%4);
REM calculate NDVI values
%8=(%2-%1)/(%2+%1);


REM SIMULATED SNOWMAP ALGORITHM AND LANDSNOW
REM to separate snow vs water
if(%2>1100)then
        REM to avoid dark targets
        if(%3>=1000)then

                REM SIMULATED SNOWMAP
                REM check for vegetation using NDVI value
                if(%8>=0.1)then
                        if(%8>=0.25)then
                                if(%7>=(0.0652*f$exp(1.8069*%8)))then
                                        %9=1;
                                else
                                        %9=0;
                                endif
                        else
                                if(%7>=((%8-0.2883)/(-0.4828)))then
                                        %9=1;
                                else
                                        %9=0;
```

```
                                        endif
                                endif
                        REM not classify as vegetation
                        else
                                if(%7>=0.4)then
                                        %9=1;
                                else
                                        %9=0;
                                endif
                        endif

                        REM LANDSNOW
                        REM check for vegetation using landcover data
                        if(%5<=722)then
                                if(%7>0)then
                                        %17=1;
                                else
                                        %17=0;
                                endif
                        REM not classify as vegetation
                        else
                                if(%7>=0.4)then
                                        %17=1;
                                else
                                        %17=0;
                                endif
                        endif

        REM pixel is dark target
        else
                %9=42;
                %17=42;
        endif
REM pixel is water
else
        %9=48;
        %17=48;
endif


REM LBSM ALGORITHM
REM to separate snow vs water
if(%2>600)then
        REM to avoid dark targets
        if(%3>=500)then
                REM check for vegetation using landcover data
                if(%5<=722)then
                        if(%7>0)then
                                %10=1;
                        else
                                %10=0;
```

```
                endif
            REM not classify as vegetation
            else
                if(%7>0.25)then
                    %10=1;
                else
                    %10=0;
                endif
            endif
        REM pixel is dark target
        else
            %10=42;
        endif
REM pixel is water
else
        %10=48;
endif


REM to exclude cloud obscured pixels using MOD10A1 data
if(%6=50)then
        %9=50;
        %10=50;
        %17=50;
endif


REM to exclude no production mask, no decision and missing data pixels using MOD10A1 data
if((%6=255)OR(%6=1)OR(%6=0))then
        %9=255;
        %10=255;
        %17=255;
endif


REM to exclude river and lake pixels using landcover data
if((%5=900)OR(%5=901))then
        %6=102;
        %9=102;
        %10=102;
        %17=102;
endif


REM exclude border pixels using landcover data
if((%5=-9999)OR(%5=0))then
        %6=-3;
        %9=-3;
        %10=-3;
        %17=-3;
endif
```

```
REM to determine spatial agreement between the algorithms
REM MOD10A1 vs Simulated Snowmap
if(%6=200)then
        if(%9=1)then
                %11=1;
        else
                %11=%9;
        endif
else
        %11=-10;
endif

REM MOD10A1 vs LBSM
if(%6=200)then
        if(%10=1)then
                %12=1;
        else
                %12=%10;
        endif
else
        %12=-10;
endif

REM MOD10A1 vs LandSnow
if(%6=200)then
        if(%17=1)then
                %18=1;
        else
                %18=%17;
        endif
else
        %18=-10;
endif


REM to save another copy of the test algorithms result
%13=%9;
%14=%10;
%19=%17;


REM to exclude lake ice and inland water pixels from MOD10A1 data
if((%6=100)OR(%6=37))then
        %13=100;
        %14=100;
        %19=100;
endif


REM MOD10A1 data that excluded rivers, lakes, and border pixels from landcover data
%15=%6;
```

```
REM MOD10A1 data that excluded water and dark targets from LBSM exclude
%16=%15;
if((%14=42)OR(%14=48))then
        %16=42;
endif
```

Appendix C – Case Studies Statistical Test Results

Case Study	Year	Sample 1	Sample 2	m	n	Wm	Wn	z	are Significant Different if
Case 4.1.1	Year 2001	LBSM	Simulated Snowmap	3	3	12	9		W ≥ 15 or W ≤ 6
		LBSM	LandSnow	3	3	12	9		W ≥ 15 or W ≤ 6
		LandSnow	Simulated Snowmap	3	3	12	9		W ≥ 15 or W ≤ 6
	Year 2002	LBSM	Simulated Snowmap	6	6	43	35		W ≥ 52 or W ≤ 26
		LBSM	LandSnow	6	6	42	36		W ≥ 52 or W ≤ 26
		LandSnow	Simulated Snowmap	6	6	42	36		W ≥ 52 or W ≤ 26
Case 4.1.2	Year 2001	MOD V3	MOD V4	9	9	95		0.84	z ≥ 1.96 or z ≤ −1.96
		MOD V3 w/o Cloudy Days	MOD V4 w/o Cloudy Days	4	4	20	16		W ≥ 25 or W ≤ 11
	Year 2002	MOD V3	MOD V4	15	15	200		-1.35	z ≥ 1.96 or z ≤ −1.96
		MOD V3 w/o Cloudy Days	MOD V4 w/o Cloudy Days	11	11	105		-1.41	z ≥ 1.96 or z ≤ −1.96
Case 4.1.3	Year 2001	LBSM	MOD V4	3	3	12	9		W ≥ 15 or W ≤ 6
		Similated Snowmap	MOD V4	3	3	12	9		W ≥ 15 or W ≤ 6
		LandSnow	MOD V4	3	3	12	9		W ≥ 15 or W ≤ 6
	Year 2002	LBSM	MOD V4	6	6	36	36		W ≥ 52 or W ≤ 26
		Similated Snowmap	MOD V4	6	6	37	41		W ≥ 52 or W ≤ 26
		LandSnow	MOD V4	6	6	37	41		W ≥ 52 or W ≤ 26

*α = 0.05

Appendix D – LBSM Results and MOD10A1 Products

LBSM Year 2001 Results

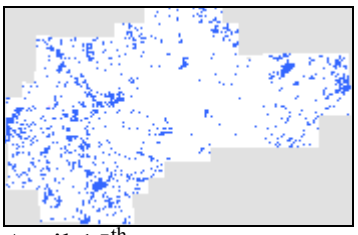
April 15th

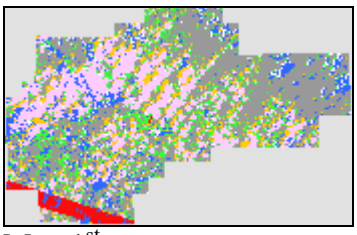
May 1st

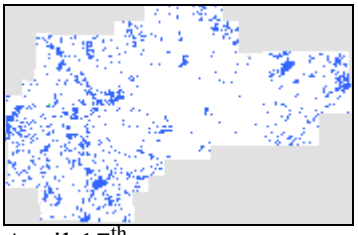
April 17th

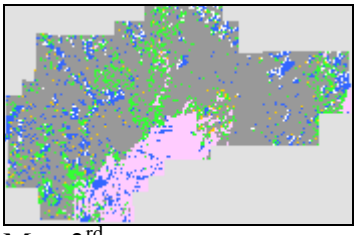
May 3rd

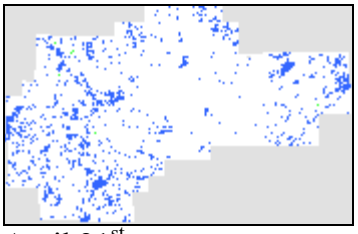
April 21st

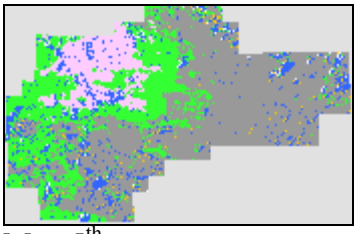
May 5th

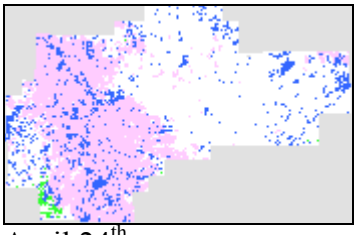
April 24th

Legend

- land
- snow
- lake ice
- missing data
- no decision
- non-production mask
- water
- dark target
- cloud obscured
- inland water
- lake or river
- boundary

MOD10A1 Year 2001 Products

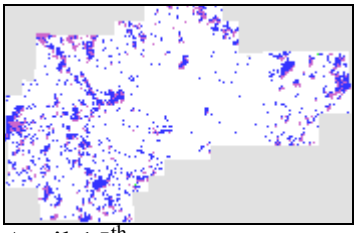
April 15th

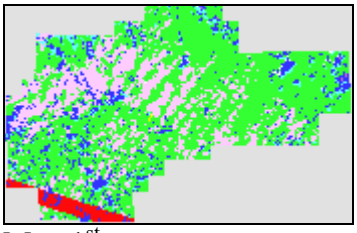
May 1st

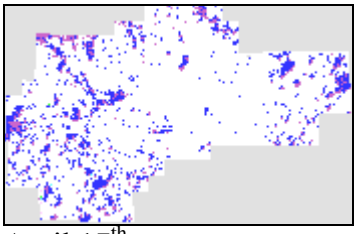
April 17th

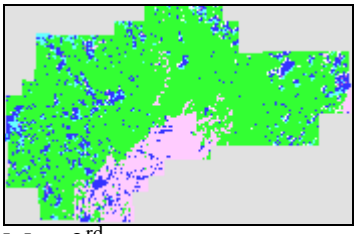
May 3rd

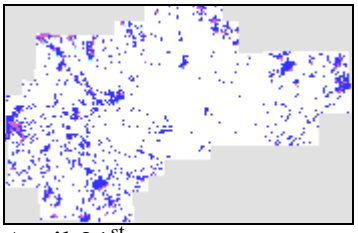
April 21st

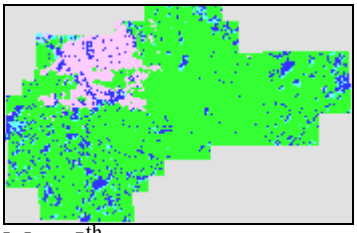
May 5th

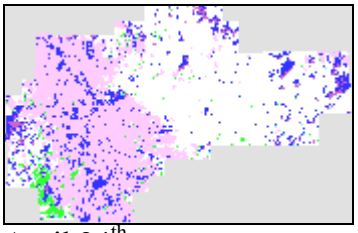
April 24th

Legend

- land
- snow
- lake ice
- missing data
- no decision
- non-production mask
- water
- dark target
- cloud obscured
- inland water
- lake or river
- boundary

LBSM Year 2002 Results

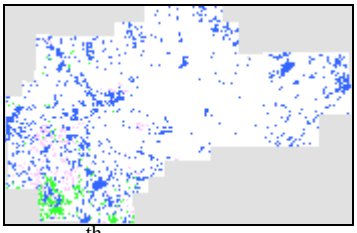
May 8th

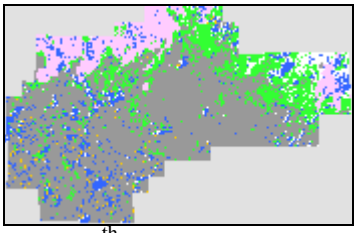
May 20th

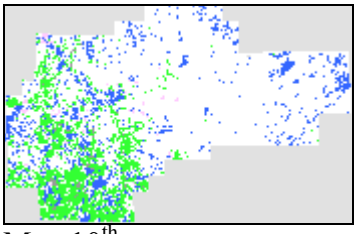
May 10th

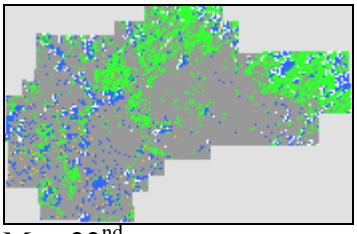
May 22nd

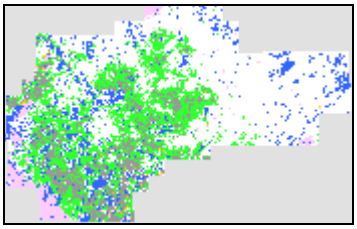
May13th

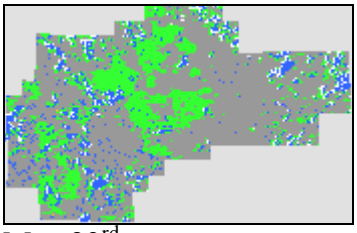
May 23rd

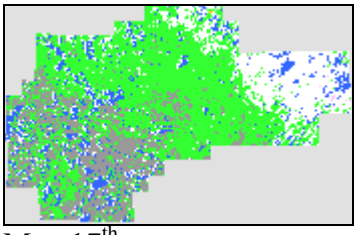
May 17th

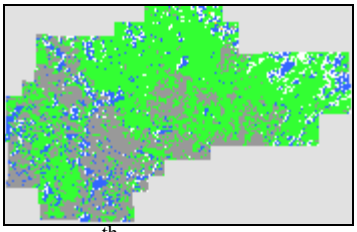
May 19th

Legend

- land
- snow
- lake ice
- missing data
- no decision
- non-production mask
- water
- dark target
- cloud obscured
- inland water
- lake or river
- boundary

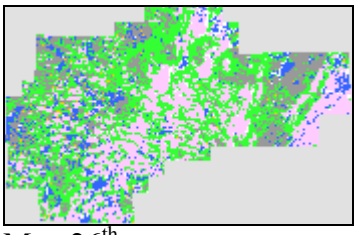

May 26th

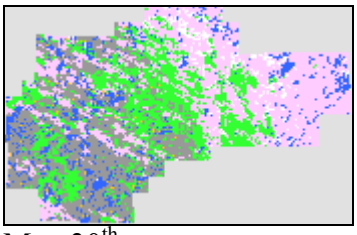

May 30th

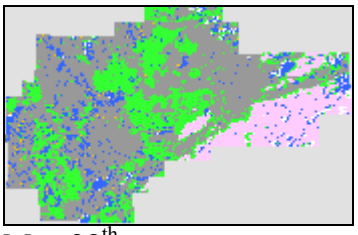

May 28th

Legend

- land
- snow
- lake ice
- missing data
- no decision
- non-production mask
- water
- dark target
- cloud obscured
- inland water
- lake or river
- boundary

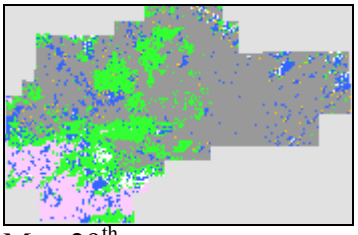

May 29th

MOD10A1 Year 2002 Products

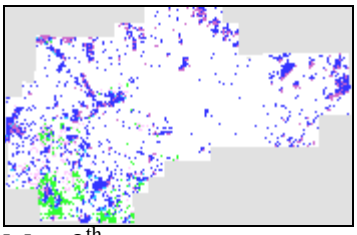
May 8th

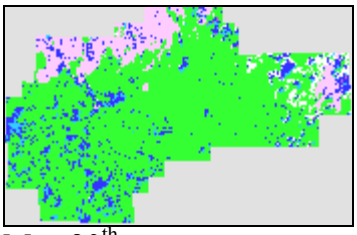
May 20th

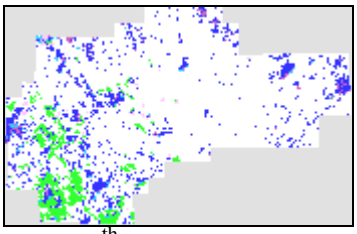
May 10th

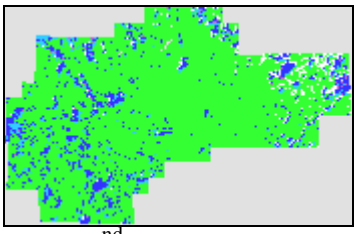
May 22nd

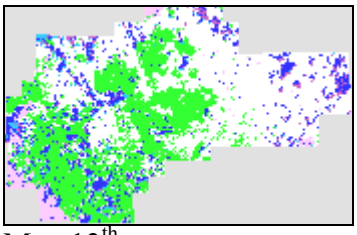
May 13th

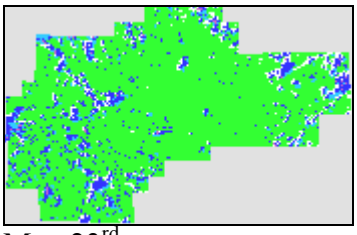
May 23rd

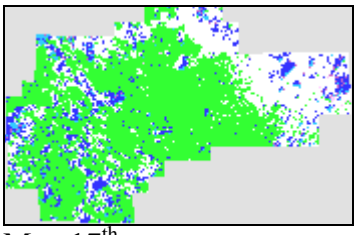
May 17th

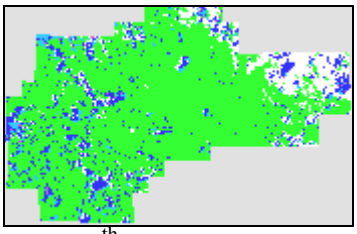
May 19th

Legend

- land
- snow
- lake ice
- missing data
- no decision
- non-production mask
- water
- dark target
- cloud obscured
- inland water
- lake or river
- boundary

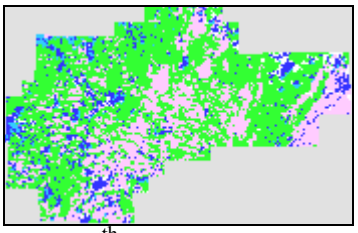

May 26th

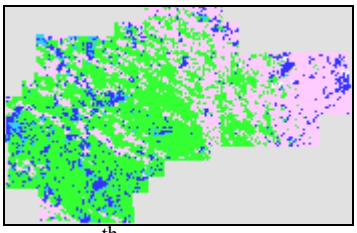

May 30th

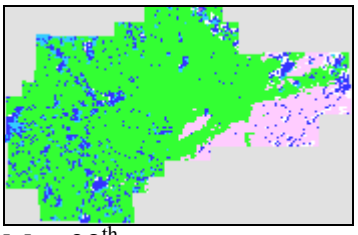

May 28th

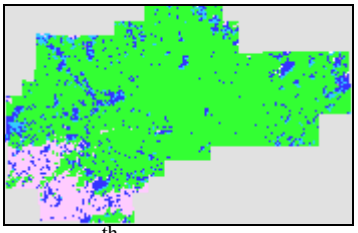

May 29th

Legend

- land
- snow
- lake ice
- missing data
- no decision
- non-production mask
- water
- dark target
- cloud obscured
- inland water
- lake or river
- boundary

Appendix E – Runoff Computation Results

Date of Year 2002	Mean Temperature (ºF)	Rain (inches)	Snow (cm)
11-Apr	36.32	0	0.5
12-Apr	37.49	0	0
13-Apr	39.11	0.007874016	0
14-Apr	34.34	0.017716535	4.5
15-Apr	21.245	0	2.15
16-Apr	22.46	0	5.15
17-Apr	23	0	8.1
18-Apr	21.47	0	0.3
19-Apr	23.09	0	0.05
20-Apr	25.97	0	0
21-Apr	36.68	0	0
22-Apr	42.215	0.017716535	0
23-Apr	30.155	0.127952756	8.65
24-Apr	15.17	0	7.45
25-Apr	18.005	0	0
26-Apr	20.165	0	0.05
27-Apr	23.72	0	0
28-Apr	33.755	0.082677165	0
29-Apr	35.78	0	0.25
30-Apr	30.83	0	0.05
01-May	26.915	0	0.5
02-May	28.4	0.098425197	1
03-May	29.435	0.076771654	8.55
04-May	21.29	0	1.85
05-May	24.125	0	0
06-May	26.51	0	0
07-May	29.345	0	0

Date of Year 2002	Mean Temperature (ºF)	Rain (inches)	Snow (cm)
08-May	33.17	0	0
09-May	35.15	0	0
10-May	36.23	0	0
11-May	46.67	0	0
12-May	45.32	0.05511811	0
13-May	43.925	0.007874016	0
14-May	42.89	0.102362205	0.1
15-May	30.2	0	0.05
16-May	32.54	0	0
17-May	37.625	0	0
18-May	41.36	0	0
19-May	44.375	0	0
20-May	51.485	0	0
21-May	44.465	0	0
22-May	35.465	0	0
23-May	35.015	0	0
24-May	39.38	0	0
25-May	46.535	0.035433071	0
26-May	51.215	0.003937008	0
27-May	59.315	0	0
28-May	50.9	0	0
29-May	52.115	0.13976378	0

Date of Year 2002	Burntwood River Watershed					
	LBSM K = 0.103			MODIS K = 0.098		
	Melt (mm)	SWE (mm)	Q(mm)	Melt (mm)	SWE (mm)	Q(mm)
11-Apr	11.30	139.66	11.30	10.75	140.21	11.30
12-Apr	14.36	125.30	14.36	13.67	126.54	13.67
13-Apr	19.88	105.41	19.88	18.98	107.56	18.98
14-Apr	7.40	102.51	7.40	7.10	104.96	7.10
15-Apr	0.00	104.66	0.00	0.00	107.11	0.00
16-Apr	0.00	109.81	0.00	0.00	112.26	0.00
17-Apr	0.00	117.91	0.00	0.00	120.36	0.00
18-Apr	0.00	118.21	0.00	0.00	120.66	0.00
19-Apr	0.00	118.26	0.00	0.00	120.71	0.00
20-Apr	0.00	118.26	0.00	0.00	120.71	0.00
21-Apr	12.24	106.02	12.24	11.65	109.06	11.65
22-Apr	28.03	77.99	28.03	26.73	82.33	26.73
23-Apr	0.00	86.64	0.00	0.00	90.98	0.00
24-Apr	0.00	94.09	0.00	0.00	98.43	0.00
25-Apr	0.00	94.09	0.00	0.00	98.43	0.00
26-Apr	0.00	94.14	0.00	0.00	98.48	0.00
27-Apr	0.00	94.14	0.00	0.00	98.48	0.00
28-Apr	5.89	88.26	5.89	5.66	92.82	5.66
29-Apr	9.89	78.62	9.89	9.41	83.66	9.41
30-Apr	0.00	78.67	0.00	0.00	83.71	0.00
01-May	0.00	79.17	0.00	0.00	84.21	0.00
02-May	0.00	80.17	0.00	0.00	85.21	0.00
03-May	0.00	88.72	0.00	0.00	93.76	0.00
04-May	0.00	90.57	0.00	0.00	95.61	0.00
05-May	0.00	90.57	0.00	0.00	95.61	0.00
06-May	0.00	90.57	0.00	0.00	95.61	0.00
07-May	0.00	90.57	0.00	0.00	95.61	0.00
08-May	3.06	87.64	2.93	2.91	92.96	2.65
09-May	8.24	80.52	7.12	7.84	85.89	7.07
10-May	11.07	72.00	8.52	10.53	76.48	9.41
11-May	38.38	47.14	24.86	36.52	49.69	26.79
12-May	36.25	28.10	19.70	34.56	29.86	20.43
13-May	32.48	15.01	13.20	30.97	17.03	12.94
14-May	29.96	5.52	11.36	28.58	7.15	11.67
15-May	0.00	5.57	0.00	0.00	7.20	0.00
16-May	1.41	5.35	0.22	1.34	6.91	0.30
17-May	14.72	4.28	1.07	14.00	4.74	2.17
18-May	24.49	2.91	1.38	23.30	2.46	2.28
19-May	32.38	1.62	1.29	30.80	1.19	1.26
20-May	50.98	0.62	1.00	48.50	1.10	0.09

Date of Year 2002	Taylor River Watershed					
	LBSM K = 0.066			MODIS K = 0.061		
	Melt (mm)	SWE (mm)	Q(mm)	Melt (mm)	SWE (mm)	Q(mm)
11-Apr	7.24	143.72	7.24	6.69	144.27	6.69
12-Apr	9.20	134.51	9.20	8.51	135.76	8.51
13-Apr	13.20	121.32	13.20	12.30	123.46	12.30
14-Apr	5.20	120.62	5.20	4.90	123.06	4.90
15-Apr	0.00	122.77	0.00	0.00	125.21	0.00
16-Apr	0.00	127.92	0.00	0.00	130.36	0.00
17-Apr	0.00	136.02	0.00	0.00	138.46	0.00
18-Apr	0.00	136.32	0.00	0.00	138.76	0.00
19-Apr	0.00	136.37	0.00	0.00	138.81	0.00
20-Apr	0.00	136.37	0.00	0.00	138.81	0.00
21-Apr	7.85	128.52	7.85	7.25	131.56	7.25
22-Apr	18.43	110.09	18.43	17.13	114.43	17.13
23-Apr	0.00	118.74	0.00	0.00	123.08	0.00
24-Apr	0.00	126.19	0.00	0.00	130.53	0.00
25-Apr	0.00	126.19	0.00	0.00	130.53	0.00
26-Apr	0.00	126.24	0.00	0.00	130.58	0.00
27-Apr	0.00	126.24	0.00	0.00	130.58	0.00
28-Apr	4.24	122.01	4.24	4.01	126.57	4.01
29-Apr	6.34	115.92	6.34	5.86	120.96	5.86
30-Apr	0.00	115.97	0.00	0.00	121.01	0.00
01-May	0.00	116.47	0.00	0.00	121.51	0.00
02-May	0.00	117.47	0.00	0.00	122.51	0.00
03-May	0.00	126.02	0.00	0.00	131.06	0.00
04-May	0.00	127.87	0.00	0.00	132.91	0.00
05-May	0.00	127.87	0.00	0.00	132.91	0.00
06-May	0.00	127.87	0.00	0.00	132.91	0.00
07-May	0.00	127.87	0.00	0.00	132.91	0.00

Date of Year 2002	Taylor River Watershed					
	LBSM K = 0.066			MODIS K = 0.061		
	Melt (mm)	SWE (mm)	Q(mm)	Melt (mm)	SWE (mm)	Q(mm)
08-May	1.96	125.91	1.96	1.81	131.10	1.81
09-May	5.28	120.63	5.28	4.88	126.22	4.88
10-May	7.09	113.54	7.09	6.55	119.66	6.55
11-May	24.59	88.94	24.59	22.73	96.93	22.73
12-May	23.73	65.21	23.73	22.04	74.89	22.04
13-May	21.28	44.07	21.15	19.76	55.78	19.12
14-May	19.72	25.47	18.83	18.34	38.68	17.36
15-May	0.00	25.52	0.00	0.00	38.73	0.00
16-May	0.91	24.75	0.77	0.84	38.00	0.74
17-May	9.43	17.12	7.63	8.72	30.59	7.40
18-May	15.69	10.00	7.12	14.50	21.79	8.81
19-May	20.75	7.96	2.04	19.17	14.79	7.00
20-May	32.66	3.86	4.10	30.19	8.75	6.04
21-May	20.90	2.14	1.72	19.31	5.77	2.97
22-May	5.81	1.92	0.22	5.37	5.20	0.58
23-May	5.05	1.78	0.13	4.67	4.92	0.28
24-May	12.37	1.51	0.27	11.43	4.37	0.55
25-May	25.73	1.06	1.33	23.88	3.51	1.73
26-May	33.50	0.64	0.52	31.06	2.74	0.86
27-May	45.79	0.24	0.40	42.32	2.05	0.70
28-May	31.68	0.08	0.16	29.28	1.80	0.24
29-May	35.49	0.04	3.58	32.94	1.80	3.55

Date of Year 2002	Burntwood River Watershed			Taylor River Watershed		
	Traditional K = 0.051			Traditional K = 0.024		
	Melt (mm)	SWE (mm)	Q(mm)	Melt (mm)	SWE (mm)	Q(mm)
11-Apr	5.60	145.36	5.60	2.63	148.33	2.63
12-Apr	7.11	138.25	7.11	3.35	144.98	3.35
13-Apr	10.49	127.76	10.49	5.61	139.37	5.61
14-Apr	4.31	127.95	4.31	2.70	141.16	2.70
15-Apr	0.00	130.10	0.00	0.00	143.31	0.00
16-Apr	0.00	135.25	0.00	0.00	148.46	0.00
17-Apr	0.00	143.35	0.00	0.00	156.56	0.00
18-Apr	0.00	143.65	0.00	0.00	156.86	0.00
19-Apr	0.00	143.70	0.00	0.00	156.91	0.00
20-Apr	0.00	143.70	0.00	0.00	156.91	0.00
21-Apr	6.06	137.64	6.06	2.85	154.06	2.85
22-Apr	14.53	123.11	14.53	7.53	146.53	7.53
23-Apr	0.00	131.76	0.00	0.10	155.08	0.10
24-Apr	0.00	139.21	0.00	0.00	162.53	0.00
25-Apr	0.00	139.21	0.00	0.00	162.53	0.00
26-Apr	0.00	139.26	0.00	0.00	162.58	0.00
27-Apr	0.00	139.26	0.00	0.00	162.58	0.00
28-Apr	3.57	135.69	3.57	2.37	160.21	2.37
29-Apr	4.90	131.04	4.90	2.30	158.16	2.30
30-Apr	0.00	131.09	0.00	0.00	158.21	0.00
01-May	0.00	131.59	0.00	0.00	158.71	0.00
02-May	0.00	132.59	0.00	0.00	159.71	0.00
03-May	0.00	141.14	0.00	0.00	168.26	0.00
04-May	0.00	142.99	0.00	0.00	170.11	0.00
05-May	0.00	142.99	0.00	0.00	170.11	0.00
06-May	0.00	142.99	0.00	0.00	170.11	0.00
07-May	0.00	142.99	0.00	0.00	170.11	0.00
08-May	1.52	141.47	1.52	0.71	169.39	0.71

Date of Year 2002	Burntwood River Watershed			Taylor River Watershed		
	Traditional K = 0.051			Traditional K = 0.024		
	Melt (mm)	SWE (mm)	Q(mm)	Melt (mm)	SWE (mm)	Q(mm)
09-May	4.08	137.39	4.08	1.92	167.47	1.92
10-May	5.48	131.91	5.48	2.58	164.89	2.58
11-May	19.00	112.91	19.00	8.94	155.95	8.94
12-May	18.66	94.26	18.66	9.52	146.43	9.52
13-May	16.73	77.52	16.73	8.56	137.87	8.56
14-May	15.58	62.05	15.58	8.11	129.87	8.11
15-May	0.00	62.10	0.00	0.00	129.92	0.00
16-May	0.70	61.40	0.70	0.33	129.59	0.33
17-May	7.29	54.11	7.29	3.43	126.16	3.43
18-May	12.12	41.99	12.12	5.71	120.45	5.71
19-May	16.03	25.95	16.03	7.54	112.91	7.54
20-May	25.24	0.71	25.24	11.88	101.03	11.88
21-May				7.60	93.43	7.60
22-May				2.11	91.32	2.11
23-May				1.84	89.48	1.84
24-May				4.50	84.98	4.50
25-May				10.22	74.76	10.22
26-May				13.00	61.77	13.00
27-May				35.38	26.38	35.38
28-May				11.52	14.86	11.52
29-May				14.03	0.83	14.03

Appendix F – SCA versus Accumulated Degree-days

Height Range (m)	Number of Pixels
185-195	7596
195-205	11602
205-215	18549
215-225	27361
225-235	33406
235-245	65913
245-255	71626
255-265	85399
265-275	117247
275-285	158688
285-295	202502
295-305	227502
305-315	187556
315-325	135295
325-335	77551
335-345	45622
345-355	8214
355-365	1196
> 365	37

LBSM SCA 2002

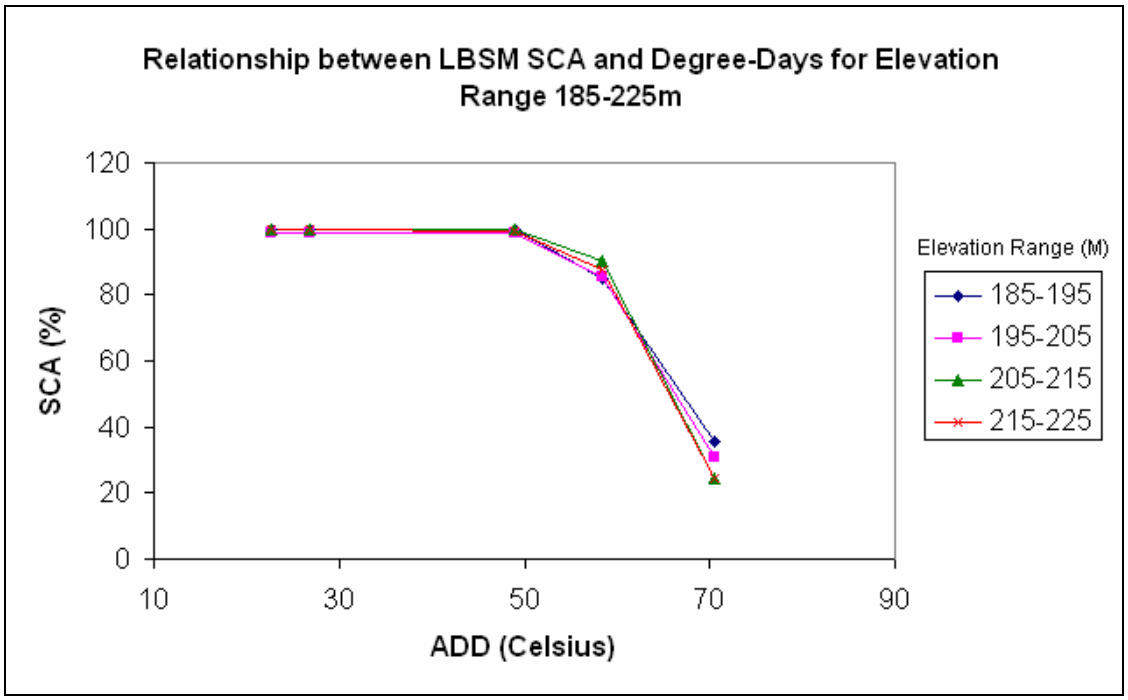

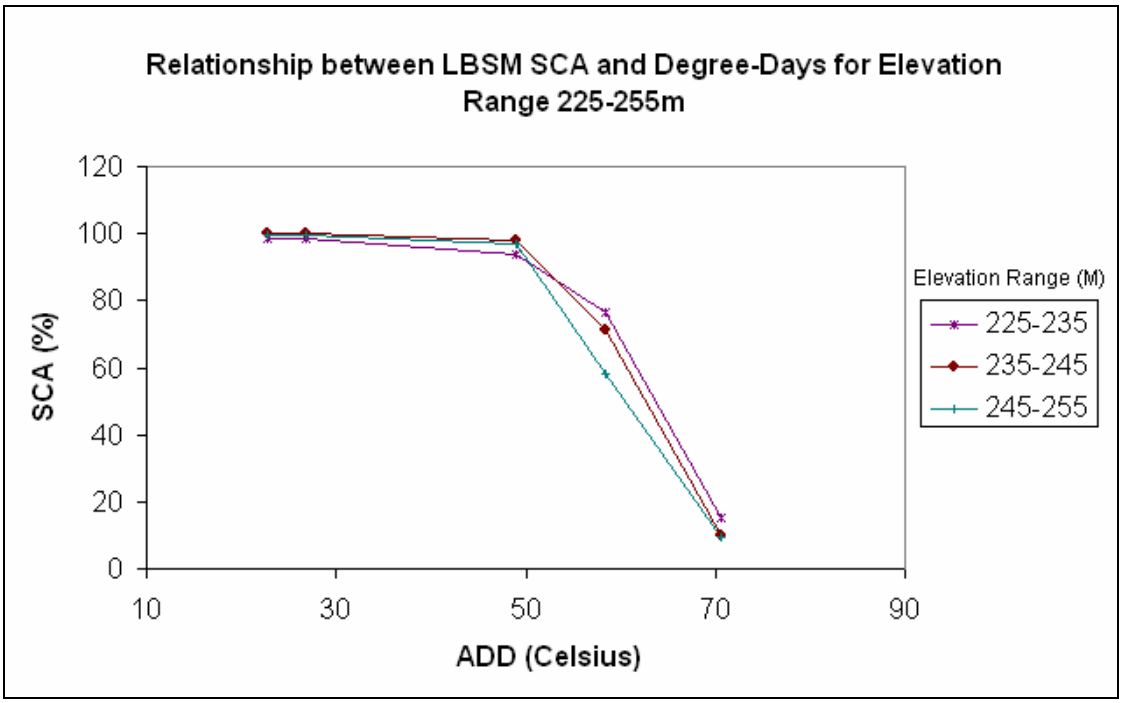

LBSM SCA 2002

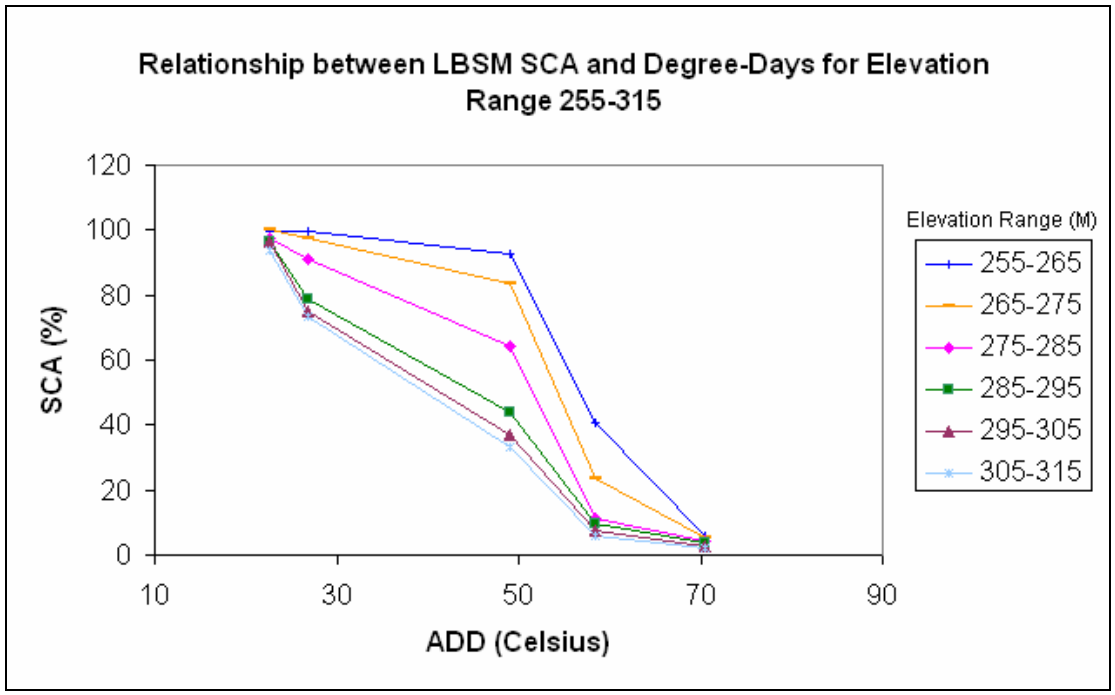

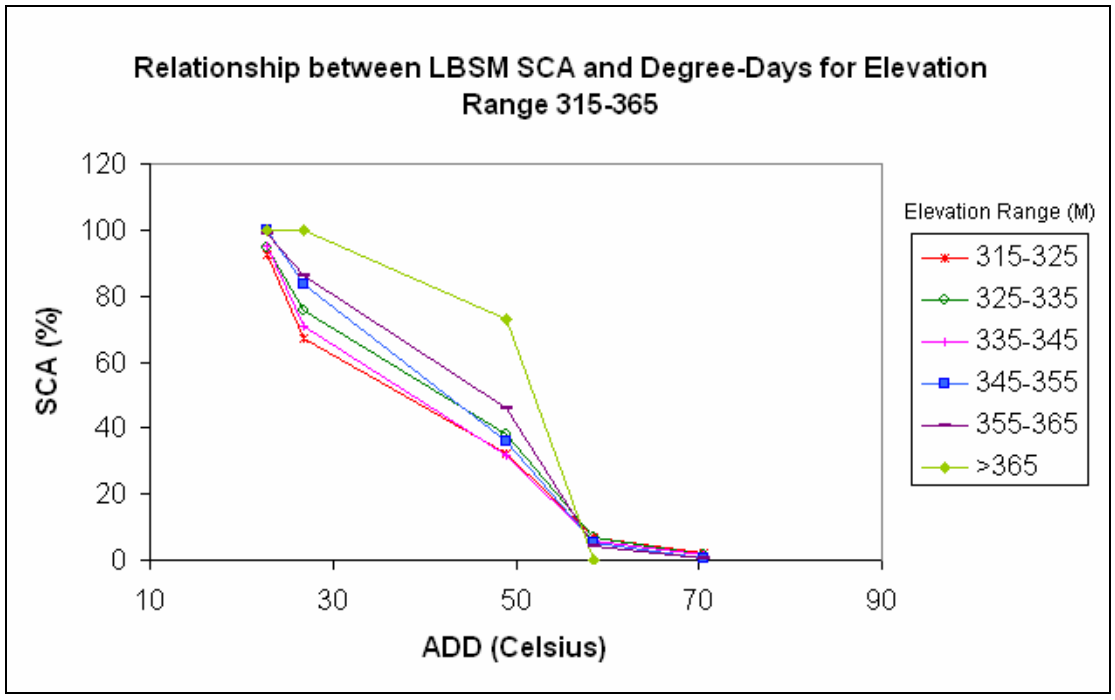

MOD10A1 SCA 2002

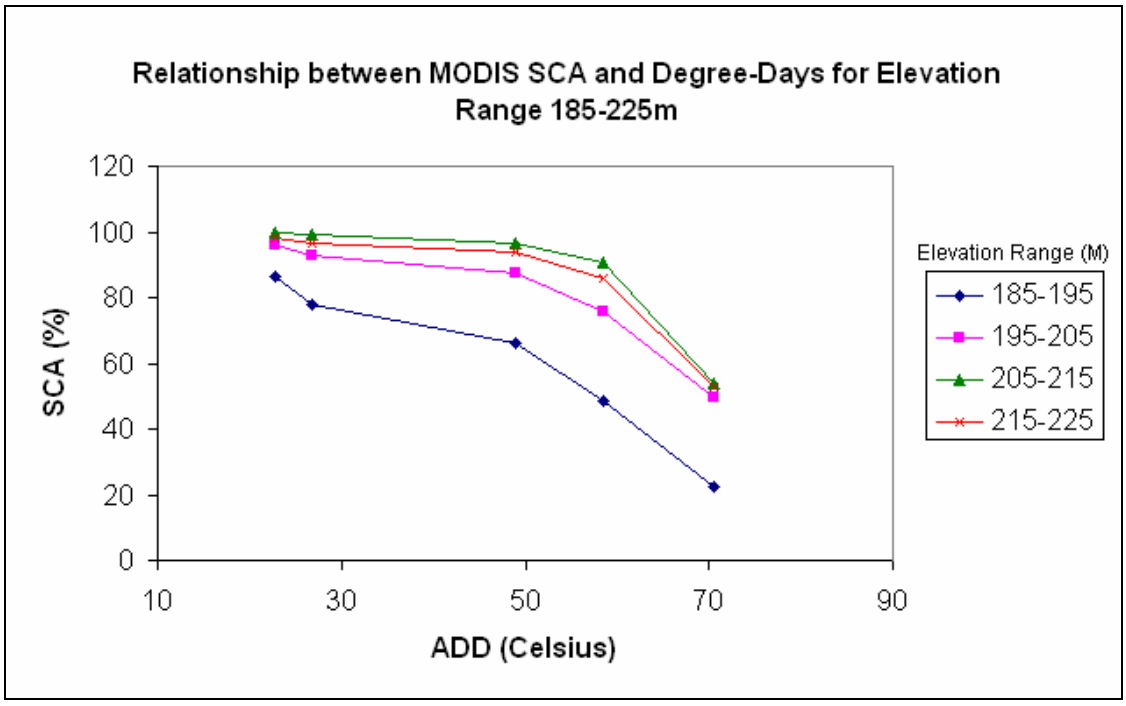

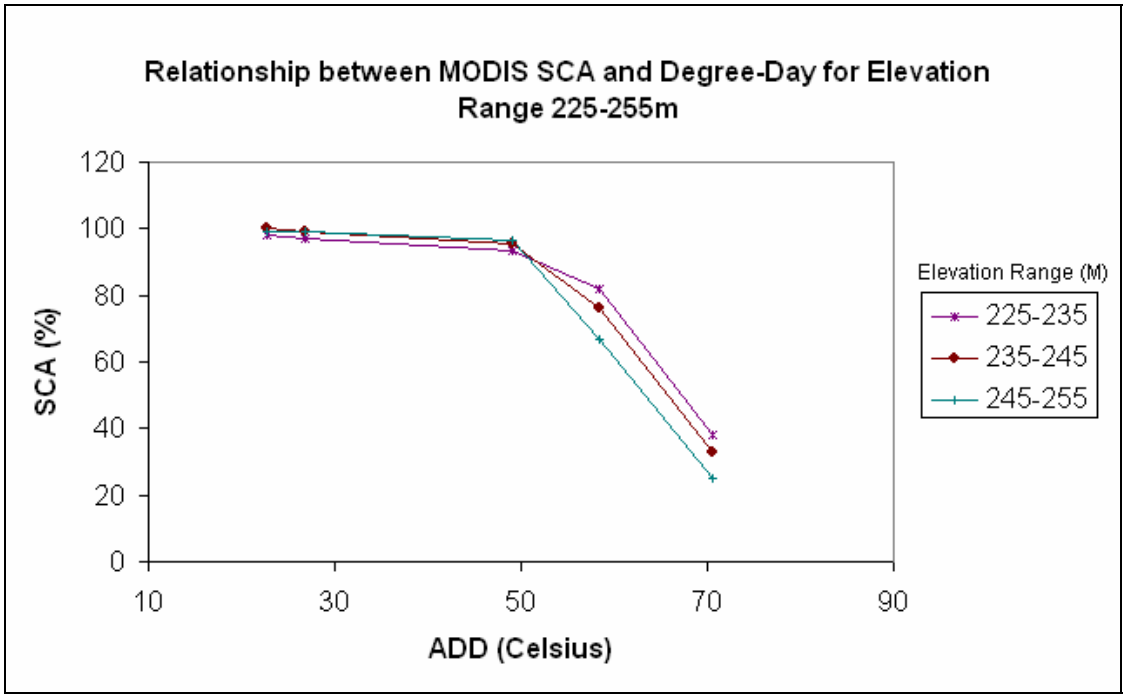

MOD10A1 SCA 2002

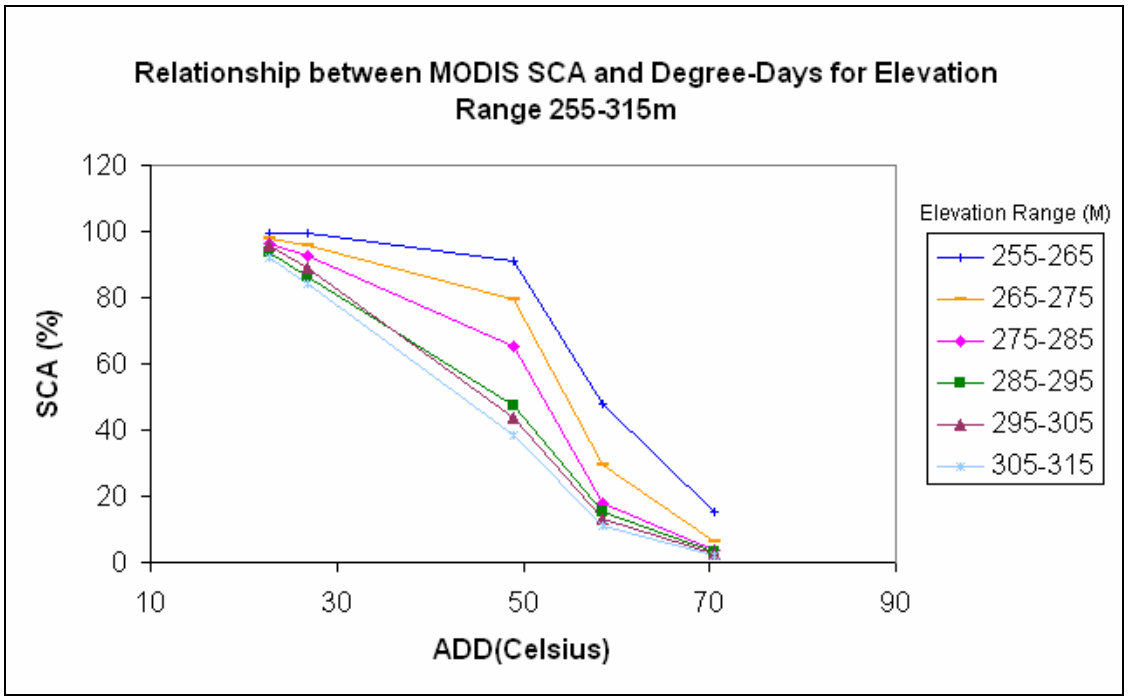

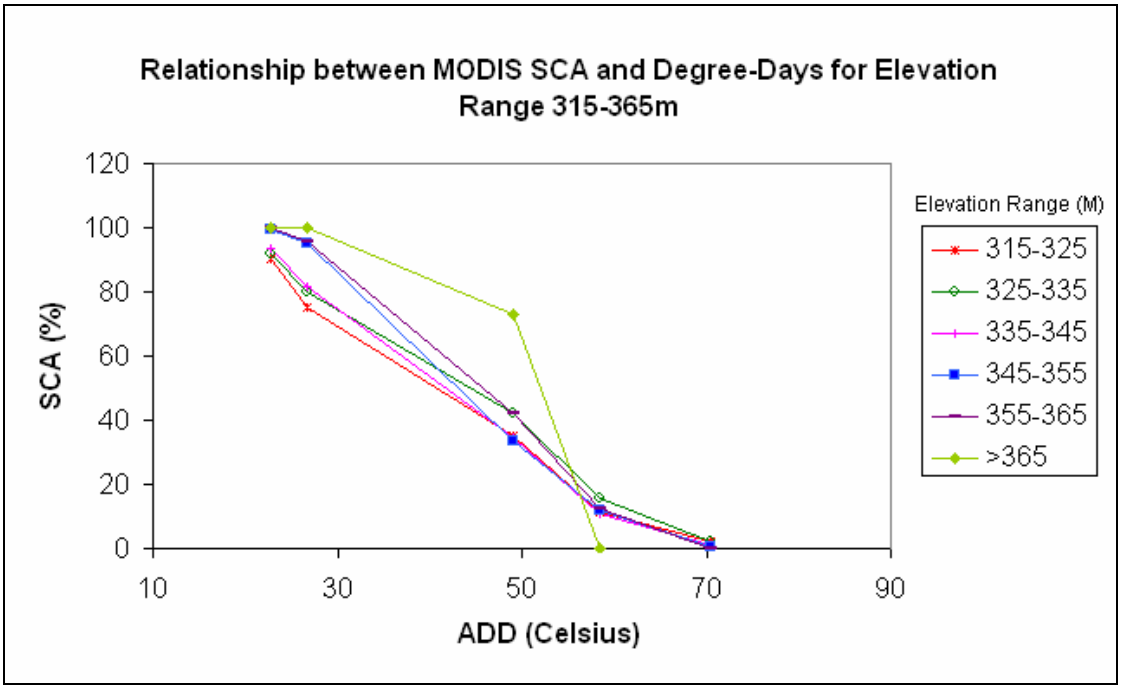

MOD10A1 SCA 2003

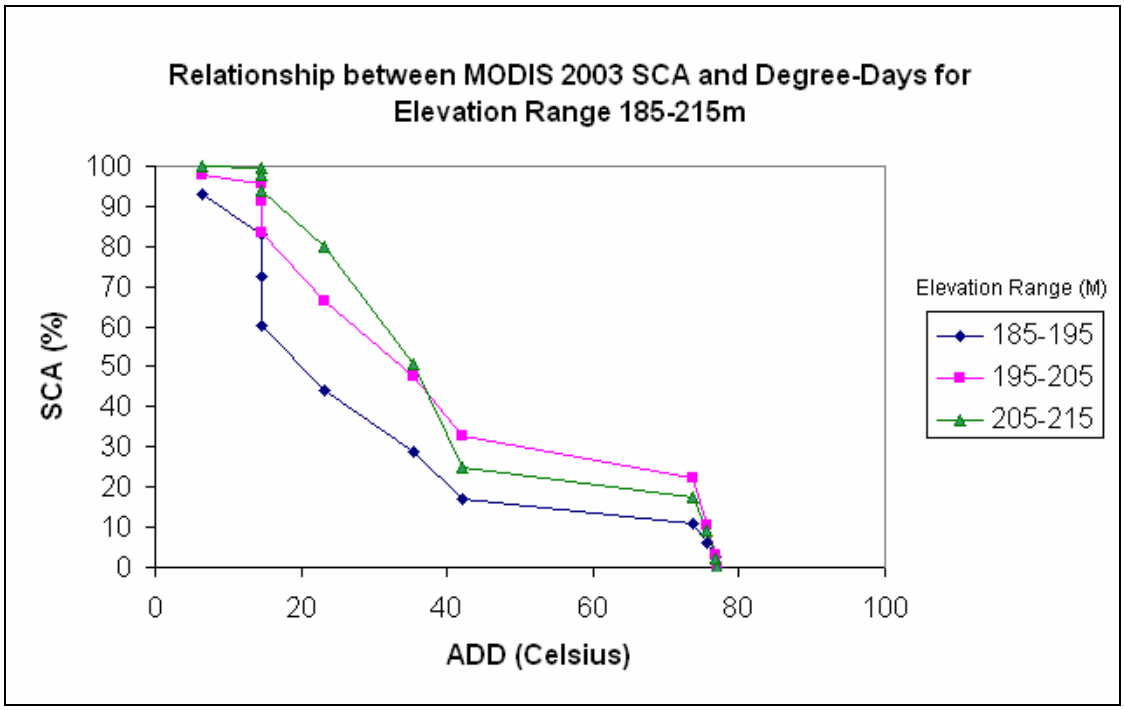

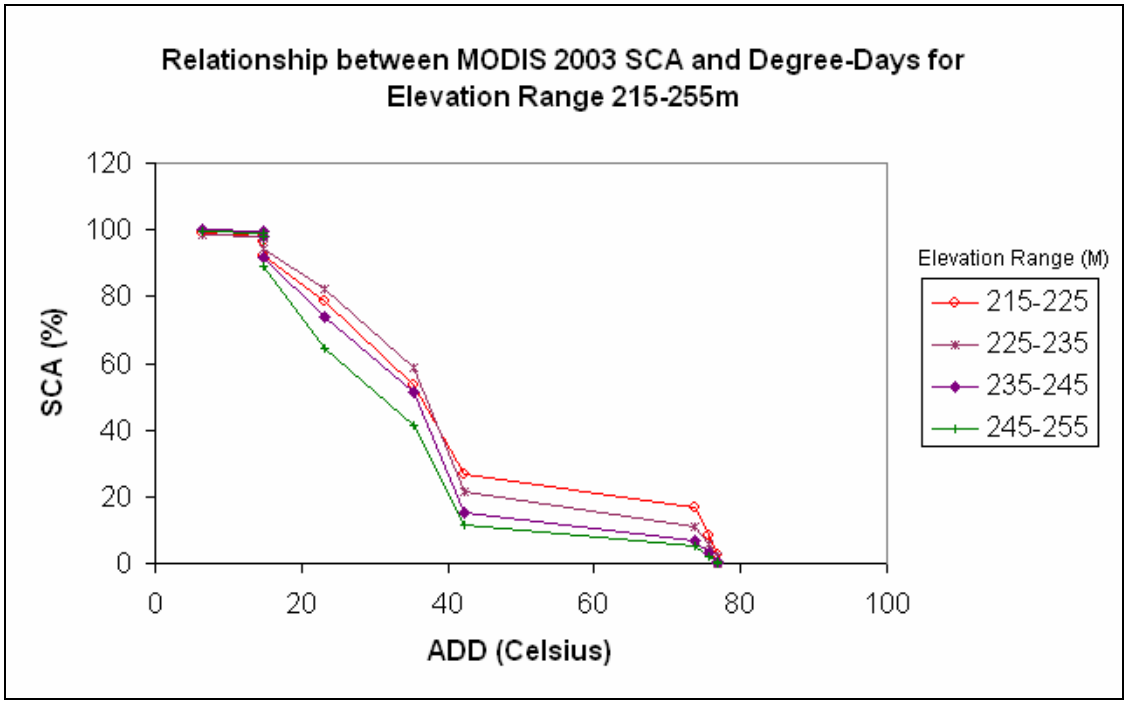

MOD10A1 SCA 2003